Zentrum für Entwicklungsforschung (ZEF)

The hidden risk of conventional floodplain mapping

Diagnosis in Cali, Colombia

Dissertation

Zur

Erlangung des Grades
Doktor der Ingenieurwissenschaften
(Dr. -Ing.)

der
Landwirtschaftlichen Fakultät

der
Rheinischen Friedrichs-Wilhelm-Universität Bonn

von
Cesar Canon

aus
Bogota, Kolumbien

Bonn 2022

Referent: Prof. Dr. Janos Bogardi

1. Korreferent: Prof. Dr. Jürgen Kusche

2. Korreferent: Prof. Dr. Bernd Diekkrüger

Tag der Promotion: 31. Januar 2022

ABSTRACT

Flood hazard maps display the geographical areas inundated by water bodies after extreme rainfall events take place, helping governments focus their efforts and resources on performing works to mitigate disasters produced by such inundations. However, rainfall also triggers small disasters at other moments, which are not included in these maps, such as traffic impedance and water-borne diseases, both inside and outside the mapped floodplain.

Unfortunately, small disasters are overlooked in traditional risk management for being tolerable, mild, and scattered. Though they do occur with high frequency, and citizens and utility companies must constantly attend them. Besides, it is challenging to get data sources to describe them accurately. Therefore, efforts should be made to base analyses on available on-site reports. Mitigation of small disasters triggered by rainfall can save money to build resilience, foster the development of a city, and reduce inequality.

This research seeks to relate the occurrence and types of small disasters triggered by rainfall to rainfall parameters and neighborhood attributes, and to prioritize neighborhoods for intervention in Cali, Colombia, for which secondary data is collected and its suitability evaluated for this sort of analysis; once small disasters are counted and characterized, an estimation of their potential economic impact is proposed; finally, the impact of rainfall events on the drainage network in a selected neighborhood is simulated through a hydrodynamic model, which includes scenarios such as obstructed pipelines, and low impact development solutions (LIDS) installed, in order to better understand the influence of ground and underground conditions on nuisance floods.

Contributions provided here about correlation analysis, hydrodynamic simulations, and diagnosis of information gaps are useful to prioritize areas in other cities, to follow better data gathering practices, and to understand the potential economic losses if prompt action is not taken.

Das verborgene Risiko der konventionellen Überschwemmungskartierung: Diagnose in Cali, Kolumbien

KURZFASSUNG

Hochwassergefahrenkarten zeigen die geografischen Gebiete, die nach extremen Regenfällen an Wasserläufen und Seen überflutet werden und unterstützen somit Regierungen und Verwaltungen, ihre Bemühungen und Ressourcen auf die Durchführung von Arbeiten zur Eindämmung von Katastrophen zu konzentrieren, die durch solche Überschwemmungen verursacht werden. Regenfälle lösen jedoch zu anderen Zeitpunkten auch kleinere Katastrophen aus, die in diesen Karten nicht enthalten sind, wie z. B. Verkehrsstau und durch Wasser übertragene Krankheiten. Diese können sowohl innerhalb als auch außerhalb der kartierten Überschwemmungsgebiete auftreten.

Leider werden diese kleineren Katastrophen im traditionellen Risikomanagement übersehen, weil sie als erträglich, mild und vereinzelt gelten. Sie treten jedoch mit hoher Häufigkeit auf, und daher werden Bürger und Versorgungsunternehmen ständig mit solchen Ereignissen konfrontiert. Außerdem es ist eine Herausforderung, die geeignete Daten zu erhalten, um diese Ereignisse genau zu beschreiben. Daher sollten Anstrengungen unternommen werden, um Analysen auch auf verfügbaren Vor-Ort-Berichte zu stützen. Die Eindämmung kleiner Katastrophen, die durch Regenfälle ausgelöst werden, kann Geld sparen, um Widerstandsfähigkeit aufzubauen, die Entwicklung einer Stadt zu fördern und Ungleichheit zu verringern.

Diese Forschung versucht, das Auftreten und die Arten kleiner Katastrophen, die durch Regenfälle ausgelöst werden, mit Niederschlagsparametern und Attributen städtischer Nachbarschaften in Beziehung zu setzen und Nachbarschaften für notwendige Interventionen in Cali, Kolumbien, zu priorisieren. Dafür wurden Sekundärdaten gesammelt und ihre Eignung wurde für diese Art von Analysen bewertet. Nach der Identifizierung und Charakterisierung kleineren Katastrophen, wurde eine Schätzung ihrer potenziellen wirtschaftlichen Auswirkungen vorgeschlagen.; Schließlich wird die Auswirkung von Niederschlagsereignissen auf das Entwässerungsnetz in einer ausgewählten Nachbarschaft durch ein hydrodynamisches Modell simuliert; die dabei erarbeiteten Szenarien berücksichtigen verstopfte Rohrleitungen und beziehen auch installierte „Low Impact Development Solutions (LIDS)“ (nebenwirkungsarme Entwicklungslösungen) eint, um die Auswirkungen von Oberflächenbeschaffenheit und Untergrundbedingungen bei Überschwemmungen besser zu verstehen.

Die hier bereitgestellten Beiträge zu Korrelationsanalysen, hydrodynamischen Simulationen und der Diagnose von Informationslücken sind nützlich, um Gebiete in anderen Städten zu priorisieren, bessere Datenerfassungspraktiken einzuführen und die potenziellen wirtschaftlichen Verluste einzuschätzen, die entstehen, wenn nicht umgehend Maßnahmen ergriffen werden.

DEDICATION

To my son Samuel, and to the family of my friend María del Pilar (the first of us).

TABLE OF CONTENTS

LIST OF ACRONYMS AND ABBREVIATIONS

AI	Aedic Index
CVC	Corporación Regional Autónoma del Valle del Cauca
DANE	Departamento Administrativo Nacional de Estadística
DAPM	Departamento Administrativo de Planeación Municipal
DESINVENTAR	Sistema de Inventario de Desastres
EMCALI	Empresas Municipales de Cali
ENSO	El Niño Southern Oscillation
FA	Fondo Adaptación
FNFA	Flood versus Non-Flood Analysis
GLM	Generalized Linear Models
GR	Green Roofs
ICA	Impact Classification Analysis
ICT	Instituto de Crédito Territorial
IDESC	Infraestructura de Datos Espaciales Santiago de Cali
LIDS	Low Impact Development Solutions
LULC	Land use/Land coverage
OR	Odds Ratio
PP	Porous pavement
PUJC	Pontificia Universidad Javeriana Cali
RG	Rain Gardens
SEL	Socioeconomic Level
SUDS	Sustainable Drainage Systems
TAZ	Transport Analysis Zones

1 INTRODUCTION

1.1 Flood management in Colombia

Floods are significant events in Colombia because of the frequency of their episodes, the extent of the areas involved, and the number of people and livelihoods compromised. This natural phenomenon has caused tragedies such as human casualties, forced migration and social and economic losses, been partially due to the absence of clear unified policies on water management, urban planning, disaster prevention and disaster follow-up throughout the country, and to poorly distributed hydrometeorological stations, incomplete time series and insufficient analysis of the consequences of weather events (Campos et al 2012; González and Alfaro 2001; Sedano et al. 2013).

The cold phase of El Niño Southern Oscillation (ENSO), known as La Niña, increases the intensity and total volume of precipitation in the mountain range and coasts of Colombia. The 2010-2011 La Niña event was one of the strongest registered in the last sixty years, producing floods and landslides that affected nearly four million people and led to losses in infrastructure, farming, and government subsidies for around US $7.8 billion (Hoyos et al. 2013).

The severity of the negative impacts derived from the 2010-2011 La Niña event drove the Colombian Government to declare state of emergency and to create a special fund – Fondo Adaptación (FA), in order to mitigate further impacts on society, economy, and ecology. Four main critical spots in Colombia were financed by FA to rebuild infrastructure, rehabilitate the economy, and protect the population (Decree 4819 2010). One of these spots was the *Aguablanca* dike, which protects the city of Cali from floods.

1.2 Problems related to the study area: Cali, Colombia

The city of Cali in Colombia started to expand towards the Cauca River in the 1950's once a 17-km dike was built along it, which allowed the district to grab land from the floodplain. This new land, intended first for agricultural use only, ended up engaged

mainly for urban activities. By 2016, more than 800,000 people were living in the floodplain area and 40,000 on top of the dike itself.

According to a diagnose by Royal Haskoning DHV and OSSO (Corporación OSSO 2012), if there are segments along the dike with a length in excess of 30 m where the top would stay at least 1.5 m below the water level during a 100-year flood, then these segments are prone to break; six points met these conditions in the longitudinal profile.

When the six breaches are included in 100-year, 250-year and 500-year flood simulations, the populated lowlands of eastern Cali and critical infrastructure along the Cauca River get inundated, such as the main water and wastewater treatment plants, electrical substations and pumping stations, potentially depleting the supply of drinking water, electrical power and drainage capacity. On top of that, because of its flat topography and lack of suitable infrastructure, the city also suffers from minor floods, which affect transportation, health and education services, and public health all over the city.

Moreover, one of the two access roads to the harbor of Buenaventura – the only harbor in the Colombian Pacific – goes through Cali and would reduce its capacity in case of flooding, compromising the emerging participation of the country in the Asia Pacific market.

No flood-risk study in Cali has ever analyzed floods outside the floodplain, or any type of floods down to street level (Corporación OSSO 2012). This study considers neighborhoods as basic areal units of analysis: a neighborhood is a political subdivision of the boroughs in a city, which tries to ensure a predominant land use (residential, industrial, universities, etc.); neighborhoods in Cali can be as small as a couple hectares and as big as 8 square kilometers.

1.3 Small disasters triggered by rainfall

Small disasters are chronic and localized; they can happen anywhere in a city, any time after rainfall events occur, and often in physically separated areas, with non-evident proximity to a cause or set of causes, and mostly with consequences that are difficult to estimate (Figure 1.2). Small disasters may curb the development of a city by frequently

affecting the population's general well-being and assets. By only considering floodplain problems in flood risk management plans, cities and governments run the hidden risk of overlooking the potential losses of small disasters in general.

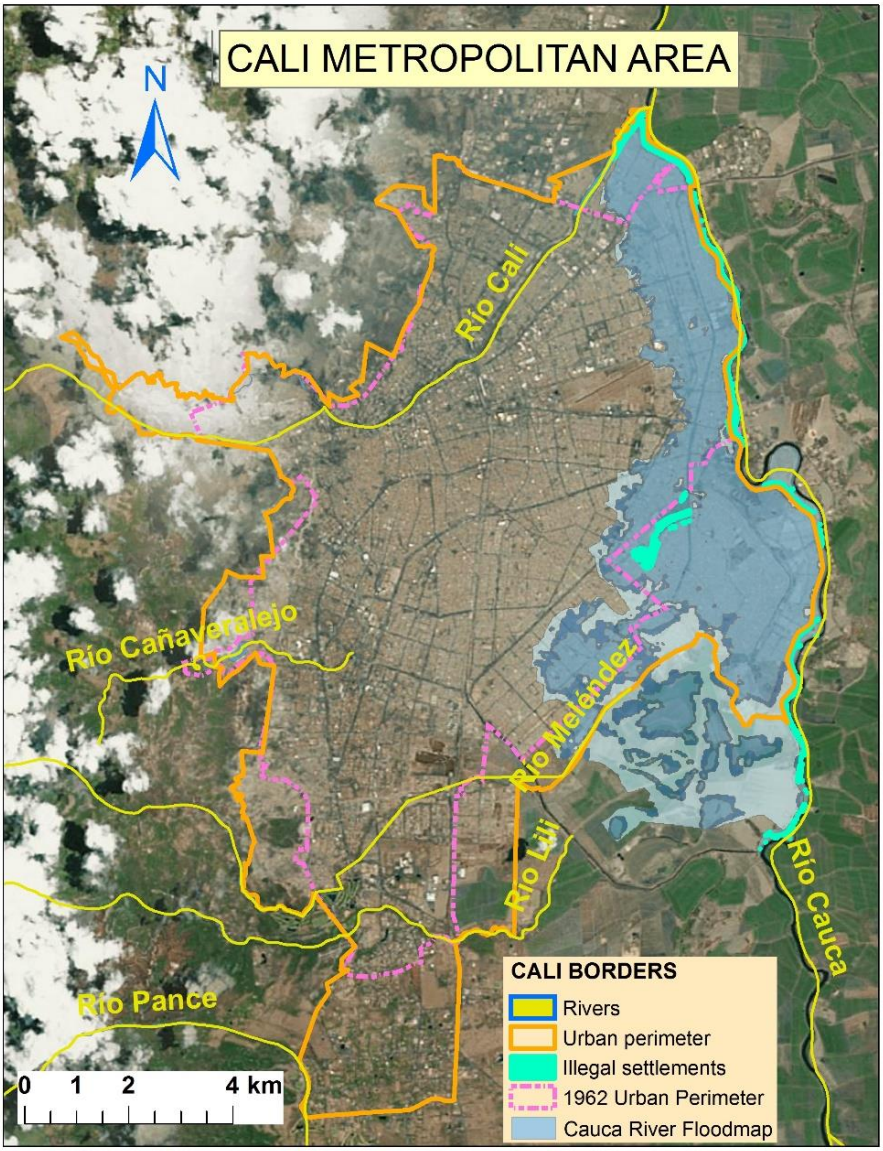

Figure 1.1: Extent of main floods between 1998 and 2011 in Cali. All illegal settlements on the Cauca River dike (around 40,000 people) and several legal neighborhoods (around 800,000 people) live within the flooded areas.

There are many possible types of small disasters triggered by rainfall, which are not captured by flood hazard maps; this study chose the following types of small

disasters for their recurrence in consulted reports, and grouped them together under the heading 'small disaster': *traffic impedance* and *water-borne diseases* (as a result of nuisance floods in one or several neighborhoods), *trees falling over properties*, and *power cuts* (due to trees falling, wind gusts, and/or electric storms).

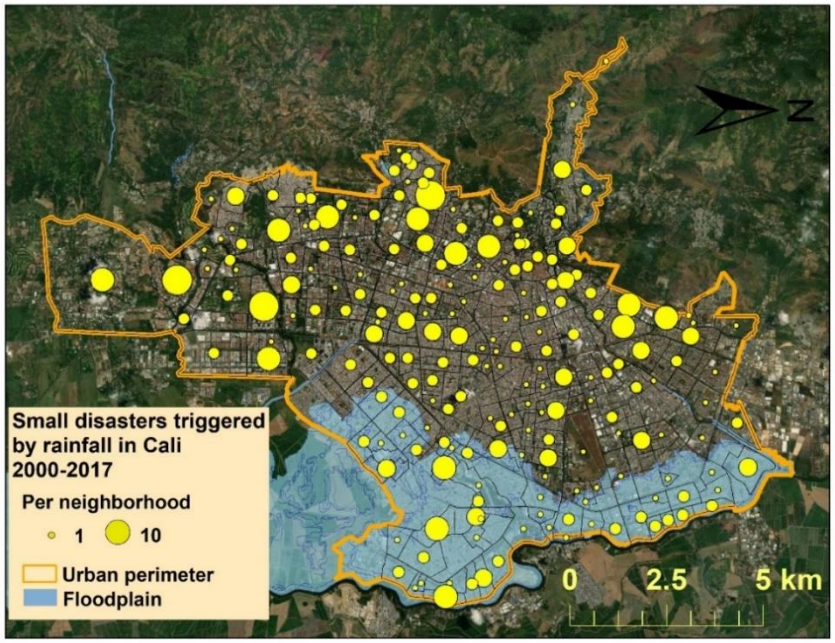

Figure 1.2: Small disasters triggered by rainfall reported per neighborhood in Cali during 2000-2017. Most neighborhoods have been affected both inside and outside the mapped floodplain.

Small disasters may be a consequence of unplanned urbanization, topography and hydrogeology, unsound cultural practices such as littering and wastewater illegal connections, insufficient or misplaced drainage infrastructure (University of Maryland and Texas A&M University 2018), poor drainage maintenance, and local or regional environmental degradation among other causes. Small disasters may indirectly take human lives, for instance, in car accidents due to a poorly drained road.

The concept of small disaster adopted in this study is similar to those for *local disaster: "social and environmental risks resulting from more recurrent lower level events, which are often chronic at the local and subnational levels"* (Cardona and Carreño 2011), and *extensive risks: "minor but recurrent disaster risks responsible for*

most disaster morbidity and displacement, eroding development assets, such as houses, schools, health facilities, roads and local infrastructure. However, the cost of extensive risk is not visible and tends to be underestimated, as it is usually absorbed by low-income households and communities and small businesses" (UNISDR 2015).

1.4 Main objective of the research

The main goals of this research are to make a selection process of the most vulnerable neighborhoods, based on spatiotemporal analyses involving rainfall parameters and neighborhood attributes; to estimate the economic impacts that these small disasters have had on Cali during this century; and to assess the efficiency of LIDS to minimize small disasters triggered by rainfall.

1.4.1 Detailed objectives

- Find correlations between rainfall parameters and neighborhood attributes with minor floods reported in Cali. Depending on the type of variables the correlation coefficients can be Pearson, Nagelkerke, or McFadden.
- Estimate economic losses due to minor floods in the city in the areas of transportation, health, and education. Economic losses are expressed first as time lost by citizens under different situations, such as time lost by commuters in traffic congestion, or hours with no class at educational institutions due to power cuts; time is also translated into money.
- Simulate drainage network response to rainfall events in a selected neighborhood by using a hydrodynamic model that has the capacity to include clogging and obstruction problems, as well as implementation of LIDS.

1.4.2 Research questions

- Is there a significant correlation between rainfall parameters (e.g., intensity, duration) and neighborhood attributes (such as population density and distance to rivers) with the occurrence of minor floods in Cali? Can areas of attention be prioritized by knowing these rainfall parameters and neighborhood attributes?

- How much can minor floods cost to the city of Cali in aspects such as traffic impedance, water-borne diseases, and interruption of health and education services?
- Can a hydrodynamic model simulate accurately backwater and waterlogged areas observed in a selected neighborhood in Cali?
- How effective can LIDS be to reduce flooding volumes in neighborhoods in Cali?

1.5 Structure of the thesis

Chapter 1: Introduction. This chapter provides a background for flood management in Cali, Colombia and defines its specific flood-risk challenges. It outlines the main and secondary objectives and the research questions, as well as the structure of the following chapters in the thesis.

Chapter 2: Description of the study area. This chapter describes the physical features of the city of Cali, its hydrology and hydrometeorological characterization, and presents a historical overview of its population dynamics.

Chapter 3: Minor floods correlated to rainfall events and neighborhood attributes in Cali. Rainfall events are split and characterized, along with neighborhood attributes, in order to find correlations with reported minor floods in Cali during 2000-2017.

Chapter 4: Economic loss estimation due to minor floods in Cali. Congestion time in transportation, water-borne diseases and interruption of health and education services caused by minor floods along with their monetary costs are estimated.

Chapter 5: Hydrodynamic simulation of drainage network response to rainfall events and LIDS implementation in a neighborhood in Cali. The drainage network of a neighborhood in Cali, along with its physical and demographic properties, is represented in a hydrodynamic model down to street level. Clogged outlets, pipeline obstructions and implementation of LIDS are simulated to see the drainage network response to rainfall events and the flooding volumes produced under the different scenarios.

Chapter 6: Conclusions and recommendations. Contributions, suggestions, and analysis limitations from chapters 3 to 5 are presented in here.

Chapter 7: References.

2 DESCRIPTION OF THE STUDY AREA: THE CITY OF CALI

2.1 Introduction

Cali is the capital city of the Valle del Cauca state (Figure 2.1, below). It is the third most populated city in Colombia, with over 2.4 million inhabitants, and it is also the economic and cultural pole of development for the Pacific region, even though it is not located on the pacific basin (west from the Andes), but in between the Andes west and center mountain ranges (Bahamón Dussán 2014); the Pacific region is comprised additionally by the states of Chocó, Cauca, and Nariño. Cali is under the jurisdiction of a few governmental entities for having both urban and rural district areas. 51.4% of the Valle del Cauca population lives in Cali (Alcaldía de Santiago de Cali 2014).

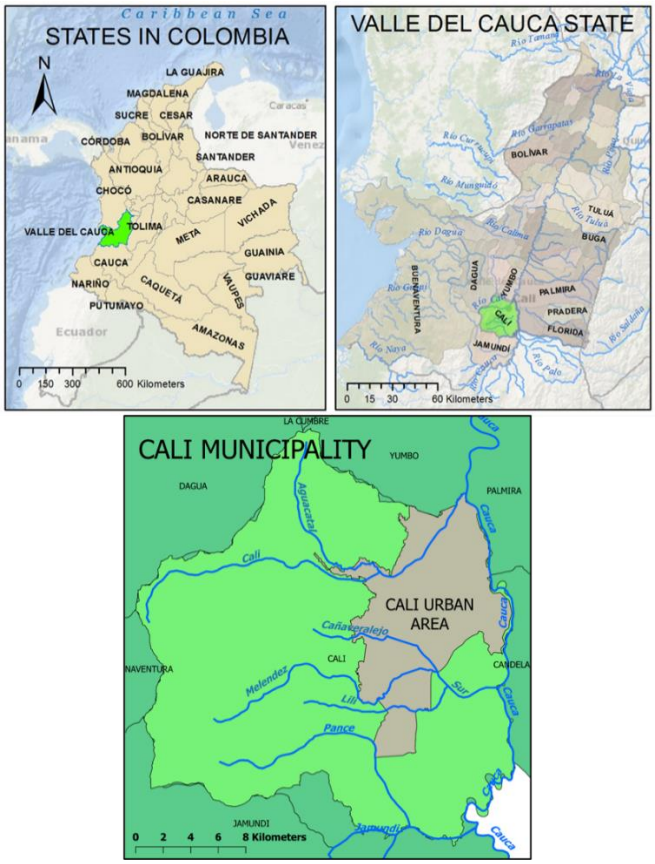

Figure 2.1: Valle del Cauca State in the Colombian Pacific region (upper left); Cali municipality in the state (upper right); and rivers crossing Cali (below).

2.2 Location and weather

Cali is in the Southwest of Colombia, along the eastern piedmont of the western Andes Mountain range, influenced by a warm and dry continental weather. It has an area of 560.3 km² on an elevation range between 939 m.a.s.l. by the Cauca River in the east and 1,442 m.a.s.l. on the western mountains (Figure 2.1**Error! Reference source not found.**, below). Its average temperature is 23.9°C, raising at noon up to 31°C and going down to 19°C at dawn. Relative humidity of air is slightly below 70% during dry months, and between 75% and 76% during rains. There is a bimodal precipitation regime in the Cauca valley, with two rainy seasons throughout March-May and October-December, and two dry, or less rainy seasons in the other months, being June-August more severe, with around six rainy days per month; in rainy months there can be around 18 rainy days per month. Annual average precipitation in Cali is 1,483 mm, measured at the Universidad del Valle station: monthly average values for precipitation and evapotranspiration are shown in Figure 2.2 (González O 2012, Guzmán D et al 2015).

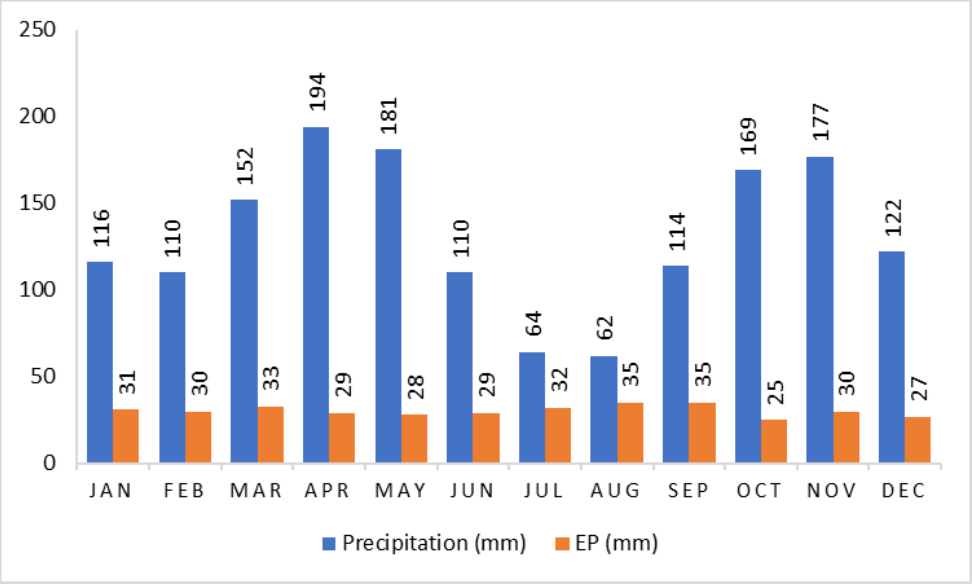

Figure 2.2: Average monthly values of Precipitation and Evapotranspiration (EP) in Cali between 1985 and 2008 at Universidad del Valle station. Source: (García 2010, report on water balance for Cali).

The metropolitan area of Cali is crossed by four rivers –*Cali*, *Cañaveralejo*, *Meléndez*, and *Lili*, all of them flowing into the Cauca River, to the east of the city. There are three other rivers in rural Cali: *Aguacatal* and *Pichindé* flowing into *Cali* River, and *Pance*, which turns into *Jamundí* river before flowing into the *Cauca* River (Figure 2.1, below).

2.3 Population Dynamics

2.3.1 Initial settlement of Cali

Before inhabited, the Cauca valley displayed exuberant tropical vegetation along with rapid mountain rivers, which turned into meanders as they crossed the flatlands to meet the Cauca River, putting in nutrients, feeding lakes and marshes, and widening their beds for flooding seasons (CVC 2007).

The city of Cali was originally built in the 16th century along the alluvial cone of the *Cali* River (*Cauca* River tributary), protected from natural hazards in general (Figure 2.3, below). During the 20th century, *Cauca* and *Cali* riverbanks were occupied by informal settlers (Buitrago Bermudez et al. 2011) that confined the streams, disconnecting them from lakes, meanders and *madreviejas* (dormant meanders) that received their excess flow (Figure 2.3, above). From all the original lakes ever known in the Valle del Cauca state, the *Sonso* lake is the only one remaining, about 50 km northeast from Cali (CVC 2007). In the 1930s, the city had already expanded over the steep slopes of the western hillside and over the river floodplains, opposing its original plan of linear development along the foothills (Figure 2.3). The first disasters produced by flood and landslides were reported around this time, as it is expected from rapidly urbanized areas (Palanisamy and Chui 2015). The city administration mitigated the damages by improving urban equipment, confining disasters towards the periphery. Disasters came back eventually to improved neighborhoods whenever La Niña event was stronger than expected (Jiménez and Velásquez 2011).

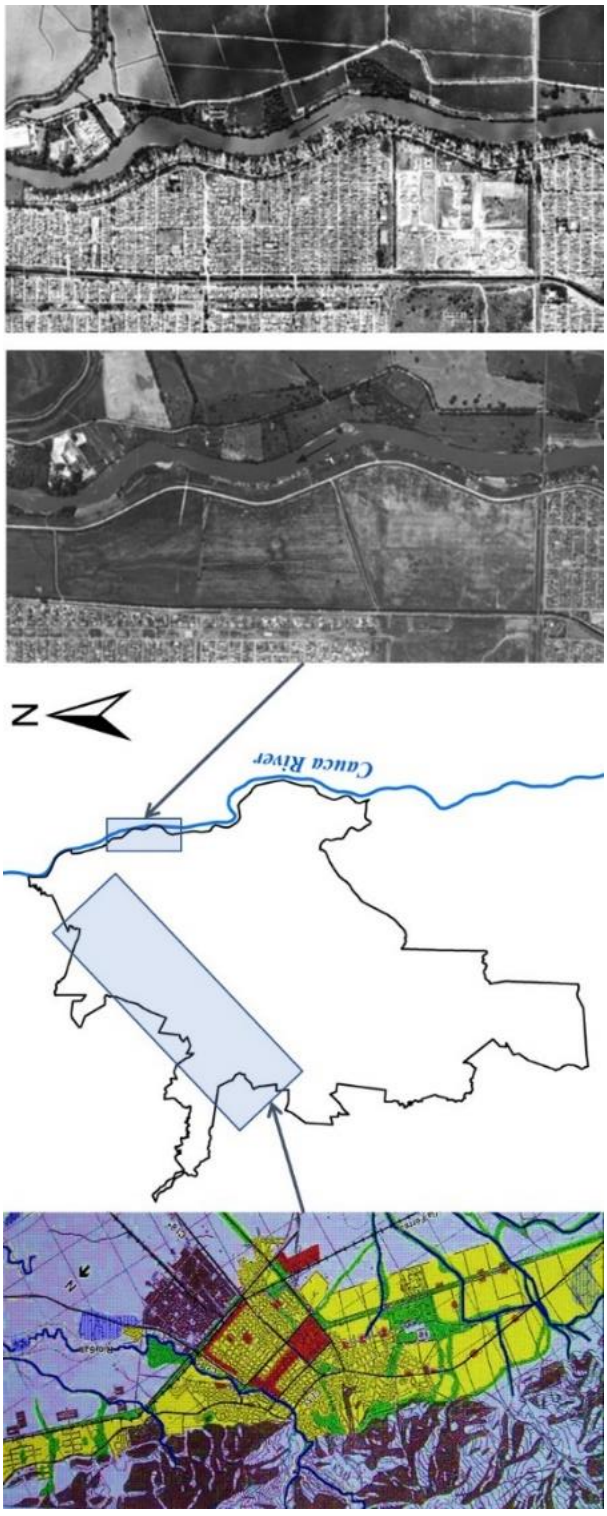

Figure 2.3: Urban growth in Cali. Below: urban projection of Cali in 1950 close to western cordillera (source: Jiménez and Velásquez 2011); above: aerial photographs of Cauca River floodplain in 1981 and 1998 (source: CVC 2007).

2.3.2 The quest for development

By the 1950s, electric power in Colombia just covered a fifth of the demand for energy; meanwhile, mountain settlers threatened river springs and basin flow regulation with deforestation practices, in part due to forced migration from rural to urban areas sped by bipartisan political violence. To face these challenges, several leaders and major landowners in Cali created in 1954 the *Regional Autonomous Corporation of the Cauca Valley* (CVC), inspired by the *Tennessee Valley Act* in the United States. CVC pursued regional development and local and foreign investment through power generation, water regulation for agriculture, industry, housing, and fishery, water quality, land use improvement, flora and fauna protection, and strengthening of transportation and telecommunications (CVC 2007).

CVC reckoned around 100,000 ha in the valley for agricultural and industrial use (CVC 2007), despite the fact that this area had many natural aspects that would make these economic activities hard to perform and become profitable, such as frequent floods, long dry periods, slow drainage and lack of certain soil nutrients. To meet CVC goals, projects like *Salvajina* and *Timba* reservoirs for flow regulation, *Calima* reservoir for power generation, and *Aguablanca* district for drainage, farmland suitability and flood control were carried out (CVC 2007).

2.3.3 Aguablanca Project and illegal settlements

Aguablanca, which literally means “White Water”, so called for looking like a sky mirror when flooded, is the western flood plain area of *Cauca* River within the city of Cali. Before the project, it received frequent floods from the rivers *Cañaveralejo*, *Lili*, *Meléndez* and *Cauca*, in addition to 70% of rain drainage and sewage from Cali (CVC 2007), but still was a fertile land, and CVC considered that establishing households for the poor, and farming and industrial activities, would both develop the region and solve housing and communication basic needs.

Aguablanca Project promised to control floods by means of a 17-km dike along the left margin of the Cauca river (from *Paso de Navarro* down to *Cali* River mouth), a 9-km open channel intercepting and conveying *Cañaveralejo*, *Lili* and *Meléndez* rivers

southwest and out of the district into the *Cauca* River (*south channel*), and the east drainage: a channel system draining rain and sewage from the city towards the *Paso del Comercio* pump station into the Cauca river as well (Figure 2.4). CVC was in charge of the works, which took place between 1958 and 1961, and of the subsequent maintenance and operation (CVC 2007).

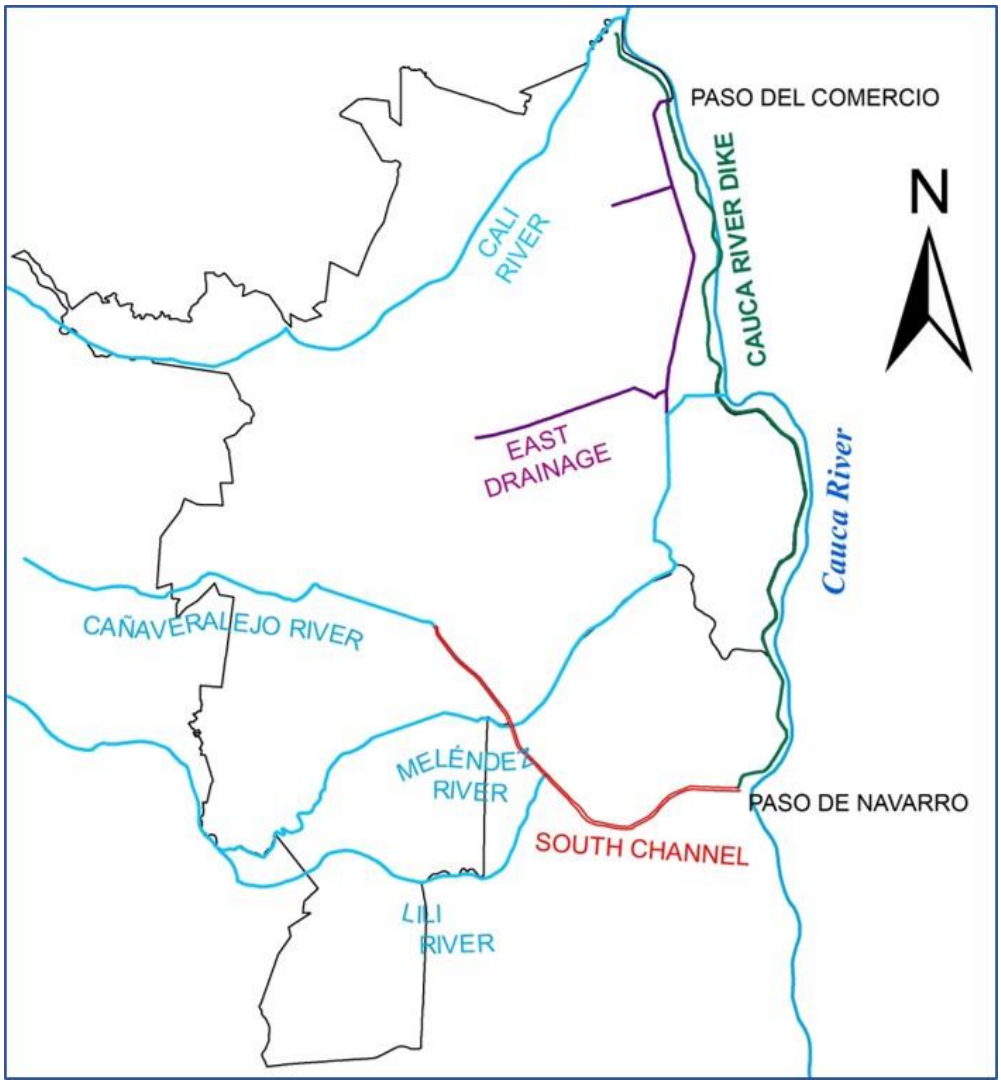

Figure 2.4: Main rivers and canals involved in Aguablanca project. East drainage and South channel are both open channels.

In the 1950s, the city started harboring informal, low-paid workers with no social protection. Cali´s growth was 70% illegal between 1949 and 1979 (Jiménez and

Velásquez 2011), due to forced displacement from rural areas than to a raise in the fertility rate. Original landowners of the *Aguablanca* floodplain area eventually decided that it was more profitable to urbanize the land than to keep it for agroindustry purposes (Uribe and Holguín 2012) . By 1980, the Cauca river dike itself started to get invaded by families, first legally under the direct support of the municipal government that promoted agricultural parcels (Jiménez and Velásquez 2011), but then illegally, until there were over 7,000 families (7,852 families were identified by Plan Jarillón in 2012).

The massive settlement of *Aguablanca* was evident. Dwellers got flooded frequently since the draining systems were not conceived originally for urban use. In 1987, CVC ceded the jurisdiction to the Cali Utility Company (EMCALI) so they would adapt the drainage infrastructure to urban (CVC 2007; Uribe and Holguín 2012). The biggest threat that the invasion of families on the dike poses to the city is that EMCALI is unable to perform the regular dike maintenance that prevents its breakage.

2.3.4 The recent response of government and risk authorities

Response from authorities to occupation since the 1980's has varied from forced evictions to negotiations and official upgrades of substandard settlings into neighborhoods.

The economic openness in Colombia, formalized through the 1991 political Constitution, took State-subsidized land use and services, and offered them to industrial multinational firms. Moreover, the financial and institutional crises in the mid-90's due to links between government and drug trafficking ruined the climate for a long-term public policy on risk management (Jiménez and Velásquez 2011), and left the country under a rather reactive, short-sighted policy of emergency response alone.

In 2000, the city administration proposed a strategic plan to recover and preserve the Cauca River dike. The plan consisted in relocating the people to reinforce the dike (Uribe and Holguín 2012). Unfortunately, sustained financial deficits in the city and unwillingness from some of the families that earn money from their activities on the dike have not allowed this relocation to come to an end even in 2019, when 4,578 families are still living on the dike (Alcaldía de Santiago de Cali 2019).

3 MINOR FLOODS CORRELATED TO RAINFALL PARAMETERS AND NEIGHBORHOOD ATTRIBUTES IN CALI

Diagnosing the causality between meteorological phenomena and each minor flood reported in a city is a complex and challenging task, especially if relevant details of exact time and location have not been provided. However, when all collected reports are lumped and linked to rainfall parameters and neighborhood attributes, some general causes can be derived.

Due to budget constraints, the city cannot perform overall maintenance and repairs permanently to prevent minor floods (assuming that infrastructure is the main cause), therefore, this study can help to prioritize some hot spots to work on first.

Strategies to develop more forward-looking, sound urban plans in the future can be also derived from this study by avoiding the practices that have increased vulnerability to minor floods in the different neighborhoods.

3.1 Input data

Secondary data on rainfall parameters, neighborhood attributes, and reports of minor floods for the metropolitan area of Cali were gathered and tabulated for correlation analysis between them. The time frame selected for this analysis goes from 2000 to 2017 (Table 3.1), mainly for two reasons: first, lack of reliable information before 2000, or no information at all, regarding high-resolution rainfall; and second, because neighborhood attributes were considered constant in time (such as population density) due to lack of information and to simplify calculations; since this assumed behavior for neighborhood attributes is not realistic, then the shorter the time frame, the milder the consequences of this assumption are.

3.1.1 Rainfall data

The Cauca Valley Environmental Authority (CVC) manages 22 stations (17 pluviographic and 5 climatologic; Table 3.1 and Figure 3.1) inside the tributary area that conveys runoff through Cali. These stations can collect rainfall information in 10-min intervals with a tipping bucket collector connected to a satellite transmitter. The data are presented in

two columns: date (*MM/DD/YYYY hh:mm*) and rainfall (mm). While the time frame for the analysis is 2000-2017, not all these stations were operational in 2000 (Table 3.1). Two applications of ArcGIS software (ESRI 2015) were used for producing maps: ArcMap, which displays and explores GIS datasets as a collection of layers and other elements in a map, and Arcscene, a 3D viewer well suited to generate perspective scenes from raster data.

Table 3.1: Characteristics of the 22 rainfall stations for Cali. OC = ordinary climatologic station, PG = pluviographic station. Area of influence for each station is computed through Voronoi polygons in Arcmap.

Starting year	**Rainfall station**	**Type**	**Sub-basin**	**Area of influence [km²]**
2000	El Topacio	OC	Pance	27.1
	La Teresita	OC	Felidia	18.2
	Planta Río Cali	PG	Lower Lili	5.1
	Cañaveralejo	PG	Cañaveralejo	11.6
	Aguacatal	PG	Aguacatal	32.7
	Edificio CVC	OC	Lower Lili	12.4
	Peñas Blancas	PG	Pichindé	30.8
	Planta Río Cauca	PG	Lower Lili	25.7
	San Bosco	PG	Lower Lili	10.5
	San Luis	PG	Lower Cali	17.0
2010	Pance-Chorrera	PG	Pance	39.1
	Lili-San Sebastián	PG	Lili	36.0
2013	Cali Bocatoma	PG	Medium Cali	16.0
	Meléndez	OC	Cañaveralejo	7.5
	Pichindé	PG	Pichindé	26.5
2014	Felidia	PG	Felidia	30.3
2015	El Colegio	PG	Aguacatal	15.2
	PTAR	OC	Lower Lili	11.7
	Cañaveralejo	PG	Aguacatal	1.7
	El Ancla	PG	Lower Cali	26.6
	El Cortijo	PG	Lower Lili	74.7
	Meléndez PTAR	PG	Lower Lili	39.2
	Nápoles			

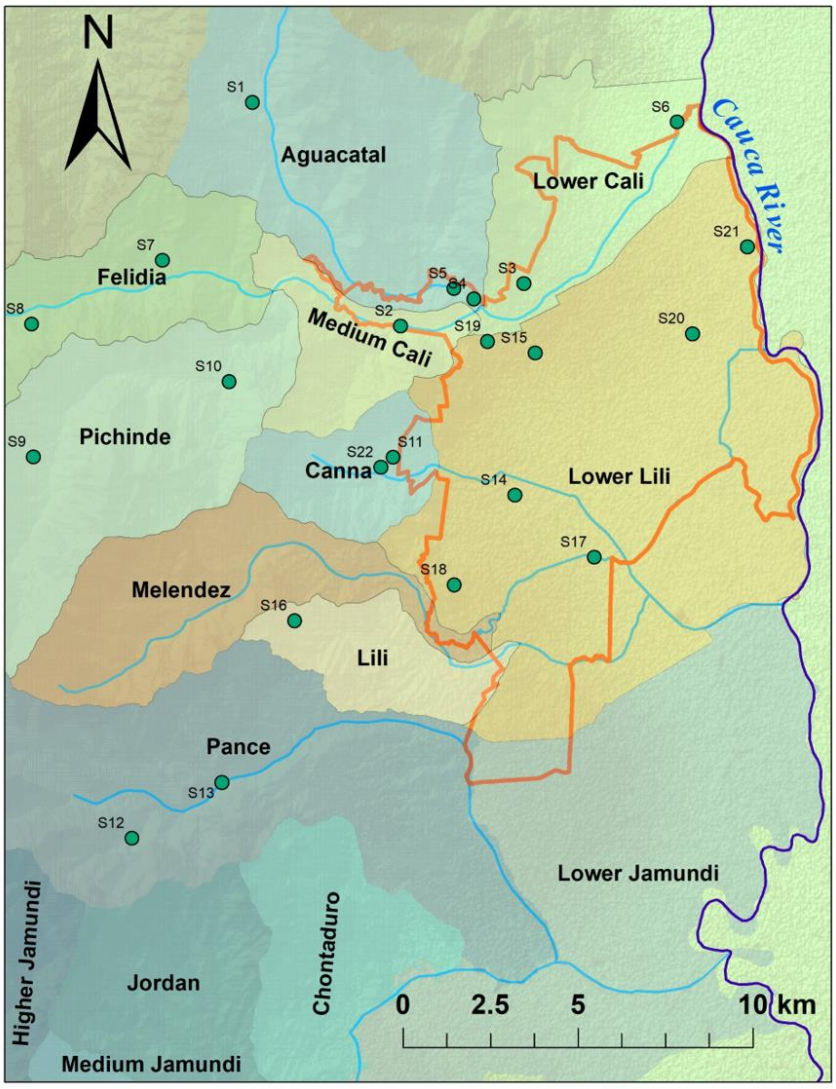

Figure 3.1: Location of the 22 rainfall stations inside the 6 sub-basins draining to Cauca River over the metropolitan area of Cali. Rivers: Aguacatal (discharging into Cali River); Lili, Meléndez, Cañaveralejo, and Pance.

3.1.2 Neighborhood attributes

The city of Cali is divided into 336 neighborhoods (see definition in section 1.2) which in turn are grouped together in 22 communes or boroughs. Demographic information and physical attributes were collected for each neighborhood:

- Population per neighborhood taken from the projections for 2017 based on the 2005 census by the National Administrative Department of Statistics (DANE). There has only been one official census in Colombia between 2000 and 2017.

- Terrain data were taken from diverse sources and formats:
    - A topographic survey with a 1-meter contour line resolution for the urban area of Cali, commissioned by the mayor's office for its 2014 land-use plan.
    - Elevation data from the 66,962 manholes across the city within the combined sewer drainage network operated by EMCALI.
    - A raster elevation model of the district of Cali, 15-m cell size, horizontal error associated to a 1:5000 scale provided by the Spatial Data Infrastructure of Cali (IDESC).
- Socioeconomic levels (SEL): Ranked from 1 (lowest) to 6 (highest), they are a classification given to real properties in order to charge them differential rates for utilities; subsidies are given to levels 1, 2 and 3 while contributions are charged to levels 5 and 6. Factors used to determine the SEL of a property are: external characteristics (size of entrance garden, type of garage, type of façade, type of door), urban environment (types of roads, types of sidewalks), and urban setting (location within the city). The Municipal Planning Department (DAPM) defines a SEL per neighborhood in Cali by averaging the SEL of all the properties within each neighborhood (Escobar G 2016).
- Aquifer map: Discharge zones, recharge zones, and sealed areas of the aquifer projected as polygons over the city (Escobar G 2016).
- Official limits of all neighborhoods provided in shapefile format by DAPM, as well as the sub-basin limits for the district of Cali.

3.1.3 Reports on minor floods

The Inventory System of the Effects of Disasters (DESINVENTAR) gathers information about small, medium, and greater impact disasters in Latin America reported by newspaper sources, groups of citizens, and institutions such as the police and the fire fighter departments. Even though several reports were complemented with photographs found in press, they were basically made with observations on site and

with the the locations and the collection of testimonies from people affected; reports lack backup technologies such as satellite imagery or water-level sensors.

All disasters reported in Cali were compiled, whether they came from the national (Colombia), regional (Valle del Cauca), or local (Cali) databases. From the many types of disaster categories (e.g., fire, flood, gale, plague, landslide, accident, earthquake) only those associated with floods caused by heavy rains were selected (Table 3.2). The DESINVENTAR database covers disaster reports between 2000 and 2015; disasters occurring during the years 2016 and 2017 were added in this study from local newspapers. For this study, the word 'disaster' used in the DESINVENTAR database is considered synonym with minor flood.

The spatial unit used for a minor flood is the neighborhood. Most reports give a detailed list of the neighborhoods that were affected. A few reports even give details about streets or blocks. However, other reports only generalize about zones like south-east Cali or northern Cali or a long segment of a highway, so further investigation had to be made on newspaper sources to determine more accurately which neighborhoods were affected. Should it still not have been possible to detect individual neighborhoods, then all neighborhoods in such an area were counted, even if that implies including some neighborhoods that were not involved in the minor floods. There were 156 minor-flood-related reports between 2000 and 2017, including 122 with neighborhood accuracy in their detail (Table 3.2).

Each minor flood reported comes along with information that helps determine what type of minor flood it is; this information is classified into several items such as 'Deaths, missing, wounded', 'transportation congestion and accidents', or 'Power cuts' (Table 3.3).

Table 3.2: Minor-flood-related events reported in DESINVENTAR and local newspapers. Details can be found at neighborhood (N), street (S), or zone (Z) scale. Events in bold were reported for two consecutive days on press; events shaded were reported for three consecutive days.

ID	Start date	Detail	ID	Start date	Detail	ID	Start date	Detail	ID	Start date	Detail
1	31-Jan-2000	N, Z	40	21-Mar-2006	N	79	3-May-2010	N, S	118	16-Sep-2013	N, S, Z
2	4-May-2000	N, Z	**41**	**24-Mar-2006**	**N**	80	31-May-2010	N, S	119	14-Oct-2013	S, Z
3	20-Jul-2000	N, S, Z	42	1-Apr-2006	N, S	81	1-Sep-2010	N	120	31-Oct-2013	Z
4	**5-Sep-2000**	**N, S, Z**	43	12-Apr-2006	N, Z	82	28-Oct-2010	N, S, Z	121	23-Dec-2013	N, S, Z
5	7-Jan-2001	N, S	44	14-Apr-2006	N, S	83	4-Nov-2010	N	122	12-Mar-2014	N, S
6	22-Jan-2001	N, S, Z	**45**	**1-May-2006**	**N, S**	84	12-Nov-2010	Z	123	16-Apr-2014	N
7	21-Feb-2001	N, S, Z	46	7-May-2006	N, S	85	22-Nov-2010	N	124	28-Apr-2014	N
8	22-Mar-2001	N, Z	47	2-Oct-2006	S	86	25-Nov-2010	N	125	20-May-2014	N, S
9	16-Apr-2001	N, S	48	7-Nov-2006	N, S	87	25-Feb-2011	N	126	7-Jun-2014	N, Z
10	13-Jul-2001	N, S, Z	49	24-Nov-2006	N	88	6-Apr-2011	N, S, Z	127	18-Sep-2014	S, Z
11	13-Sep-2001	N, S	50	12-Dec-2006	N, S	**89**	**22-Apr-2011**	**N**	128	13-Oct-2014	S, Z
12	29-Sep-2001	N	51	20-Jan-2007	N	90	25-Apr-2011	N, S, Z	129	20-Oct-2014	N, S, Z
13	23-Oct-2001	Z	52	27-Mar-2007	N, S	91	5-May-2011	N	130	26-Nov-2014	N, S
14	14-Nov-2001	Z	53	2-Apr-2007	S	92	8-May-2011	N, S, Z	131	23-Jan-2015	Z
15	13-Dec-2001	N, S	54	16-Apr-2007	N, S, Z	93	15-Jun-2011	Z	132	30-Mar-2015	N, S, Z
16	2-Apr-2002	N, S	55	18-May-2007	N, S	94	1-Jul-2011	N	133	6-May-2015	N, S
17	8-Apr-2002	Z	56	25-May-2007	N	95	6-Jul-2011	N	134	1-Nov-2015	N, S
18	18-Apr-2002	Z	57	27-May-2007	N, S	96	6-Sep-2011	N	135	7-Nov-2015	S
19	22-Apr-2002	N	58	30-Oct-2007	Z	97	14-Oct-2011	N	136	13-Mar-2016	S
20	21-May-2002	N, Z	59	1-Nov-2007	N	98	6-Nov-2011	N, Z	137	30-Mar-2016	S
21	17-Jul-2002	S	60	20-Dec-2007	N	99	12-Nov-2011	N	138	11-Apr-2016	S, Z
22	24-Oct-2002	N, S, Z	**61**	**18-Feb-2008**	**N, S**	100	16-Dec-2011	N	139	26-Apr-2016	N, Z
23	25-Apr-2003	N, S, Z	62	25-Apr-2008	N,S	**101**	**8-Feb-2012**	**N, Z**	140	10-May-2016	N, S
24	12-May-2003	N	63	28-Apr-2008	Z	102	21-Mar-2012	N	141	28-May-2016	N, Z
25	5-Oct-2003	Z	64	1-May-2008	N, S	**103**	**25-Mar-2012**	**N, Z**	142	13-Jun-2016	N, S
26	13-Oct-2003	N	65	11-Jun-2008	N, Z	104	10-Apr-2012	N	143	20-Jun-2016	N, S
27	7-Jan-2004	Z	66	24-Jun-2008	N	105	18-Apr-2012	N, S, Z	144	30-Sep-2016	N
28	26-Mar-2004	N, Z	67	3-Jul-2008	N, S, Z	106	28-Apr-2012	N, S	145	2-Oct-2016	S
29	3-May-2004	N, Z	68	8-Jul-2008	N, S	107	1-May-2012	N, S	146	7-Oct-2016	S
30	12-May-2004	N, S, Z	69	4-Oct-2008	N	108	5-May-2012	N, Z	147	1-Dec-2016	N, S, Z
31	27-Oct-2004	N	70	20-Nov-2008	N, S	**109**	**7-May-2012**	**N, S**	148	28-Feb-2017	Z
32	29-Mar-2005	N	**71**	**26-Nov-2008**	**N, S**	110	25-Jun-2012	N, Z	149	10-Mar-2017	N, S
33	21-May-2005	N, S	72	7-Mar-2009	N	111	23-Oct-2012	Z	150	24-Mar-2017	Z
34	2-Jul-2005	N	73	9-Mar-2009	N	112	24-Feb-2013	Z	151	26-Mar-2017	S
35	24-Jul-2005	N, S	**74**	**19-Mar-2009**	**N, S, Z**	113	23-Apr-2013	N, S, Z	152	14-Apr-2017	N, S
36	28-Sep-2005	N, S, Z	75	8-Apr-2009	Z	114	29-Apr-2013	N, S, Z	153	18-Apr-2017	N, S
37	14-Dec-2005	N	76	8-Dec-2009	S, Z	115	21-May-2013	N, S, Z	154	26-Apr-2017	N, S, Z
38	1-Feb-2006	Z	77	23-Feb-2010	S	116	27-May-2013	N, S, Z	155	30-Apr-2017	N, S
39	17-Mar-2006	N, S	78	29-Apr-2010	S, Z	117	11-Aug-2013	N, S, Z	156	6-May-2017	N

Table 3.3: Types of minor floods reported in DESINVENTAR and local newspapers. The right column shows how many times each type of minor flood has occurred during the 156 events reported.

Reported impacts from minor floods	**Occurrence**
Deaths, missing, wounded	25/156
Homes destroyed and/or affected	89/156
Education and health centers affected	21/156
Transportation congestion and accidents	44/156
Sewerage blockage and saturation	25/156
Power cuts	52/156
Trees falling	44/156
Main rivers overflow	15/156

3.2 Methodology

The present section pursues two main goals: the first one is to determine whether rainfall parameters and neighborhood attributes have significant correlations with the occurrence or not of minor floods in the city, in which case, the latter could be predicted, and priority could be given to those existing or projected neighborhoods with attributes that make them prone to minor floods; it will also be useful to prevent new neighborhood projects from having these attributes that make them vulnerable in the first place. The methodology for this first goal is referred further down as *Flood versus Non-Flood Analysis* (FNFA).

The second goal is to determine whether rainfall parameters and neighborhood attributes are significantly correlated with the different types of minor floods once they have occurred, in which case a more detailed spatial characterization of the consequences can be accomplished. The methodology for this second goal is called *Impact Classification Analysis* (ICA).

For both goals it was necessary to split the continuous 10-min rainfall records into rainfall events: the methodology to do so varies for each goal, as it will be explained

later. Neighborhood attributes are also important, but they have no time component since they were considered constant for the interval studied.

Input data on rainfall, neighborhoods, and reported minor floods were chronologically ordered for correlation and statistical analysis. In the first part of the analysis, statistical differences in rainfall parameters (t-test, F-test, Wilcox test) between minor-flood-related and non-minor-flood-related rainfall events were determined; regressions were made to see if rainfall parameters from a rainfall event can predict whether this event will cause minor floods or not (logistic regression), whether it can predict the number of neighborhoods affected (Poisson regression), and also whether neighborhood attributes are significantly correlated with the number of minor floods reported on those neighborhoods (Poisson regression). In the second part, only rainfall events related to minor floods were chosen, to see if their parameters were significantly correlated with the types of minor floods observed during each event.

3.2.1 Rainfall event separation

Rainfall events must be clearly defined and split from other events before performing statistical analysis and prediction models based on them; rainfall data, however, is presented as an ongoing record. Separation techniques for rainfall events are suggested in literature, always emphasizing the uncertainty in their accuracy (Lisonbee et al. 2019; Gariano et al. 2019; Argüeso et al. 2016; Cea and Fraga 2018). For the present analysis, two separation methods were applied to the continuous rainfall data set: one for FNFA, and another one for ICA.

Flood versus Non-Flood Analysis (FNFA)

A rainfall event is defined for this analysis as any period or group of periods of non-zero rainfall record separated by several periods of no rain before and after, so it can be clearly distinguished from the previous and following event. One main challenge was to define how long this no-rain period should be. Some studies split rainfall events by days, because hourly rainfall data is not available all the time (Garcia-Urquia and Axelsson 2015; Liang and Ding 2017); for this rainfall dataset, a no-rain period of 24 hours was

selected, basically to avoid several rainfall events occurring in a single day, which is the minimum time resolution for the minor-flood reports.

Rainfall information is available in continuous 10-min time series from each of the 22 stations (around 52,600 values per station per year if no values are missing, as a result of dividing 365.25 days by 10 minutes); more than 300,000 values had to be checked. It was therefore practical to use a programming language to split the rainfall events. RStudio (RStudio Team 2015) was chosen for its data handling and storage capabilities, and its suite of operators for calculations on arrays (matrices). In order to delimitate these events, the following steps were performed:

- Rainfall readings from all stations were collected and sorted chronologically. Sometimes there is more than one reading for the same 10-min period, as many stations may capture rainfall simultaneously (Figure 3.2, left).
- The readings were split every time there was a period of 24 hours or longer of no rain (Figure 3.2, right). The dataset separation produced 791 rainfall events.
- Those rainfall events with less than 1.0 mm of cumulative rainfall were discarded (29 events); 762 rainfall events remained.
- Events that only lasted 10 minutes or one observation, even if it was registered at several stations, were also discarded (18 events); 744 rainfall events remained for the analysis (approximately 290,000 data values).
- Within the 744 rainfall events, some can be found as short as 20 min, and one as long as 58 days, that is, for 58 days there was not a single 24-hour zero-rain period during 58 days; this length depends on the arbitrary 24-hour separation period chosen. Different separation periods would give also different amounts and lengths of events (Table 3.4).

Table 3.4: Change in amount and length of rainfall events with different separation periods (24 h, 12 h, 6 h and 1 h).

	24-hour separation	12-hour separation	6-hour separation	1-hour separation
Initial events	791	1,194	1,508	2,168
Less than 1.0 mm events	29	95	172	373
Single observation events	18	53	82	161
Remaining events for analysis	744	1,036	1,254	1,634
Shortest duration event	20 min	20 min	20 min	20 min
Longest duration event	58 days	36 days	36 days	22 days

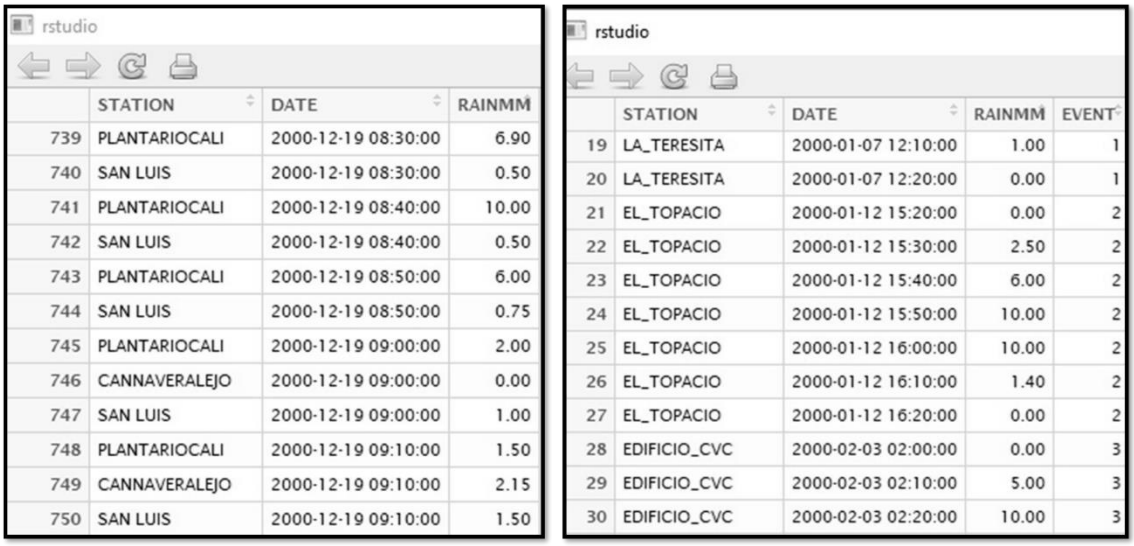

rstudio

	STATION	DATE	RAINMM
739	PLANTARIOCALI	2000-12-19 08:30:00	6.90
740	SAN LUIS	2000-12-19 08:30:00	0.50
741	PLANTARIOCALI	2000-12-19 08:40:00	10.00
742	SAN LUIS	2000-12-19 08:40:00	0.50
743	PLANTARIOCALI	2000-12-19 08:50:00	6.00
744	SAN LUIS	2000-12-19 08:50:00	0.75
745	PLANTARIOCALI	2000-12-19 09:00:00	2.00
746	CANNAVERALEJO	2000-12-19 09:00:00	0.00
747	SAN LUIS	2000-12-19 09:00:00	1.00
748	PLANTARIOCALI	2000-12-19 09:10:00	1.50
749	CANNAVERALEJO	2000-12-19 09:10:00	2.15
750	SAN LUIS	2000-12-19 09:10:00	1.50

rstudio

	STATION	DATE	RAINMM	EVENT
19	LA_TERESITA	2000-01-07 12:10:00	1.00	1
20	LA_TERESITA	2000-01-07 12:20:00	0.00	1
21	EL_TOPACIO	2000-01-12 15:20:00	0.00	2
22	EL_TOPACIO	2000-01-12 15:30:00	2.50	2
23	EL_TOPACIO	2000-01-12 15:40:00	6.00	2
24	EL_TOPACIO	2000-01-12 15:50:00	10.00	2
25	EL_TOPACIO	2000-01-12 16:00:00	10.00	2
26	EL_TOPACIO	2000-01-12 16:10:00	1.40	2
27	EL_TOPACIO	2000-01-12 16:20:00	0.00	2
28	EDIFICIO_CVC	2000-02-03 02:00:00	0.00	3
29	EDIFICIO_CVC	2000-02-03 02:10:00	5.00	3
30	EDIFICIO_CVC	2000-02-03 02:20:00	10.00	3

Figure 3.2: Simultaneous readings from different rainfall stations can occur, as well as zero-rainfall periods within an event (left); each event is separated 24 hours or longer from the others (right).

Impact classification analysis (ICA)

This analysis emphasizes rainfall events occurring on the dates of minor-flood reports, in order to see whether variability in rainfall parameters is related to different types of minor floods in the city (Table 3.3). Here, another methodology to split events was performed: for minor floods reported in press for one day, it is assumed that the rainfall

event causing that minor flood in particular starts at 00:00 hours the day before it is reported in press and ends along with the day of the report (Figure 3.3, above). Sometimes, however, minor floods are in press for up to three days in a row (Table 3.2), in which case the rainfall event ends with the last day of the reports (Figure 3.3, below).

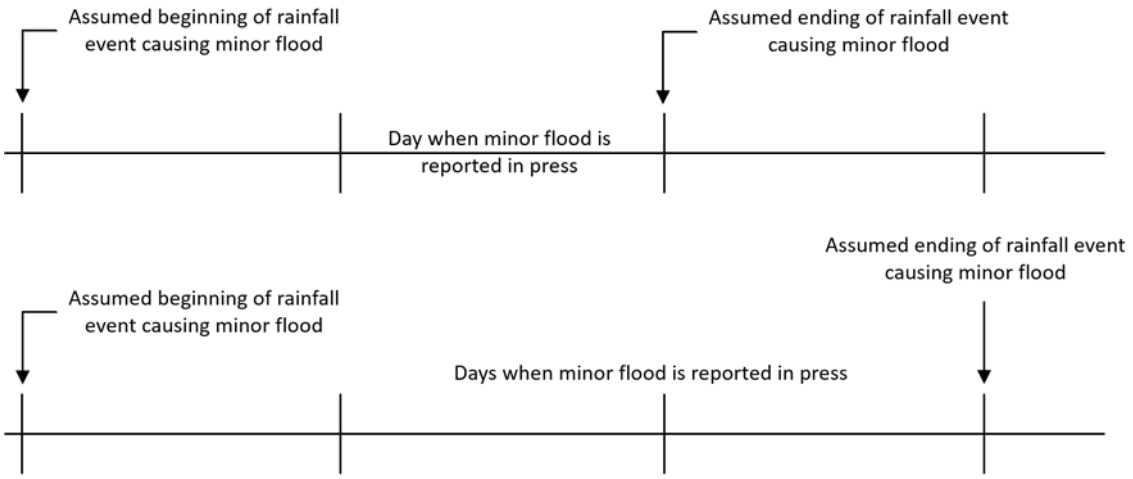

Figure 3.3: Assumed beginning and ending of rainfall events causing minor floods: minor-flood reports that last one day in press (above); whenever the report lasts two or three days (below). Reports do not specify the hour of the day.

3.2.2 Rainfall parameters used for the analysis

There is a generalized need to use statistical methods to determine which rainfall parameters relate better with minor floods in city sub-zones instead of following the traditional approach where empirical rainfall thresholds are based on expert criteria only (Ramos-Cañón et al. 2016). The following parameters were chosen to describe rainfall events. Some of them were based on literature review:

- *Total rainfall* (mm): this is the total amount of rainfall during an event. Total rainfall seems to be strongly correlated with intensity at daily level, but not at sub-daily levels (Cooley and Chang 2017), for which it deserves to be considered separately in this analysis.
- *Maximum intensity* (mm/min): this parameter corresponds to the highest 10-min reading within each rainfall event, divided by 10. Rainfall-runoff models and pollutant wash-off sub-models use rainfall intensity as input rather than flow

rate to achieve better performance and be less affected by coarser time resolutions in data (Manz et al. 2013).

- *Peak position*: this is the position where the maximum intensity value is located within the event, considering every 10-min reading as a position (dimensionless parameter). In case of two or more periods sharing the maximum intensity value, the first one is considered.
- *Peak hour*: this is the round hour of the day when maximum intensity within the event takes place. As with *peak position*, in case of two or more periods sharing *maximum intensity* values, the first one is considered. Hours of the day are expressed as round numbers between 0 and 23.
- *Starting year day*: this is the day of the year when the rainfall event starts, with January 1st as day 1 and December 31st as day 365 (366 for leap year). Seasonal phenomena can be directly associated with the time of year. It can also help to predict which moments of the year are more prone to minor floods.
- *Duration* (min): this parameter accounts for the entire length of the event from the first record to the last one.
- *Rain periods*: rain does not fall continuously along an event, i.e., there are some periods with zero values. In this analysis, there is no limit for the number of interruptions within an event: in an extreme hypothetical example, there could be only three readings in 48 hours, with 23 hours and 50 min of separation in between them, and yet they would be accepted as a single rainfall event. This parameter counts the amount of non-zero 10-min readings within each event as an indicator of the time it actually rained, or the effectiveness of the rainfall.
- *Triangular shape*: this is the ratio between *total rainfall* and the area of a triangle with *duration* as its base and *maximum intensity* as its height. A value of 2 means a perfectly homogeneous rainfall; values close to 1 represent highly triangular hyetographs, while values close to 0 mean abrupt changes in rainfall intensity, concentrating volume in short periods of time (Sofia and Tarolli 2017).
- *Asymmetry*: this is the ratio between the amount of rainfall that has fallen before and after the *maximum intensity* period; values close to 1 imply a symmetry of

the rainfall volumes, while values smaller than 1 imply that the rainfall volume after the burst is higher than the one before (Sofia and Tarolli 2017). In case of two or more periods sharing *maximum intensity*, the first one is taken.

- *Spots*: this is the number of rainfall stations that detect an event. There are events detected by only one station, as well as others detected by all 22. Not all the 22 stations were functioning during all the years of the time frame (2000-2017), so the spatial coverage of rainfall events in those years could have been undervalued by *Spots*. Therefore, every year with fewer stations was weighted by a factor to level it with the other years: this factor is the total number of stations (22) divided by the number of stations functioning in that year, being always greater than one and thus reducing this possible undervaluing.

3.2.3 Demographic and physical attributes per neighborhood

Neighborhood attributes are either collected from street to neighborhood level as in SEL or downscaled from larger resolutions as in aquifer areas. ArcGIS mapping tools were used to extract data for each neighborhood.

All attributes were assumed to remain unaltered overall during the 2000-2017 period: physical features such as topography, aquifer areas and distance to rivers are not expected to change within neighborhood resolution during this time frame, and p*opulation density*, which would be the more reluctant attribute to fit into this assumption because it evidently changes more rapidly in time, only has one value for each neighborhood during all the time frame, based on a census performed at national level in 2005 (previous census had been in 1993, DANE 2010), and even though the Census Bureau emits yearly estimates, these are merely linear projections at neighborhood level. The neighborhood attributes used for this analysis were:

- *Area* (km^2): the shapefile delimiting the neighborhoods is projected over the *MAGNA_Cali_Valle_del_Cauca_2009* coordinate system, and each area is computed with the ArcMap Field Calculator from ArcGIS.
- *Population density* (inhabitants per km^2): this is computed as the ratio of the projected population for each neighborhood in 2017 (the unique value chosen) over the corresponding area of the neighborhood.

- *SEL* (1 to 6): they are calculated per block side based on visible features of residential property (not including drainage infrastructure or public services), immediate surroundings, and landscape context (commercial use, industry, low-density residential, etc.). Then the values of all block sides inside each neighborhood are averaged.
- *Mean elevation* (m): the elevation map for the city of Cali was made by downscaling the 15-meter resolution raster to a 5-meter horizontal resolution and 1-meter vertical resolution raster through the 1-m contour lines, using the ArcMap interpolation tool (Figure 3.4, upper left). The raster file was then calibrated with elevation data from the drainage network manholes. It was actually the produced raster that helped to correct the elevation of four of the manholes that were evidently off due to typos (e.g., 9,790 m instead of 979 m). With *zonal statistics* tool, elevation values of all pixels inside a neighborhood were averaged. This average is the mean elevation of the neighborhood.
- *Distance to river* (m): it is the distance from each neighborhood's centroid to its nearest river, computed with the ArcMap Near tool. For this attribute, all rivers crossing the city were considered (*Aguacatal*, *Cali*, *Cañaveralejo*, *Lili*, *Meléndez*, *Pance*, and *Cauca*), even along those stretches where rivers are channelized and become part of the drainage network (Figure 2.4).
- *Mean slope* (degrees): the elevation raster file previously obtained was converted to a slope file keeping the same 5-meter resolution using the ArcMap slope tool (Figure 3.4, upper right). The range of slope values found in pixels over Cali is 0.0 to 71.06 degrees. The mean slope per neighborhood was computed with the zonal statistics tool by averaging the pixel values.
- *Slope range* (degrees): with the same procedure and data used for *mean slope*, this parameter shows the range of slope values present in each neighborhood as the maximum value minus the minimum value; it is an indicator of topographic heterogeneity. For instance, the neighborhood *Menga* has a mean slope of 13.11°, but it has a slope range of 65.29°, computed as the difference between its highest slope pixel (69.21°) and its lowest slope pixel (3.92°).

- *Aquifer areas*: Recharge, discharge, and sealed areas of the aquifer underneath Cali are shown as polygons (Figure 3.4, below). Some neighborhoods may cover parts of discharge, recharge, and/or sealed areas, so an average must be estimated. Aquifer areas are given values of +1 for recharge, -1 for discharge, and zero for sealed. The parameter may then range between -1 and +1. Average values for each neighborhood were computed with the *zonal statistics* tool.

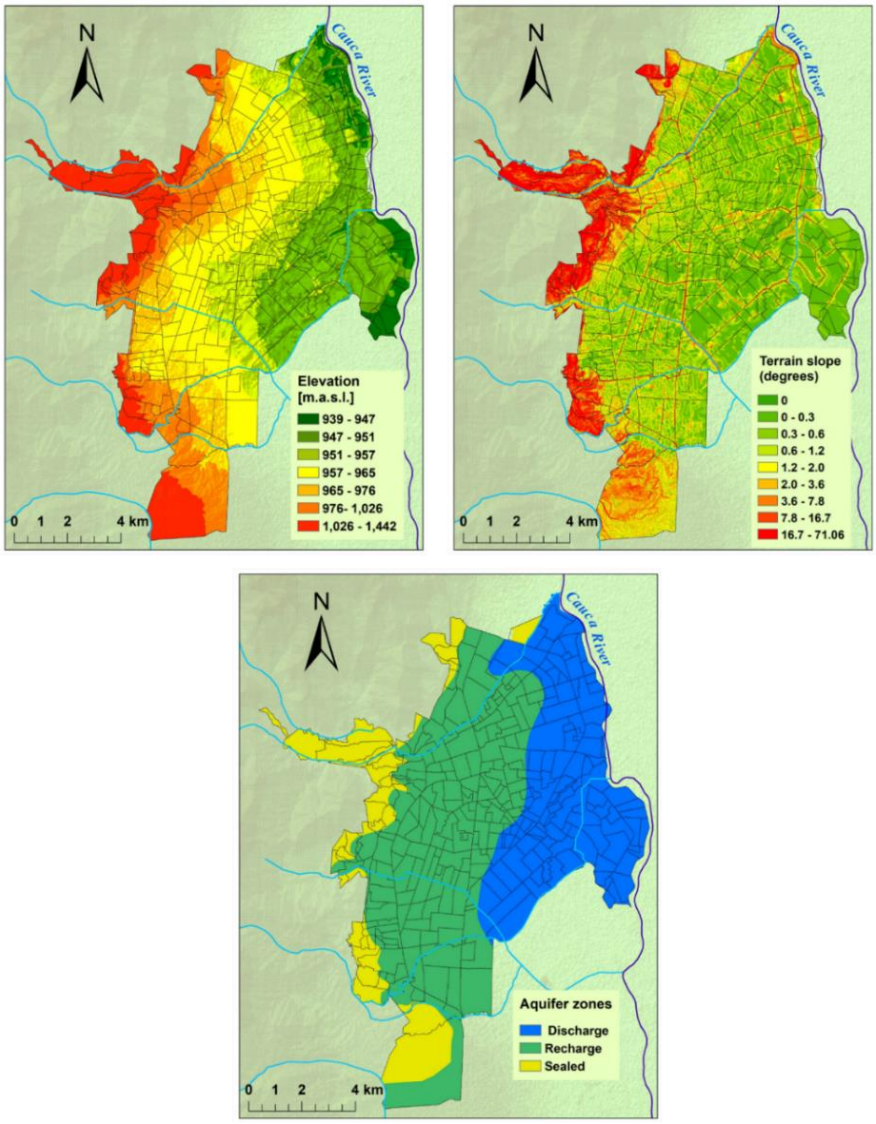

Figure 3.4: Upper left: elevation (m.a.s.l.) for 5-meter resolution pixels. Upper right: terrain slope in 5-meter resolution pixels. Below: aquifer zones for the urban area. Neighborhood boundaries are displayed on each map.

3.2.4 Statistical tests on rainfall parameters for FNFA

Once all FNFA rainfall events had been defined, the next step was to determine which ones coincided in date with minor floods reported; three possibilities arise: one is that there is a coincidence, another is that a rainfall event takes place and no minor floods are reported, and the other is that minor floods are reported when no rainfall event occurs.

The criterion to match rainfall events and minor-flood reports is as follows: if the first day of any minor flood has been reported on the day a rainfall event starts and up to two days after the event ends, then this minor flood is considered as a direct consequence of that rainfall event (one day for the physical consequences to take place in the city and another day for possible delays releasing the reports, Figure 3.5). Matching the dates was manually made on an Excel spreadsheet for the 156 minor-flood events reported.

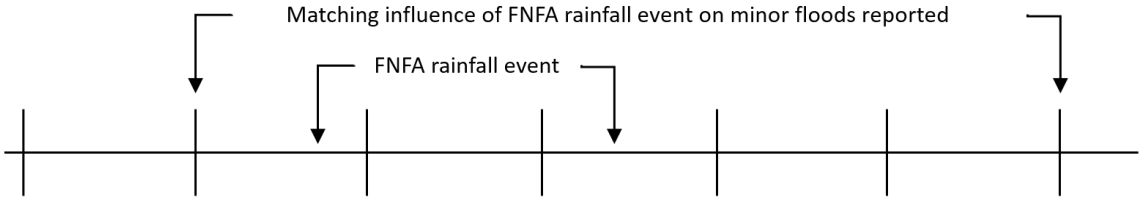

Figure 3.5: A rainfall event can cause minor floods reported before or after, due to time delay for consequences to show, delays on publications of reports, and time resolution of the reports.

Rainfall parameter differences between minor flood and non-minor-flood events

Out of the 744 rainfall events detected, 114 matched dates with minor-flood reports; as for minor-flood reports, 126 of them were matched to rainfall events and 30 were not, that is, there were 30 minor floods that were reported on dates when no rainfall event was registered. Rainfall parameter differences were considered between two samples: those rainfall events related to minor floods (114) and those that were not (630).

Descriptive statistics for each sample was computed using functions *fivenum* and *mean* from R (Table 3.5): *fivenum* summarizes a continuous univariate dataset by

calculating five numbers: minimum, first quartile, median, third quartile, and maximum (RStudio Team 2015); *mean* supplements the summary with the mean value.

Table 3.5: Descriptive statistics for all rainfall parameters, disaggregated between minor flood and non-minor flood events.

Rainfall parameter	min		1st quartile		Median		Mean		3rd quartile		Max	
	Flood	Non	Flood	Non	Flood	Non	Flood	Non	Flood	Non	Flood	Non
Total rainfall [mm]	1.4	1.0	60.2	13.0	120.0	34.7	157.5	56.3	196.2	71.4	1173.1	393.8
Max. intensity [mm/min]	0.03	0.02	1.00	0.44	1.78	0.92	1.84	1.06	2.40	1.49	5.00	5.45
Peak Position [-]	1	1	6	3	36	6	570	114	364	36	7340	5611
Begin Year day [day]	5	2	97	86	127	169	168	176	271	267	356	365
Peak hour [h]	0	0	6	5	14	13	0	0	16	18	23	23
Duration [min]	25.0	20.0	230.1	100.1	1556.0	325.2	7096.0	1627.4	7755.0	1731.1	83893.7	25146.1
Rain periods [-]	2	2	27	8	75	19	444	96	372	65	5025	2543
Triangular shape [-]	0.005	0.004	0.019	0.046	0.118	0.240	0.251	0.423	0.445	0.727	1.288	2.000
Asymmetry [-]	-40.4	-228.0	-1.5	0.3	0.5	0.7	0.003	0.7	1.4	1.4	47.9	336.0
Spots [-]	1.5	1.0	1.8	1.8	4.4	2.9	7.3	5.1	11.0	5.9	22.0	21.0

Visual comparisons between Flood and Non-Flood related samples were made through violin and box plots (Figure 3.6): the upper ends of the distributions for *total*

rainfall, *maximum intensity*, *Peak position*, *duration*, *rain periods* and *spots* were higher for rainfall events related to minor floods; *maximum intensity* actually contains two isolated records from Non-Flood related rainfall events in the highest position, but these did not affect the overall distribution. On the other hand, upper ends from *begin year day*, *triangular shape* and *asymmetry* were higher for non-Flood events.

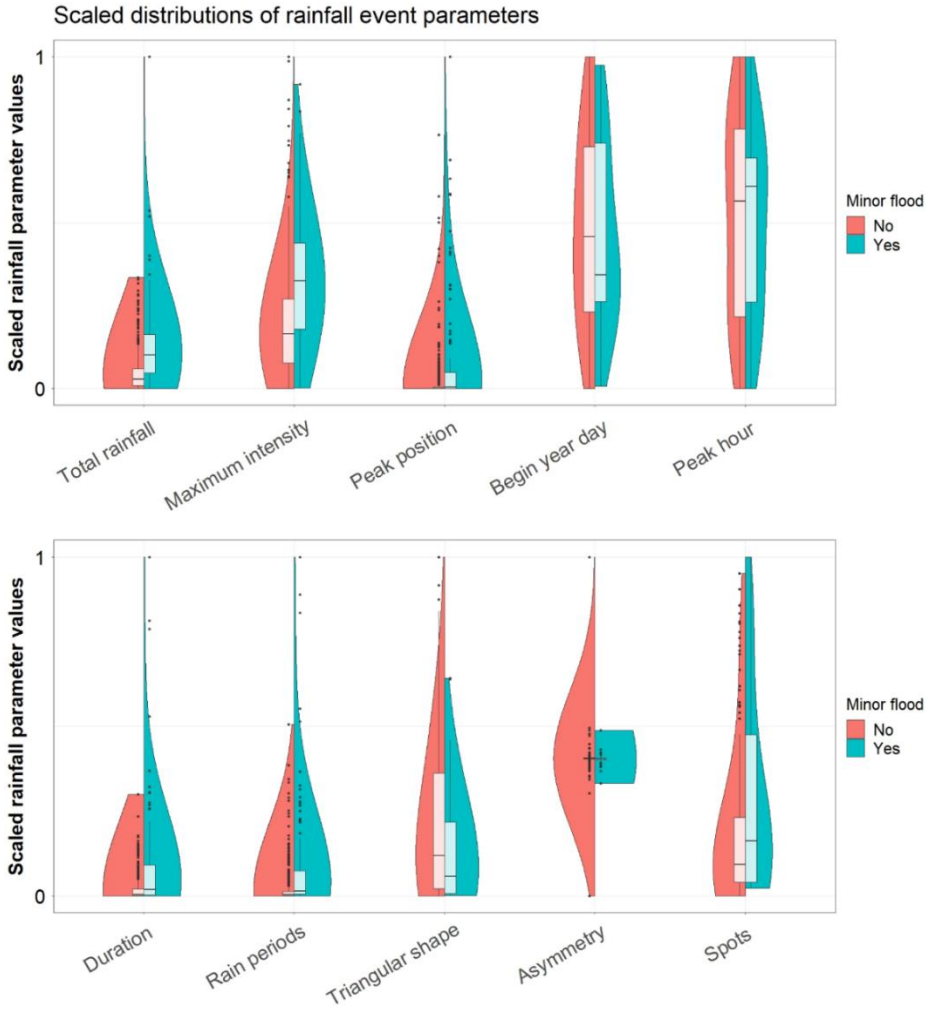

Figure 3.6: Rainfall-parameter data distribution shown in solid colors for minor flood and non-minor-flood events. Light-colored bars represent 1st quartile (bottom), mean (line in between) and 3rd quartile (top) for each rainfall-parameter subset. Dots are individual records. All parameter values were scaled between 0 and 1 to ease overall visual comparison.

Numeric comparisons were also made for FNFA samples, via statistical tests that allowed to identify significant differences and to determine value ranges that might be useful to eventually calibrate an early warning system (Table 3.6).

T-tests were used to compare the means from both samples for each rainfall parameter and to find the difference in means along with its confidence interval with a 0.05 significance level: the function *t.test* from R was used, in which it must be stated whether both samples have the same length or not (paired or not paired) and the significance of the confidence interval (0.95).

F-tests (function *var.test* in R) were also used to detect heteroscedasticity between samples: it means that the variability of a variable (e.g., *maximum intensity* in Flood related events) is not uniform along the range of values of another variable correlated to it (*maximum intensity* in non-Flood related events). Whenever the t-test was significant, and the corresponding F-test was significant as well, a Wilcox test (W-test) was performed to verify the initial t-test results: the W-test is more robust in cases of heteroscedasticity and non-normal distributions. The *wilcox.test* function from R was used, for which an alternative hypothesis must be chosen from "two sided", "greater", and/or "less" (all three were chosen since the difference between means is important regardless of its sign), the confidence level set to 0.95, and a parameter μ that represents the difference between means (zero by default).

Table 3.6: Statistical differences between minor flood and non-minor flood related events. T-tests are verified by W-tests whenever F-test is significant.

Rainfall parameter	F-test	t-test	diff(mean)	CI 0.95	Units	W-test	μ
Total rainfall	p<0.05 *	p<0.05 *	**101.1**	(84.0_118.3)	mm	p<0.05 *	**58.0**
Maximum intensity	p<0.05 *	p<0.05 *	**0.8**	(0.61_0.96)	mm/min	p<0.05 *	**0.6**
Peak Position	p<0.05 *	p<0.05 *	**456**	(328_584)	[-]	p<0.05 *	**7**
Begin Year day	p=0.28	p=0.47	**No diff**	(-28_13)	day	[-]	
Peak hour	p=0.13	p=0.44	**No diff**	(-2_1)	h	[-]	
Duration	p<0.05 *	p<0.05 *	**5468.6**	(4290.8_6645.9)	min	p<0.05 *	**250.2**
Rain periods	p<0.05 *	p<0.05 *	**348**	(266_429)	10 min	p<0.05 *	**23**
Triangular shape	p<0.05 *	p<0.05 *	**-0.172**	(-0.255_-0.088)	[-]	p<0.05 *	**-0.026**
Asymmetry	p<0.05 *	p=0.65	**No diff**	(-3.96_2.47)	[-]	[-]	
Spots	p<0.05 *	p<0.05 *	**2.2**	(1.2_3.3)	[-]	p<0.05 *	**0.4**

* significant result (<0.05)

Rainfall parameters as predictors of minor floods

How well can rainfall parameters alone or all together predict whether a rainfall event in particular will cause minor floods or not? A binary variable called 'Flood' takes a value of 1 for minor flood-related rainfall events and zero otherwise. As it was stated before, there were 114 rainfall events related to minor floods (Flood=1) and 630 events that were not (Flood=0).

Since the variable 'Flood' is categorical, the most suitable generalized linear model (GLM) to predict it is the binary logistic regression. In binary logistic regression, the predictors or independent variables can be categorical and/or continuous; in this case, each of the rainfall parameters were continuous; R function *glm* was used, under the option *binomial family* (Friedman 2010). Results from this function include the estimate from the independent variable and its corresponding p-value ($p<0.05$ is considered significant).

The odds ratio of an independent variable represents the increase in its chance of success "p" of the dependent variable (a rainfall event being related to a minor flood) as the independent variable moves up one unit. This increase is measured from 1.0, that is, an odds ratio of 1.0 means no increase, while an odds ratio of 1.5 means an increase of 50% in success chances as the independent variable moves up one unit. The odds ratio shows how influential an independent variable is over the dependent variable; in the binary logistic regression, the estimate is equal to the logarithm of the odds ratio (equation 3.1).

$$Odds\ ratio = \frac{\mathrm{p}}{\mathrm{1\text{-}p}} = \mathrm{e}^{\mathrm{estimate}} \qquad 3.1$$

This chance, however, increases differently depending on the initial value of the parameter: for instance, the effect of increasing rainfall intensity from 1 to 2 mm/min is different than if it went from 10 to 11 mm/min. The logistic regression estimates rather an average odds ratio along the complete range of values. Sometimes changing the units of a variable may take odds ratio away from 1.0 and make it easier to interpret: when total rainfall is converted from millimeters to inches, the odds ratio

increases from 1.010 to 1.308, that is, an extra inch in rainfall increases the chances of a minor flood by 30.83% (Table 3.7). The significance of the parameter, however, remains the same regardless of the change in units.

Table 3.7: Results from each rainfall parameter predicting binary variable 'Flood' (logistic regression). Shaded parameters were not significant.

	Binary Logistic regression		
Parameter	**Odds ratio**	**Estimate**	**p**
Total rainfall [mm]	1.0107	0.0106	<0.05 *
Total rainfall [in]	1.3083	0.2679	<0.05 *
Max. intensity [mm/min]	2.2547	0.8137	<0.05 *
Peak Position [-]	1.0007	0.0007	<0.05 *
Begin Year day [day]	0.9993	-0.0007	0.46
Peak hour [h]	0.9885	-0.0114	0.43
Duration [min]	1.0002	0.0002	<0.05 *
Duration [h]	1.0089	0.0089	<0.05 *
Rain periods [-]	1.0016	0.0016	<0.05 *
Triangular shape [-]	0.3041	-1.2065	<0.05 *
Asymmetry [-]	0.4777	-0.0033	0.645
Spots [-]	1.0675	0.0653	<0.05 *

* significant result (<0.05)

Rainfall parameters can also predict variable 'Flood' in a joint manner (Table 3.8). A joint logistic regression is performed in this case using R function *glm* again, under the same binomial logistic option. GLM do not have an R^2 coefficient as Ordinary Lineal Models do; however, there are some Pseudo-R^2 coefficients available for GLM, such as Cox-Snell and Nagelkerke (Lumley 2017), which use the maximized likelihood values available in logistic regressions to indicate the proportional reduction in squared prediction error from using the model prediction instead of the mean (the same purpose of a regular R^2). For this analysis, Nagelkerke Pseudo-R^2 was chosen because it is rescaled for binary variables (taking values between 0 and 1) such as 'Flood'. Function *Nagelkerke* from R Studio is used for computations.

Table 3.8: All rainfall parameters predicting 'Flood' (joint logistic regression).

Joint logistic regression			
	Number of observations		744
	Pseudo R2		0.262
Parameter	**Odds Ratio**	**Estimate**	**p**
Total rainfall [mm]	1.0056	0.0056	<0.05
Max. intensity [mm/min]	1.6182	0.4813	<0.05
Peak Position [-]	1.0003	0.0003	0.15
Begin Year day [day]	0.9987	-0.0013	0.24
Peak hour [h]	0.9949	-0.0051	0.76
Duration [min]	1.0000	0.00004	0.17
Rain periods [-]	1.0006	0.0006	0.25
Triangular shape [-]	0.5894	-0.5286	0.17
Asymmetry [-]	1.0028	0.0028	0.66
Spots [-]	0.9153	-0.0885	<0.05
Constant	0.1066	-2.2390	<0.05

Stepwise regression determines whether some independent variables can be removed from the overall model without lowering its prediction capabilities: variables are removed one at a time from the original model, then placed one at a time from scratch, to check if there is a better combination than the current model; the process is repeated until there is no further improvement. Function *stepAIC* from R was used for stepwise regression. Results from stepwise regression performed on the joint logistic regression for 'Flood' (Table 3.8) are shown in Table 3.9.

Table 3.9: Stepwise estimation to predict variable 'Flood' (joint logistic regression). Shaded parameters were removed in the process.

Stepwise regression on Joint logistic regression			
	Number of observations		744
	Pseudo R2		0.251
Parameter	**Odds Ratio**	**Estimate**	**p**
Total rainfall [mm]	1.0062	0.0062	<0.05
Max. intensity [mm/min]	1.5613	0.4455	<0.05
Peak Position [-]	1.0004	0.0004	0.06
Begin Year day [day]			
Peak hour [h]			
Duration [min]	1.0001	0.0001	<0.05
Rain periods [-]			
Triangular shape [-]			
Asymmetry [-]			
Spots [-]	0.9482	-0.0532	<0.05
Constant	0.0566	-2.8720	<0.05

Some rainfall parameters had odds ratio values very close to 1 (Table 3.8) and might be easier to interpret if their units are changed. With *total rainfall* in inches instead of millimeters, and *peak position* and *duration* in hours, joint logistic regression was run again along with its corresponding *stepwise* estimation (Table 3.10 and Table 3.11). Once again, changing the units of a variable does not change its significance.

Table 3.10: Results for all rainfall parameters predicting variable 'Flood' (joint logistic regression) after changing units for *total rainfall*, *peak position,* and *duration.*

Joint logistic regression			
	Number of observations		744
	Pseudo R2		0.262
Parameter	**Odds Ratio**	**Estimate**	**p**
Total rainfall [in]	1.1542	0.1434	<0.05
Max. intensity [mm/min]	1.6182	0.4813	<0.05
Peak Position x6 [-]	1.0019	0.0019	0.15
Begin Year day [day]	0.9987	-0.0013	0.24
Peak hour [h]	0.9949	-0.0051	0.76
Duration [h]	1.0024	0.0024	0.17
Rain periods [-]	1.0006	0.0006	0.25
Triangular shape [-]	0.5894	-0.5286	0.17
Asymmetry [-]	1.0028	0.0028	0.66
Spots [-]	0.9153	-0.0885	<0.05
Constant	0.1065	-2.2392	<0.05

Table 3.11: Stepwise estimation to predict variable 'Flood' (joint logistic regression), after changing units for *total rainfall*, *peak position*, and *duration*. Shaded parameters were removed in the process.

Stepwise regression on Joint logistic regression			
	Number of observations		744
	Pseudo R2		0.251
Parameter	**Odds Ratio**	**Estimate**	**p**
Total rainfall [in]	1.1698	0.1568	<0.05
Max. intensity [mm/min]	1.5611	0.4454	<0.05
Peak Position x6 [-]	1.0023	0.0023	0.06
Begin Year day [day]			
Peak hour [h]			
Duration [h]	1.0037	0.0037	<0.05
Rain periods [-]			
Triangular shape [-]			
Asymmetry [-]			
Spots [-]	0.9482	-0.0532	0.07
Constant	0.0566	-2.8723	<0.05

Rainfall parameters as predictors of number of neighborhoods affected by minor floods

While the categorical variable 'Flood' indicates whether a rainfall event coincides or not with a minor flood, the variable 'Occurrences' counts how many neighborhoods were reported as affected for every minor flood. Not all 156 minor flood reports were suitable for this part of the analysis: only those with at least neighborhood accuracy in their descriptions were considered (122 reports, Table 3.12). However, from these 122 events, there were 25 that did not coincide with any rainfall event at all; these events were also not considered for the analysis, leaving 98 events to work with.

In each of the 98 reports, the neighborhoods affected were identified and counted; and the number entered in the variable 'Occurrences' for each of the 92 rainfall events coinciding with the 98 reports. There are fewer rainfall events than reports because the length of some of the rainfall events covered several individual reports.

Since 'Occurrences' is a counting variable that takes values from 1 to 34, a Poisson regression is ideal to fit this dependent variable with the usual rainfall parameters as independent variables. Poisson regression belongs to the GLM family and is used to predict count variables (positive integer numbers), such as neighborhoods affected.

Poisson regression is performed through *glm* function in R, under the *poisson* option. Each rainfall parameter alone was taken as a predictor first (Table 3.13), and then all parameters were used together in a joint Poisson regression (Table 3.14). This time, McFadden Pseudo-R^2 was chosen to measure the goodness of fit for Poisson regression instead of the previous Nagelkerke's for three reasons: first, because Nagelkerke's is rescaled for Bernoulli or binary variables (Lumley 2017), second, because due to the high intercept weight on the model (Constant estimate and odds ratio in Table 3.14), it is better to compare the intercept-only model with the full estimated model than the null model with the full model, which is what McFadden does (RStudio Team 2015), and third, because the McFadden test is the most widely used measure for goodness of fit for discrete models (Mokhtarian 2016).

Table 3.12: Minor floods with neighborhood (N) accuracy (122 events with original ID sequence from Table 3.2). Shaded reports do not coincide with rainfall events (25). Reports in bold share the rainfall event with the previous report (6) and were discarded (92 events left). 'Count' shows number of neighborhoods affected; press refers to days in press.

ID	Start date	Press	Accuracy	Count	ID	Start date	Press	Accuracy	Count	ID	Start date	Press	Accuracy	Count
1	31-Jan-2000	1	N, Z		46	7-May-2006	1	N, S	6	97	14-Oct-2011	1	N	7
2	4-May-2000	1	N, Z	21	48	7-Nov-2006	1	N, S		98	6-Nov-2011	3	N, Z	8
3	20-Jul-2000	1	N, S, Z	5	49	24-Nov-2006	1	N	3	99	12-Nov-2011	1	N	2
4	5-Sep-2000	2	N, S, Z	14	50	12-Dec-2006	1	N, S	4	100	16-Dec-2011	1	N	1
5	7-Jan-2001	1	N, S		51	20-Jan-2007	1	N	2	101	8-Feb-2012	2	N, Z	3
6	22-Jan-2001	1	N, S, Z	3	52	27-Mar-2007	1	N, S		102	21-Mar-2012	1	N	6
7	21-Feb-2001	1	N, S, Z	3	54	16-Apr-2007	1	N, S, Z	5	103	25-Mar-2012	2	N, Z	9
8	22-Mar-2001	1	N, Z	13	55	18-May-2007	1	N, S	2	104	10-Apr-2012	1	N	2
9	16-Apr-2001	1	N, S		56	25-May-2007	1	N	4	105	18-Apr-2012	1	N, S, Z	3
10	13-Jul-2001	1	N, S, Z		**57**	**27-May-2007**	**1**	**N, S**	**1**	106	28-Apr-2012	1	N, S	3
11	13-Sep-2001	1	N, S	1	59	1-Nov-2007	1	N		107	1-May-2012	1	N, S	1
12	29-Sep-2001	1	N	1	60	20-Dec-2007	1	N		108	5-May-2012	1	N, Z	5
14	14-Nov-2001	1	N, S, Z		61	18-Feb-2008	2	N, S		**109**	**7-May-2012**	**2**	**N, S**	**2**
15	13-Dec-2001	1	N, S	15	62	25-Apr-2008	1	N,S	4	110	25-Jun-2012	1	N, Z	
16	2-Apr-2002	1	N, S	4	64	1-May-2008	1	N, S	3	113	23-Apr-2013	1	N, S, Z	4
17	8-Apr-2002	1	N, Z	3	65	11-Jun-2008	1	N, Z		114	29-Apr-2013	1	N, S, Z	12
19	22-Apr-2002	1	N		66	24-Jun-2008	1	N		115	21-May-2013	1	N, S, Z	1
20	21-May-2002	1	N, Z	13	67	3-Jul-2008	1	N, S, Z	4	116	27-May-2013	1	N, S, Z	
22	24-Oct-2002	1	N, S, Z	6	68	8-Jul-2008	1	N, S	3	117	11-Aug-2013	1	N, S, Z	14
23	25-Apr-2003	1	N, S, Z	9	69	4-Oct-2008	1	N	1	118	16-Sep-2013	1	N, S, Z	1
24	12-May-2003	1	N	2	70	20-Nov-2008	3	N, S		121	23-Dec-2013	1	N, S, Z	17
25	5-Oct-2003	1	N, S, Z	10	71	26-Nov-2008	2	N, S	3	122	12-Mar-2014	1	N, S	18
26	13-Oct-2003	1	N	2	72	7-Mar-2009	1	N	5	123	16-Apr-2014	1	N	5
27	7-Jan-2004	1	N, S, Z	5	73	9-Mar-2009	1	N	1	124	28-Apr-2014	1	N	3
28	26-Mar-2004	1	N, Z		74	19-Mar-2009	2	N, S, Z		125	20-May-2014	1	N, S	6
29	3-May-2004	1	N, Z	7	79	3-May-2010	3	N, S	12	126	7-Jun-2014	1	N, Z	16
30	12-May-2004	1	N, S, Z		80	31-May-2010	1	N, S	2	129	20-Oct-2014	1	N, S, Z	17
31	27-Oct-2004	1	N	3	81	1-Sep-2010	1	N	8	**130**	**26-Nov-2014**	**1**	**N, S**	**8**
32	29-Mar-2005	1	N	1	82	28-Oct-2010	1	N, S, Z	3	132	30-Mar-2015	1	N, S, Z	21
33	21-May-2005	1	N, S	4	83	4-Nov-2010	1	N	1	133	6-May-2015	1	N, S	17
34	2-Jul-2005	1	N	2	85	22-Nov-2010	1	N	1	134	1-Nov-2015	1	N, S	2
35	24-Jul-2005	1	N, S		**86**	**25-Nov-2010**	**1**	**N**	**2**	141	28-May-2016	1	N	5
36	28-Sep-2005	1	N, S, Z	2	87	25-Feb-2011	1	N		142	13-Jun-2016	1	N, S	13
37	14-Dec-2005	1	N	1	88	6-Apr-2011	1	N, S, Z	10	144	30-Sep-2016	1	N, Z	8
39	17-Mar-2006	1	N, S	3	**89**	**22-Apr-2011**	**2**	**N**	**14**	147	1-Dec-2016	1	N, S	10
40	21-Mar-2006	1	N		90	25-Apr-2011	1	N, S, Z	5	149	10-Mar-2017	1	N, S, Z	13
41	24-Mar-2006	2	N	3	91	5-May-2011	1	N	1	152	14-Apr-2017	1	N, S	3
42	1-Apr-2006	1	N, S		92	8-May-2011	1	N, S, Z	5	153	18-Apr-2017	1	N, S, Z	8
43	12-Apr-2006	1	N, Z		94	1-Jul-2011	1	N, S, Z	8	154	26-Apr-2017	1	N, Z	3
44	14-Apr-2006	1	N, S		95	6-Jul-2011	1	N	5	155	30-Apr-2017	1	N, S, Z	34
45	1-May-2006	2	N, S	1	96	6-Sep-2011	1	N	1	**156**	**6-May-2017**	**3**	**N**	**6**

Table 3.13: Results for each rainfall parameter predicting variable 'Occurrences' (Poisson regression). *Total rainfall* and *duration* are in two different units. Shaded parameters are not significant.

	Poisson regression		
Parameter	**Odds ratio**	**Estimate**	**p**
Total rainfall [mm]	1.0017	0.0017	<0.05 *
Total rainfall [in]	1.0453	0.0443	<0.05 *
Max. intensity [mm/min]	1.2896	0.2543	<0.05 *
Peak Position [-]	1.0002	0.0002	<0.05 *
Peak Position x6 [-]	1.0012	0.0012	<0.05 *
Begin Year day [day]	0.9993	-0.0007	0.09
Peak hour [h]	1.0023	0.0023	0.72
Duration [min]	1.0000	0.00002	<0.05 *
Duration [h]	1.0012	0.0012	<0.05 *
Rain periods [-]	1.0003	0.0003	<0.05 *
Triangular shape [-]	0.4787	-0.7366	<0.05 *
Asymmetry [-]	0.9753	-0.0250	<0.05 *
Spots [-]	1.0675	0.0653	<0.05 *

* significant result (<0.05)

Table 3.14: Results for all rainfall parameters predicting variable 'Occurrences' (joint Poisson regression), and stepwise estimation to optimize regression model.

Joint Poisson regression				**Stepwise regression**		
	Number of observations		92	Number of observations		92
	Pseudo R2		0.196	Pseudo R2		0.193
Parameter	**Odds Ratio**	**Estimate**	**p**	**Odds Ratio**	**Estimate**	**p**
Total rainfall [in]	1.0185	0.0183	0.08	1.0203	0.0201	<0.05
Max. intensity [mm/min]	1.0031	0.0030	0.96			
Peak Position x6 [-]	1.0000	0.0000	0.35			
Begin Year day [day]	0.9990	-0.0010	<0.05	0.9989	-0.0011	<0.05
Peak hour [h]	0.9948	-0.0052	0.46			
Duration [h]	1.0000	0.0000	0.92			
Rain periods [-]	1.0001	0.0001	<0.05	1.0001	0.0001	0.07
Triangular shape [-]	1.1666	0.1541	0.39			
Asymmetry [-]	0.9918	-0.0082	0.14			
Spots [-]	1.0445	0.0435	<0.05	1.0362	0.0356	<0.05
Constant	4.6739	1.5420	<0.05	4.8163	1.5720	<0.05

3.2.5 Statistical tests on neighborhood attributes

Unlike rainfall parameters that change their values with every rainfall event, neighborhood attributes were assumed constant during the analysis time frame (2000-2017). The official neighborhoods in Cali in 2000 were exactly the same in 2017, keeping

their areal extent; population and population density, however, most likely grew in 17 years. Therefore, since the most recent data of population was taken (2017), this study is probably overrating vulnerability in the early years, when population was lower.

Population density does not vary in time within a neighborhood (time series analysis), but across neighborhoods (variation in space). Hence, these attributes cannot predict whether a rainfall event will cause minor floods or not because they hold the same values for both scenarios. However, they could predict which neighborhoods are more vulnerable to receive minor floods, and for that, neighborhood attributes act as independent variables that predict the variable 'Events', which contains the total number of minor floods registered in each one of the 336 neighborhoods in the city.

Neighborhood attributes as predictors of number of minor floods registered per neighborhood

A Poisson regression is appropriate to predict the total number of minor floods per neighborhood because 'Events' is a countable or discrete variable. Within the independent variables (neighborhood attributes), the only categorical one is the *socioeconomic level* (SEL); the comparison within SEL categories means SEL 2 to 6 categories were compared to SEL 1 (Table 3.15).

Table 3.15: Neighborhood attributes predicting variable 'Events' (joint Poisson regression). Shaded attributes are not significant.

Joint Poisson regression			
	Number of observations		336
	Pseudo R2		0.060
Parameter	**Odds ratio**	**Estimate**	**p**
SEL 2	0.9505	-0.0508	0.75
SEL 3	0.9585	-0.0424	0.81
SEL 4	1.8190	0.5983	<0.05
SEL 5	1.6795	0.5185	<0.05
SEL 6	1.5142	0.4149	0.08
elevation [masl]	1.0013	0.0013	0.5
distance to river [m]	0.9998	-0.0002	<0.05
mean slope [°]	0.9612	-0.0396	0.08
slope range [°]	1.0159	0.0158	<0.05
Population density [hab/km]	1.0011	0.0011	<0.05
Acquifer dummy [-]	1.0763	0.0735	0.24
Constant	0.3201	-1.1390	0.54

Units were changed for some of the attributes to take their odds ratio values away from 1.0: *distance to river* is now expressed in hundreds of meters; *mean slope* and *slope range* in tens of degrees, and *density of population* in hundreds of inhabitants per hectare. Poisson regression was again performed (Table 3.16). Changing the units of the variables does not affect their individual significance in the model nor the overall model predictive capacity. It only makes odds ratios easier to interpret.

Table 3.16: Neighborhood attributes predicting variable 'Events' (joint Poisson regression) with transformed units. Shaded attributes are not significant.

Joint Poisson regression			
		Number of observations	336
		Pseudo R2	0.060
Parameter	**Odds ratio**	**Estimate**	**p**
SEL 2	0.9505	-0.0508	0.75
SEL 3	0.9585	-0.0424	0.81
SEL 4	1.8190	0.5983	<0.05
SEL 5	1.6795	0.5185	<0.05
SEL 6	1.5142	0.4149	0.08
elevation [masl]	1.0013	0.0013	0.5
distance to river [100m]	0.9792	-0.0210	<0.05
mean slope [10°]	0.6728	-0.3964	0.08
slope range [10°]	1.1711	0.1579	<0.05
Population density [100hab/ha]	1.1115	0.1057	<0.05
Acquifer dummy [-]	1.0763	0.0735	0.24
Constant	0.3201	-1.1390	0.54

Predictive margins of minor floods by neighborhood attributes

Interpretating regression tables can be very challenging in the presence of categorical variables (Jann 2013). Predictive margins are a graphic and more understandable way to see the effects of independent variables (and categories within) on the dependent variable. With predictive margins, the independent variable of interest can be analyzed while the others remain fixed at their average values (Williams 2012).

Some helpful commands in Stata software were used to display the predictive margins of the statistically significant neighborhood attributes on the variable 'Event' (StataCorp LP 2015; Figure 3.7); Stata is a statistical package for managing, analyzing, and graphing data; it makes predictive margin calculations easily and directly with the command *margins*, and subsequently plots with the *marginsplot* command.

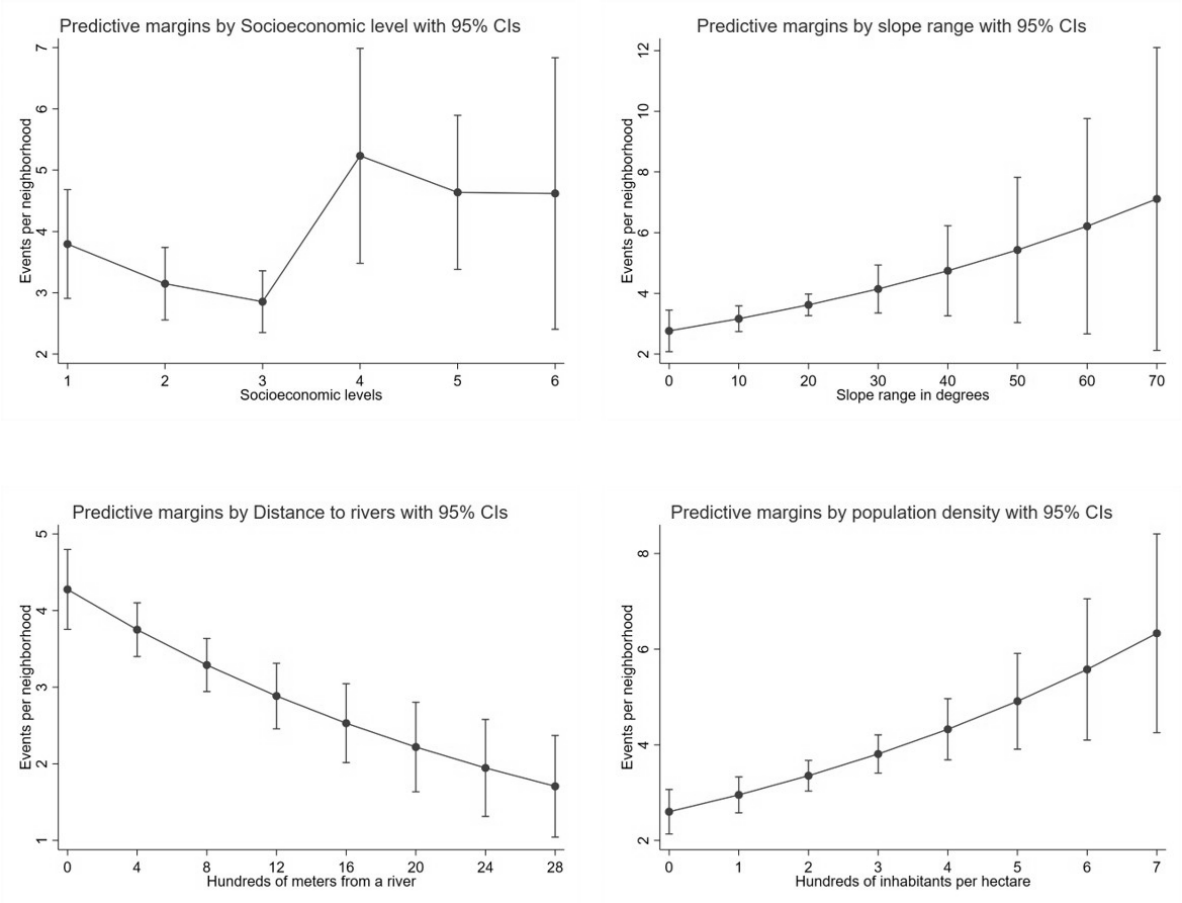

Figure 3.7: Predictive margins on dependent variable 'Events' by each statistically significant neighborhood attribute in Poisson regression (SEL, *slope range*, *distance to river*, and *population density*).

Interactions between SEL and significant attributes

Sometimes interactions between a categorical variable and a continuous variable show inner opposite trends among categories that do not arise in the overall regression. For example, *population density* has an overall positive relation to number of minor floods registered per neighborhood, but if the same analysis is made discretizing by SEL, then there could be negative trends for some of these SEL. A Poisson regression was performed including interactions between SEL (categorical variable) and the significant attributes (*distance to rivers*, *slope range*, and *population density*; Table 3.17).

Table 3.17: Results of statistically significant neighborhood attributes and their interactions with SEL predicting variable 'Events' (joint Poisson regression).

Joint Poisson regression			
	Number of observations		336
	Pseudo R2		0.084
Parameter	**Odds ratio**	**Estimate**	**p**
SEL 2	1.1709	0.1578	0.73
SEL 3	1.8932	0.6383	0.15
SEL 4	3.0160	1.1039	<0.05
SEL 5	2.7445	1.0096	<0.05
SEL 6	1.5614	0.4456	0.61
distance to river [100m]*SEL1	0.9407	-0.0611	0.08
distance to river [100m]*SEL2	0.9564	-0.0446	<0.05
distance to river [100m]*SEL3	0.9772	-0.0230	<0.05
distance to river [100m]*SEL4	1.0319	0.0314	0.07
distance to river [100m]*SEL5	1.0023	0.0023	0.92
distance to river [100m]*SEL6	0.8717	-0.1373	<0.05
slope range [10°]*SEL1	1.1264	0.1190	<0.05
slope range [10°]*SEL2	1.0613	0.0595	0.44
slope range [10°]*SEL3	1.1581	0.1468	0.07
slope range [10°]*SEL4	0.9561	-0.0449	0.62
slope range [10°]*SEL5	1.0253	0.0250	0.75
slope range [10°]*SEL6	1.4219	0.3520	0.11
Population density [100hab/ha]*SEL1	1.1873	0.1717	<0.05
Population density [100hab/ha]*SEL2	1.1978	0.1805	<0.05
Population density [100hab/ha]*SEL3	0.9508	-0.0504	0.41
Population density [100hab/ha]*SEL4	0.9773	-0.0230	0.86
Population density [100hab/ha]*SEL5	1.1388	0.1299	0.48
Population density [100hab/ha]*SEL6	0.4261	-0.8530	<0.05
Constant	0.8316	-0.1844	0.61

The interactions compare SEL 2 through SEL 6 with SEL 1. Neighborhoods with SEL 4 and 5 have a significantly higher susceptibility to be affected by minor floods than neighborhoods with SEL 1, while neighborhoods with SEL 2, 3, and 5 are not significantly more susceptible than SEL 1.

Only neighborhoods with SEL 1 are significantly susceptible to get more minor floods as their slope range increases; neighborhoods with SEL 1 and 2 are significantly more susceptible to minor floods as population density increases, while neighborhoods with SEL 6 are more susceptible as population density decreases (Figure 3.8).

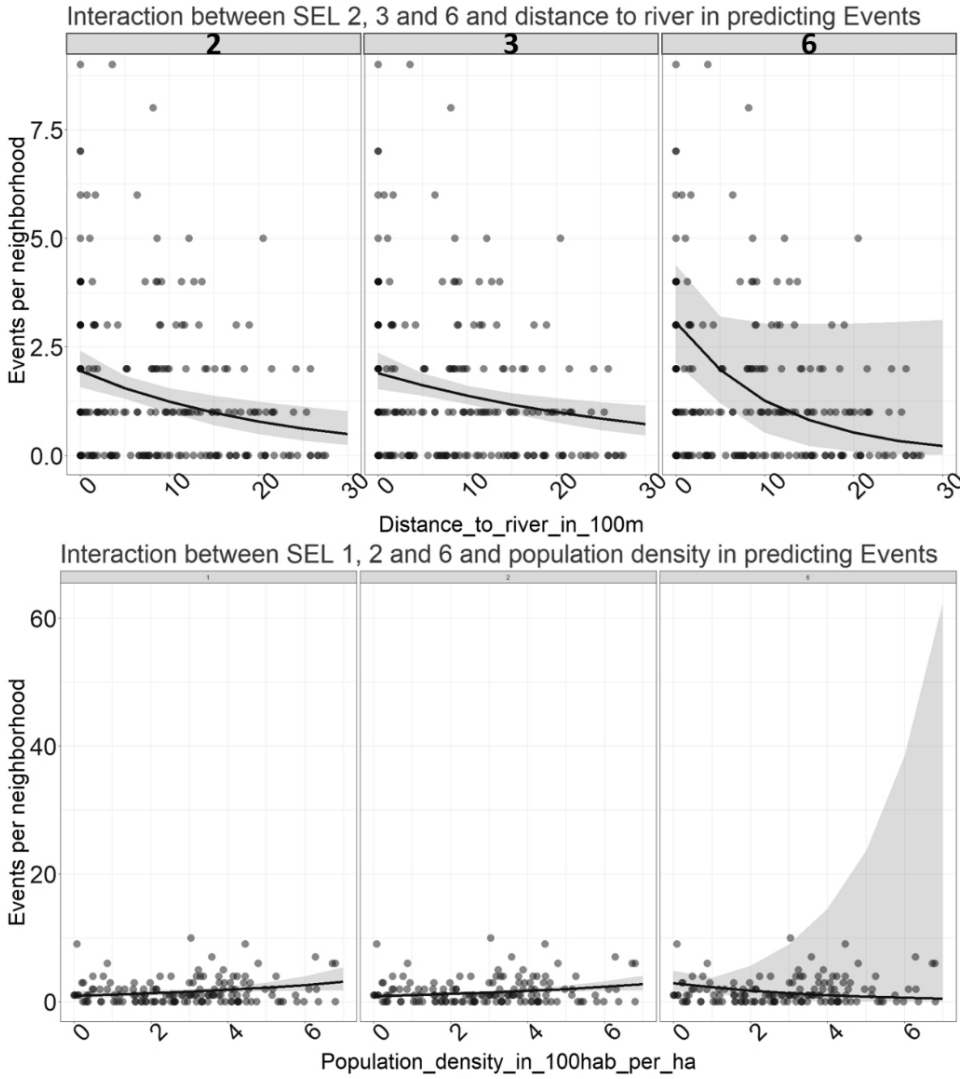

Figure 3.8: Interactions between SEL and *distance to rivers* and between SEL and *population density* to explain number of minor floods per neighborhood. Shaded surface represents the confidence interval for the events.

3.2.6 Rainfall parameters predicting types of minor floods

Rainfall events causing minor floods may also indicate what type of minor floods are triggered in the city (Table 3.3). Rainfall parameters from rainfall events split with ICA methodology (see section 3.2.1) were used as independent variables to explain the type of minor flood reported: these types of minor floods or dependent variables are dummy variables taking the value of 1 when they happen and 0 when they do not (Table 3.18). Out of the original 156 minor flood reports, 94 were used for this analysis (Table 3.21): the others were discarded for having no rainfall data in their ICA rainfall events.

Table 3.18: Types of minor floods expressed as dummy variables: DMW (deaths, missing, wounded), HDA (homes destroyed/affected), EHC (education/health centers), TCA (traffic congestion/accidents), SEW (sewer blockage), POW (power cuts), TREE (trees fallen), and RIV (rivers overflown).

Start date	DMW	HDA	EHC	TCA	SEW	POW	TREE	RIV
4-May-2000	0	1	0	1	1	1	0	1
20-Jul-2000	0	0	0	1	0	0	1	0
5-Sep-2000	1	0	0	1	1	1	1	1
22-Jan-2001	0	1	0	1	0	0	0	0
21-Feb-2001	0	0	0	1	1	0	0	0
22-Mar-2001	0	1	0	1	0	0	0	1
13-Sep-2001	0	0	0	0	0	1	0	0
29-Sep-2001	0	1	0	0	1	0	0	0
13-Dec-2001	1	1	1	1	0	0	0	0
2-Apr-2002	0	1	0	0	0	0	0	1

For the prediction, binomial logistic regression was used since dummy variables are categorical and binary. Each dummy variable was left as a dependent variable explained by all rainfall parameters (Table 3.19). R function *glm* was used.

Table 3.19: Rainfall parameters explaining types of minor floods. Estimate value is displayed along with its significance in parenthesis. DMW, EHC, SEW and POW were not significantly explained by any parameter. Shaded parameters did not significantly predict any type of minor flood. Pseudo R^2 is Nagelkerke.

Binary Logistic regression

	Impacts			
Parameter	**HDA**	**TCA**	**TREE**	**RIV**
Total rainfall [mm]	0.012 (p=0.07)			
Max. intensity [mm/min]				
Peak Position [-]				
Begin Year day [day]		-0.005 (p=0.05)		
Peak hour [h]			0.113 (p<0.05)*	
Duration [min]				
Rain periods [-]				
Triangular shape [-]		-2.745 (p=0.08)		
Asymmetry [-]				-0.129 (p=0.09)
Spots [-]				-0.311 (p=0.08)
Pseudo R2	0.1110	0.1910	0.1390	0.2550

* significant result (<0.05)

In this analysis, some dummy variables were correlated to others if the combination made sense (Table 3.20): for instance, POW explained by TREE, since it is common that fallen trees cut power lines and lead to power cuts; or EHC explained by POW, as power cuts make these facilities stop working partially or totally.

Table 3.20: Dummy variables explained by one another. Shaded combinations have no significant correlation.

Binary Logistic regression				
Variable				
Dependent	explained by	Estimate	Odds ratio	p
POW	TREE	2.24	9.39	<0.05
SEW	RIV	0.67	1.96	0.31
DMW	RIV	0.75	2.13	0.26
EHC	POW	1.87	6.46	<0.05
TCA	TREE	1.82	6.18	<0.05

Table 3.21: Reports of minor floods selected for ICA (94 reports with original ID sequence from Table 3.2).

ID	Start date	ID	Start date	ID	Start date	ID	Start date	ID	Start date
2	4-May-2000	31	27-Oct-2004	69	4-Oct-2008	98	6-Nov-2011	124	28-Apr-2014
3	20-Jul-2000	32	29-Mar-2005	71	26-Nov-2008	99	12-Nov-2011	125	20-May-2014
4	5-Sep-2000	33	21-May-2005	72	7-Mar-2009	100	16-Dec-2011	126	7-Jun-2014
6	22-Jan-2001	34	2-Jul-2005	73	9-Mar-2009	101	8-Feb-2012	129	20-Oct-2014
7	21-Feb-2001	37	14-Dec-2005	79	3-May-2010	102	21-Mar-2012	130	26-Nov-2014
8	22-Mar-2001	39	17-Mar-2006	80	31-May-2010	103	25-Mar-2012	132	30-Mar-2015
11	13-Sep-2001	41	24-Mar-2006	81	1-Sep-2010	105	18-Apr-2012	133	6-May-2015
12	29-Sep-2001	45	1-May-2006	82	28-Oct-2010	106	28-Apr-2012	134	1-Nov-2015
15	13-Dec-2001	46	7-May-2006	83	4-Nov-2010	107	1-May-2012	141	28-May-2016
16	2-Apr-2002	49	24-Nov-2006	85	22-Nov-2010	108	5-May-2012	142	13-Jun-2016
17	8-Apr-2002	50	12-Dec-2006	86	25-Nov-2010	109	7-May-2012	144	30-Sep-2016
20	21-May-2002	51	20-Jan-2007	88	6-Apr-2011	113	23-Apr-2013	147	1-Dec-2016
22	24-Oct-2002	54	16-Apr-2007	89	22-Apr-2011	114	29-Apr-2013	149	10-Mar-2017
23	25-Apr-2003	55	18-May-2007	90	25-Apr-2011	115	21-May-2013	152	14-Apr-2017
24	12-May-2003	56	25-May-2007	92	8-May-2011	117	11-Aug-2013	153	18-Apr-2017
25	5-Oct-2003	62	25-Apr-2008	94	1-Jul-2011	118	16-Sep-2013	154	26-Apr-2017
26	13-Oct-2003	64	1-May-2008	95	6-Jul-2011	121	23-Dec-2013	155	30-Apr-2017
27	7-Jan-2004	67	3-Jul-2008	96	6-Sep-2011	122	12-Mar-2014	156	6-May-2017
29	3-May-2004	68	8-Jul-2008	97	14-Oct-2011	123	16-Apr-2014		

Flow chart in Figure 3.9 summarizes the main methodology steps followed in Chapter 3.

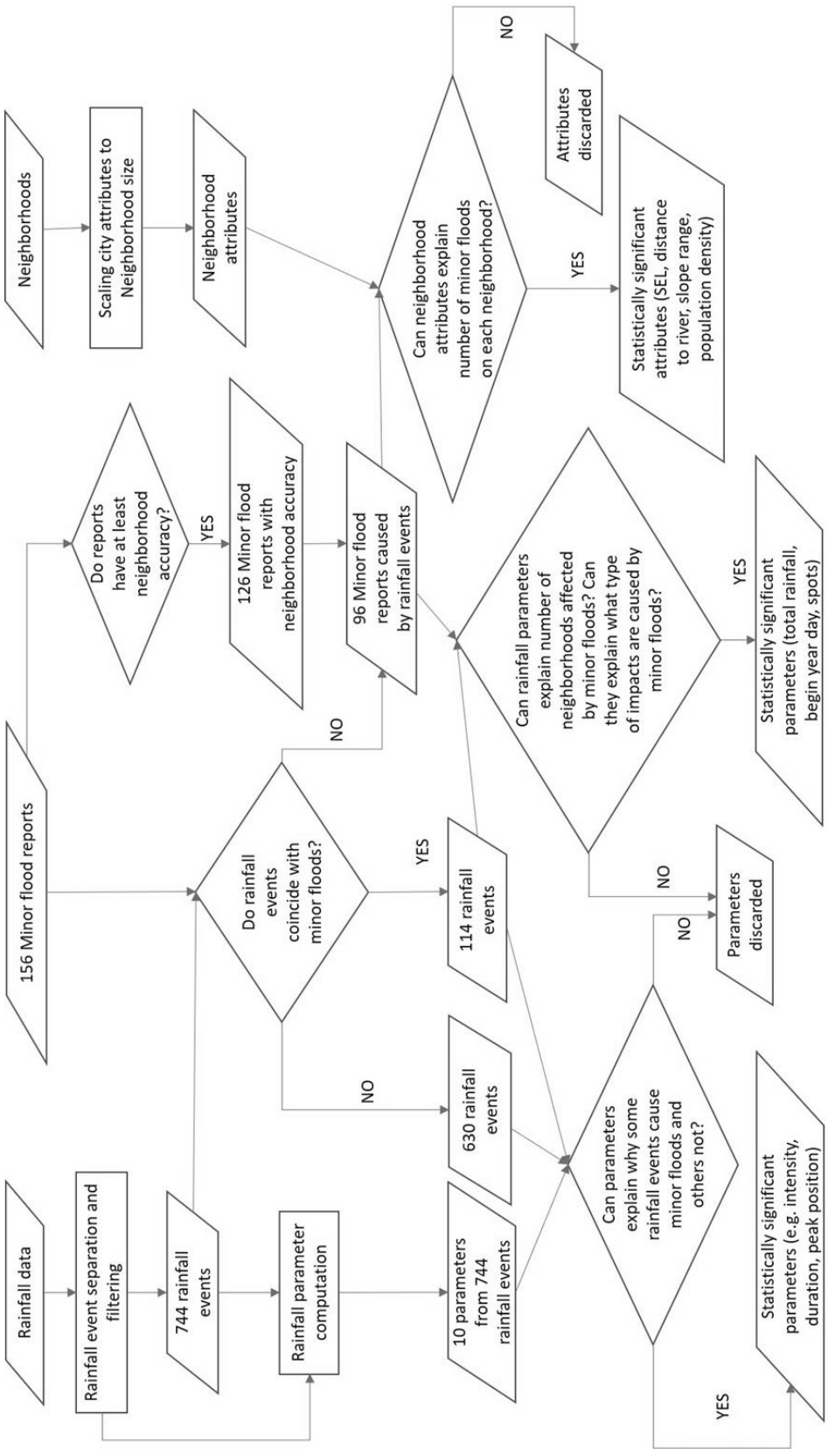

Figure 3.9: Flow chart describing the methodology in Chapter 3 that correlates rainfall parameters, minor-flood reports, and neighborhood attributes.

3.3 Analysis of results

3.3.1 Rainfall parameter differences between minor-flood and non-minor-flood-related rainfall events

All rainfall parameters (except *begin year day, peak hour* and *asymmetry*) show statistically significant differences when comparing minor flood and non-minor flood related samples (Table 3.6). Evidently, rainfall is needed for minor floods to occur, but these results indicate that rainfall features, along with other causes, determine whether minor floods occur or not after a rainfall event.

The sign in the significant mean difference between samples shows that *total rainfall* is higher during minor-flood-related rainfall events, as well as *maximum intensity*, *peak position*, *duration*, *rain periods* and *spots*. On the other hand, values for *triangular shape* are lower. Therefore, results suggest that on average, heavier, more intense, later-peaked, longer-lasting, less interrupted, and more spatially spread rainfall events are more likely to cause minor floods in Cali. Some of these minor-flood-related rainfall distinctive features coincide with characteristics that climate change could enhance, i.e. heavy rainfall lasting longer, and being more continuous within a storm (Sofia and Tarolli 2017).

Flood-triggering critical thresholds for total rainfall and rainfall intensity have been issued before by the Secretary of Risk Management in Cali (ADN Cali 2016). According to this institution, the drainage network has collapsed with rainfall intensities greater than 30 mm/h, and total rainfall over 40 mm. However, this study showed 16 rainfall events with total rainfall below 40 mm that caused minor floods (including a 1.4-mm event and three events with intensities below 30 mm/h). EMCALI allows minimum concentration times of 6 minutes to design drainages, a duration short enough to pick high rainfall intensities from Intensity-duration-frequency curves (EMCALI 2017a). On this basis, such low rainfall values causing minor floods in Cali can then only be explained by reading errors at the rainfall stations, by rainfall cells not being captured by rain gauges, by highly vulnerable areas of the city collapsing with just a few millimeters of rain, or by combinations of the former.

3.3.2 Rainfall parameters as predictors of minor floods

Individual rainfall parameters that were good at differentiating lumped minor-flood from lumped non-minor-flood-related rainfall events were also significant when predicting individual minor floods. The parameters *begin year day, peak hour,* and *asymmetry*, which were not significant for the lumped comparison, were also not significant for individual prediction of minor floods (Table 3.7).

Odds ratios (OR) show how much more likely it is for a minor flood to take place, as a rainfall parameter increases its value in one unit (Table 3.7). OR presented here consist only on the average value within the range. It is expected, however, that they have non-linear variations as rainfall parameters move along their ranges.

For instance, a rainfall event *A* having a *total rainfall* 25 mm larger than event *B*, has a **1.31**-times greater chance of causing a minor flood (from OR *total rainfall* value, Table 3.7). Furthermore, if the same event *A* had 100 mm larger *total rainfall* than event *B*, then it would have a **5.24** greater chance of causing a minor flood on average (*1.31 x 4*). The lowest *total rainfall* detected was 1.4 mm, and the highest was 1,173 mm. OR is likely to have a non-linear trend within *total rainfall* range: it is not the same to go from 20 mm to 40 mm than from 1,020 mm to 1,040 mm. OR is expected to be higher for small rainfall events; large rainfall events, on the other hand, will probably not increase their impact as much if a few millimeters are added.

Maximum intensity shows a more evident increase in probabilities of causing minor floods, i.e., through an increase of 1.0 mm/min, the rainfall event increases the chance of a flood **2.26** times on average throughout the range of values, which is not very wide (from 0.02 mm/min to 5.45 mm/min along the 744 rainfall events), making it a very sensitive parameter. In this case, higher intensities are expected to have higher OR values.

For each additional hour a rainfall event lasts, the chances of a minor flood increase **1.01** times. Rainfall events were as short as 20 min, and one as long as 58 days.

Triangular shape, a measure of the distribution of rainfall (2 being perfectly homogeneous, and asymptotic zero for very abrupt bursts) shows that an increase of

one unit, i.e., distribution becoming more homogeneous, would decrease the chances of a disaster **3.29** times (*1/0.304*).

Finally, every additional rainfall station that detects a rainfall event would indicate an increase by **1.07** in the chances of a minor flood. OR for this parameter is not easy to interpret, since it is conditioned to the current stations available. Additional stations within the same city area would produce also a different OR average value.

Joint logistic regressions

Stepwise regression on joint logistic regression of rainfall parameters explaining the dependent variable 'Flood' (Table 3.9) dropped some non-significant variables (*asymmetry*, *begin year day*, *peak hour*, *rain periods,* and *triangular shape*).

The Pseudo R^2 for the joint regression is **0.262** and for the stepwise final regression is **0.251**. Even though it is not expected in urban hydrology analysis to obtain very high R^2 values, given that the observational nature of some of the data, these R^2 values are rather low and imply that there should be more causes other than rainfall parameters that determine whether minor floods occur or not.

Parameters for early warning systems

Since final values from rainfall parameters can be known only at the end of each rainfall event (except *begin year day*), they would not be very useful at first glance to set up an early warning system. Some parameters indeed might radically change their value in the last minutes of a rainfall event: for instance, *triangular shape* may keep a value of 2 in a very homogeneous rainfall, but if in the final minutes the rainfall becomes more intense, then this parameter would quickly drop to zero. *Peak position* can also change abruptly whenever an initial maximum intensity value is registered, but the definite maximum intensity burst comes at the end of an event (it could go from 1 to 7000). *Asymmetry*, a parameter depending on *peak position*, would behave similarly.

However, there are other parameters with values that can only accumulate in time (*total rainfall*, *duration*, and *rain periods*), so they may have thresholds that trigger alarms as events develop.

3.3.3 Minor-flood reports not preceded by any rainfall event

After matching FNFA rainfall events with minor-flood reports, there were 30 minor floods that were not preceded by any rainfall event in the near past days, according to the influence criterion used (Figure 3.5): an odd result considering that rainfall is a necessary factor for minor floods to occur.

A rational explanation for this is the accuracy of minor-flood reports over time in Colombia (Figure 3.10): practically all minor floods not preceded by rain occurred before the 2010-2011 La Niña event, which raised concerns in the country for the consequences of floods, and made authorities and institutions improve data collection. It is likely that some reports before then were not very accurate in the date that they happened, and that even some rainfall stations reported no values due to lack of maintenance or personnel to read them.

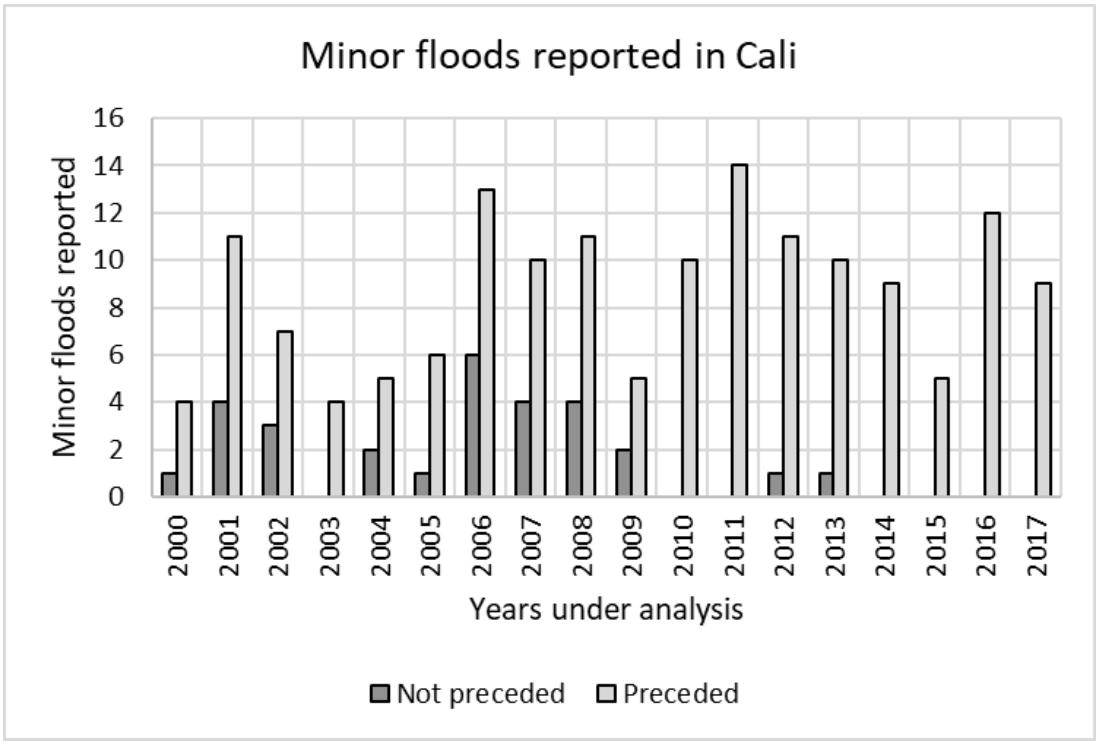

Figure 3.10: Minor floods reported in Cali preceded and not preceded by rainfall events.

3.3.4 Rainfall parameters as predictors of number of neighborhoods affected by minor floods

Compared to 'Flood', the variable 'Occurrences' adds information about the severity of the impact of the rainfall events over the city by including the number of neighborhoods affected.

All rainfall parameters except *begin year day* and *peak hour* were significant in the individual Poisson regressions to explain the variable 'Occurrences' (Table 3.13). OR shows that 25 mm more of *total rainfall* would increase the chances of affecting an extra neighborhood **1.06** times.

Maximum intensity is once again a very sensitive variable that increases the chances of affecting an extra neighborhood **1.29** times per every 1.0 mm/min increase.

A peak position taking one hour longer to appear after the start of a rainfall event would increase the probability of affecting an extra neighborhood **1.001** times. An additional hour of *duration* of a storm means also a **1.001** times higher chance of affecting an extra neighborhood.

One more rainfall station registering the event would indicate that rainfall has an increased probability of affecting an extra neighborhood **1.07** times.

Joint Poisson regressions

In the joint Poisson regression, *begin year day, rain periods,* and *spots* are significant parameters in explaining 'Occurrences' (Table 3.14). Later, in the *stepwise* estimation, *total rainfall* was included along with the previous significant variables, and all the other parameters were dropped.

3.3.5 Neighborhood attributes as predictors of number of minor floods registered per neighborhood

Distance to river, *slope range*, and *population density* significantly explained the number of minor floods registered per neighborhood in Cali (Table 3.15). The correlation coefficient (Pseudo R^2) for the Poisson regression is 0.060, which is very poor and confirms that there must be unknown variables causing minor floods in the neighborhoods other than neighborhood attributes *per se*.

The attributes *mean slope* and *mean elevation* did not significantly explain the number of minor-flood reports, probably due to a high correlation between them: when there is an increase in elevation, the surface tilts more as it enters a mountainous region. Another non-significant attribute is *aquifer areas*, probably due to the lack of a better resolution.

Odds ratios from the Poisson regression with unit-transformed variables illustrate how much a one-unit change in neighborhood attributes modifies the probability of adding a minor flood registered on average per neighborhood (Table 3.16). For instance, for every 100 meters that one moves farther away from a river, the chances of a minor flood caused by backflow are reduced by 2.1% (1-OR). For every additional ten degrees in slope range per neighborhood (higher topographic contrast), the chances of an extra minor flood reported increase by 17% (OR-1). For every additional hundred inhabitants per hectare (something like adding one story to every house in a residential block), the probability of an extra minor flood reported increases by 11.2% (OR-1).

Predictive margins for attributes and interactions between categories

Predictive margins show the expected number of minor floods per neighborhood along the range of an attribute (Figure 3.7), while interactions between variables show how categories within an attribute may have different trends that cannot be seen in the overall picture (Figure 3.8). Through predictive margins, it can be seen how higher *socioeconomic levels* expect more minor floods in the neighborhoods than lower levels, but they also show a higher variability, which may reflect the fact that not all higher SEL neighborhoods have appropriate drainage infrastructure and the minimum recommended amount of green area per capita (World Health Organization, 2012).

Lower SEL neighborhoods are not expected to become as frequently affected as higher SEL neighborhoods, but the lower variance also means that the hazard is spread more homogeneously.

Higher *slope range* values predict more minor floods significantly for SEL 1 neighborhoods only. High slope ranges allow drainage networks to convey water

effortlessly by gravity given certain design and maintenance conditions in the network. However, if these conditions are not met, then the natural topographic advantages turn into drawbacks, leading to water ponding and flash floods.

As *distance to river* increases, the expected number of minor floods per neighborhood decreases steadily while maintaining a regular variability. This is perhaps the neighborhood attribute with the greatest influence on minor floods, indicating that drainage network deficits like inadequate design dimensions or sewers clogged with garbage could be the causes that augment vulnerability to minor floods near outlet water bodies.

Population density increases along with the expected number of minor floods per neighborhood, as well as its variability. However, after revising interactions between SEL and *population density* (Figure 3.8 and

Table 3.17), it can be seen that the impact of *population density* on minor floods is greater on the lowest SEL. SEL 2 showed a milder increase, while SEL 6 did not even have neighborhoods with the highest density values. Increases in population in low-SEL neighborhoods usually occur together with an infrastructure that had been initially designed for fewer people, or even for no people at all, increasing their vulnerability. If population density increases in higher SEL neighborhoods is usually a consequence of new urban plans that deliberately seek to increase the density in the area where basic infrastructure has been previously implemented.

3.3.6 Rainfall parameters predicting types of minor floods

Only one rainfall parameter predicted significantly one type of minor flood: *peak hour* predicting *trees falling* with an estimate of 0.113, equivalent to an odds ratio of 1.12: that means that if there are two exact rainfall events, and one of them has its peak hour one hour later, then it would have 12% more chances of making trees fall. Time itself does not seem to be a reason for trees to fall easier, but Pacific jet-winds tend to be stronger in the afternoon and in the night time in the Cauca valley and mountains (Yepes et al. 2019), thus battering vegetation harder as they accompany rainfall.

Asymmetry (p=0.09) and *Spots* (p=0.08) were close to significantly predict *River overflow*. Estimates indicate that rainfall events with higher volumes after the peak and fewer spots detecting rainfall are more likely to cause rivers to spill over. Rivers in the Cauca Valley drag a large amount of sediments that eventually hold water and spill it over the banks: there are more chances of loose material in banks and mountains being dragged if large rainfall volumes follow the peak. There are also more chances of loose material being dragged if the rainfall takes place on top of the Andes mountains or upstream Cali (both locations upstream and away from the spots considered).

Impact variables explaining each other

From the five pairings highlighted in the analysis (Table 3.20), three showed significant correlations: *trees falling* explaining *power cuts*, *trees falling* explaining *traffic congestion and accidents*, and *power cuts* explaining *educational and health centers affected*. On the other hand, *river overflow* did not explain significantly either *sewer blockage* nor *death, missing and wounded*. Rainfall events with falling trees increase their chances of causing power cuts over nine times (OR 1:9.39) and traffic congestion and accidents over six times (OR 1:6.46).

3.4 Recommendations

- Finding correlations between rainfall events and minor floods poses all sorts of challenges, starting from the definitions of rainfall events and minor floods themselves and how to measure them, to the confidence in the accuracy of the information on rainfall data and minor-flood reports. Detection of more independent variables are also important to be able to prioritize vulnerable zones.
- Calibrated rainfall information should be available online in order to reduce administrative tasks for CVC workers and waiting periods for researchers. This is part of the cooperation between public and private entities regarding collection and synthesis of data for disaster risk reduction (Cutter and Gall 2015; Corfee-Morlot et al. 2011).

- Due to some very small rainfall events both in total volume and intensity associated with minor floods in Cali, it is strongly recommended that CVC periodically calibrates the rainfall stations to see whether they are correctly recording rainfall amounts, that EMCALI checks critical infrastructure points in these neighborhoods to reduce vulnerability in case low rainfall values are correct, and that research on spatial distribution of rainfall events is made, since it is possible that some events fall in very small areas in between stations and thus cannot be detected by them.
- Keeping an accurate neighborhood-level flood inventory up to date is key, so awareness of the following two data-collection challenges is necessary: first, it is very likely that during the more devastating rainfall events, rescue teams, aid organizations and civilians are busier and have less capacity to fill out detailed reports. To date, the reports simply use expressions such as “South Cali” or “East Cali”, when it is for these severe rainfall events that more detail is needed. Second, it is also very likely that illegal settlements tend not to report minor floods at all in order to avoid authorities finding out about their activities. Consequently, minor-flood reports underestimate the true impacts near illegal settlements, as well as those caused by the strongest storms. However, there are also ways to offset these challenges. One is that aid organizations could train some of their staff or part-time workers to accurately collect information immediately after the rainfall events take place. Another suggestion for better reports is to rely upon high space-time resolution synthetic aperture radar imagery (Plank 2014), or remote acquisition of multispectral imagery with drones, taken as early as possible after the rainfall events occur, as a tool to make ex-post analysis to spot minor floods overall: this gives data collectors the chance to check all places in the city (not only the ones that called to report problems), and also have more time to elaborate the reports. Since minor floods, by definition, do not take human lives or physically damage equipment, there is no need for evacuation plans, but rather for taking long-term actions to reduce

floods in detected spots, such as changes in infrastructure, along with its adequate maintenance and protection.

- Regardless of the low overall correlation between rainfall parameters and minor floods, most rainfall parameters can individually differentiate minor-flood-related from non-minor-flood-related rainfall events, and some are still significant in the joint regression. The parameters of *total rainfall*, *duration*, and *rain periods* can trigger alarms when moving away from the expected values for non-minor-flood-related events. Therefore, it must be possible for aid organizations to read these parameters in real time.
- Neighborhood attributes that significantly correlate to minor floods (*population density*, *distance to rivers*, and *slope range*) are associated with urban pressure on river buffering areas, a common phenomenon in developing countries. National and local authorities must come to terms to propose a land-use plan that protects the riverine buffer zones, not necessarily by clearing and disusing them, but on the contrary, by including protective measures for existing and new buildings (Yamin et al. 2013; Dash and Punia 2019; World Meteorological Organization 2009).

4 ECONOMIC LOSS ESTIMATION DUE TO MINOR FLOODS IN CALI DURING 2000-2017

Water depth is a parameter commonly used to describe the seriousness of main flood episodes and to compute their associated losses (Genovese and Green 2014; McGrath et al. 2015; Dottori et al. 2017). While there are more parameters that can be considered, like flow velocity, flood duration, or distance from a river (Wijayanti et al. 2017), inundation depth stands alone for analysis in most cases.

Flood loss estimation considers the water surface as a high-powered laser beam that damages objects as it touches them on its way. These objects and appliances are characterized by their relative height inside a facility in depth-impact functions (Blanco-Vogt and Schanze 2014; Kobayashi et al. 2016) and grouped in sets depending on land use. For instance, household items are expected in residential areas, while medicines and surgery equipment are expected in health centers. Rural areas are particularly exposed, since most tools, crops and animals are at ground level, just like sports courts at schools and urban water supply and sewer systems (Sánchez et al 2007).

The typical land uses included in direct flood loss estimations are residential areas, industrial estates, commercial buildings, infrastructure, and agriculture (Wu et al. 2016; Scorzini and Leopardi 2017).

Indirect losses are also sometimes considered and refer to everything besides physical damage to property. These indirect losses have all a common denominator, i.e. they are harder to translate into monetary figures, either because of more assumptions to be made (income loss due to business interruptions), or because of ethical considerations (putting a price tag to human lives and environmental damages) (Scorzini and Leopardi 2017; Chen et al. 2016).

Estimations of direct and indirect flood losses can be made based on episodes that have already occurred by adding up the corresponding costs. They can also be a forecast of losses due to a rainfall episode of certain occurrence probability. In the latter case, the total loss is calculated as current values by using the expected return period

(inverse of occurrence probability) in order to know the yearly cost to be saved to mitigate the effects.

4.1 Estimation of minor-flood impacts in Cali

Minor flood impacts cannot be detected under the current water-depth methodologies for measuring flood impacts, since water level usually does not reach homes, but only streets and sidewalks. However, depth is not the only variable that may cause losses and setbacks: stagnated water -i.e., the mere presence of puddles and backwater from sewers- is an ideal nesting site for *Aedes aegypti* larvae and pupae, so-called yellow fever mosquito, which has spread diseases such as dengue, zika and chikungunya to the population in Cali. Car traffic is also affected by flooded streets, causing impedance and productivity decline. Rainfall events are sometimes accompanied by gusty winds that lead to power cuts due to tree branches falling on electricity lines.

Hence, this study estimates economic losses due to minor floods by considering water-borne diseases (*Aedes aegypti* nesting), traffic impedance, and power cuts in healthcare facilities and educational institutions. Although owners and workers from business establishments such as restaurants, stores and shops may also be negatively affected due to power cuts, customers can find another place relatively easy, while it is extremely difficult for a person to get transferred to a different hospital if there are problems at the one, he/she is already registered to; likewise, it is practically impossible for a student to attend a different school during those days his/her school is closed. Therefore, emphasis is made in health and education.

4.2 Input data

4.2.1 Aedic index in sewers

The aedic index is the percentage of monitored sewers with *Aedes aegipti* larvae and pupae. Sewers in Cali were monitored by the Secretariat of Health between 2013 and 2015, and the index values were associated to each neighborhood observed and the day of the year of the observation. Family monthly expenditure on products to prevent dengue is taken from (Heydari et al. 2017).

4.2.2 Services in healthcare institutions

DAPM gathered information about services provided during 2014 in all public healthcare institutions in Cali (Table 4.1). All services are counted in number of patients seen. From database reports with neighborhood accuracy (92 events, Table 3.12), those reporting power cuts were taken (11 events). A power cut of 24 hours in the neighborhoods involved is assumed, in default of a better time resolution in the reports.

Table 4.1: Services provided by healthcare institutions in Cali altogether (2014). Intensive care units are not included since they run on power plants

Appointments	Procedures
General Practicioner	In-patient surgery
Specialist	Outpatient surgery
Pediatrician	Deliveries
Gynaecologist	Cytology
Dentist	Immunizations
Ophthalmologist	

4.2.3 Services in educational institutions

Average daily cost for a high school to provide services to a student is obtained from the major's office in Cali (Azcárate, Ocoró 2016); number of students enrolled at each high school institution in Cali was given by the Education Secretariat in Cali (Secretaría de Educación de Cali 2018).

For higher education, semester fees were obtained from the official websites of each institution, and the number of students enrolled at each institution in Cali was given by the Ministry of Education (Ministerio de Educación Nacional 2017).

4.2.4 Transportation

In December 2015, DAPM published a map of the average speeds during the morning rush hour on main and secondary arterial roads in Cali for both public and private transportation. Speeds (km/h) ranged from 1 km/h to 68 km/h.

Metrocali performed an origin/destination study on 510 transport analysis zones (TAZ). These zones are available in shape format and cover the whole city of Cali.

The origin destination matrix is presented in Excel and includes commuters from the MIO bus system (owned by Metrocali), public transport, and private vehicles.

The database of minor-flood reports with neighborhood accuracy was used again to list the flooded neighborhoods on each of the 109 days along which the 92 minor floods between 2000 and 2017 took place (Table 3.12).

4.3 Methodology

Economic loss triggered by minor floods in Cali from 2000 to 2017 was estimated based on three adverse phenomena, i.e., *Aedes aegypti* breeding, traffic impedance, and power cuts affecting health care and educational institutions.

4.3.1 Aedes aegypti

Water and sanitation play an important role in the lifecycle of most neglected tropical diseases (STH, Dracunculiasis, Trachoma, Schistosomiasis, Onchocerciasis, lymphatic filariasis, dengue, chikungunya) (Sheela et al. 2015). Mosquito and other disease vectors have adapted and proliferated in urban environments, leading to extensive outbreaks (e.g. chikungunya, dengue and Zika in Cali) when precipitation levels increase (Dommar et al. 2014).

Along with precipitation, the intense pollution of canals, drains and lakes, and the large wetland areas favor the occurrence of dengue (Sheela et al. 2015). Actively removing vector breeding sites through community-based interventions ensures cities that are resilient to Leishmaniasis, Chagas, dengue, chikungunya, Zika, and yellow fever (Bangert et al. 2017).

Results of a study in Ecuador, show that households spend a monthly average of US$ 2.00 of their family income on *Aedes aegypti* control measures, including aerosols, liquid sprays, repellents, mosquito coils, and unimpregnated bed nets. Most households had access to sewerage, garbage collection, and piped water in their home (Heydari et al. 2017). The study does not specify how effective these measures are to avoid the diseases.

The aedic index (AI) stands for the percentage of sewers with mosquito larvae and pupae. The Secretariat of Health in Cali has been monitoring over 65,000 drains in

the city since 2013. Due to limited staff and budget, not all sewers can be monitored on the same day, and it takes up to a year to monitor the entire city. Therefore, it is not always possible for neighborhoods where minor floods have been reported to also have a recent AI value surveyed. Nonetheless, there are some neighborhoods where dates of surveys and minor floods are close enough to analyze the contrast of AI values before and after the minor floods occur (Table 4.2).

AI values were obtained from affected neighborhoods before and after minor floods (Table 4.2). Information came out from 18 minor-flood reports between 2013 and 2015 that affected up to 129 neighborhoods.

Table 4.2: Time span between AI survey and minor-flood reports in affected neighborhoods (fragment). Numbers below minor-flood dates represent the time in days between the AI survey and each minor flood (positive if survey happened later and negative if earlier)

Aedic Index Survey		**Dates of minor flood reports**				
Date	**Neighborhoods monitored**	23-Dec-2013	12-Mar-2014	28-Apr-2014	20-May-2014	7-Jun-2014
21-Jan-2014	EL PONDAJE	29		-97		
24-Jan-2014	PAMPALINDA - CUARTO DE LEGUA					-134
24-Jan-2014	SAN FERNANDO - 3 DE JULIO	32	-47			
24-Jan-2014	TEJARES Y CRISTALES - MIRAFLORES	32				
27-Jan-2014	NORMANDÍA - CENTENARIO - JUANAMBÚ	35	-44			
31-Jan-2014	EL INGENIO					-127
31-Jan-2014	PANAMERICANO					
12-Feb-2014	GRANADA - SANTA MÓNICA RESIDENCIAL	51	-28		-97	
18-Feb-2014	MAKRO - VALLE DEL LILI					-109
21-Feb-2014	ALCÁZARES	60				
24-Feb-2014	EL PONDAJE	63		-63		
25-Feb-2014	SANTA ANITA - LIMONAR					-102
6-Mar-2014	MELÉNDEZ					-93

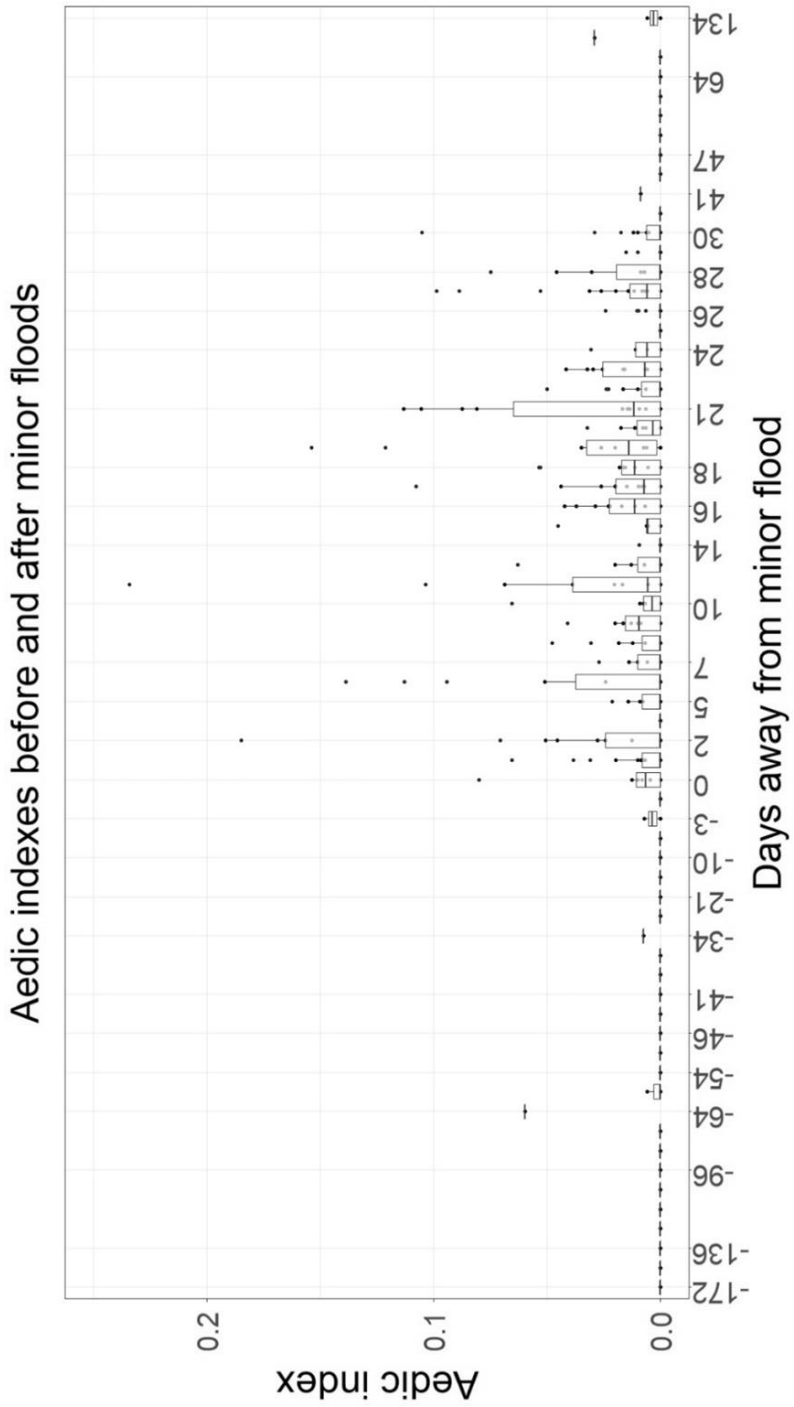

Figure 4.1: AI values in affected neighborhoods before and after minor floods (day zero). Lower and upper box hinges correspond to 1st and 3rd quartiles, while the line in between represents the median value; upper whiskers extend to 1.5 times the inter-quartile range, leaving data beyond as “outlying” points.

It can be seen how AI is triggered punctually on the days when minor floods occur (day zero), and then fades out about a month later, which is as long as the life cycle of mosquito (EPA 2017). It would then be reasonable to relate economic losses through minor floods with the household expenses to control mosquitoes in the first month following flood disasters in the affected neighborhoods.

The number of households per neighborhood is computed as the projected population per neighborhood for 2017 (DANE 2010) divided by 3.8, which is the average number of household members in Cali (Escobar G 2016); then this number of households per neighborhood is multiplied by the amount of minor floods the neighborhood reported between 2013-2015 and then multiplied by the mosquito monthly control cost of US$ 2.00 (equation 4.1).

$$Mosquito\ control\ cost = \sum_{\substack{affected \\ neighborhoods}} \frac{population \times monthly\ control\ cost \times minor\ floods}{average\ number\ of\ household\ members} \qquad 4.1$$

The estimated total economic loss due to the control of *Aedes aegypti* breeding caused by minor floods is US$ 623,832.00 (€ 536,823.00) with over 880,000 people involved (Table 4.3).

Costs of treatment for infected people are not considered in this study, but according to Cali epidemiology bulletins (Rojas 2016a) there were 6,594 hospitalizations at an early dengue stage, 751 of which developed into dengue hemorrhagic fever cases between 2013 and 2015; costs for early-stage dengue hospitalization in Colombia between 2000 and 2010 averaged US$ 599.00 per patient and US$ 2,361.00 per patient reaching hemorrhagic fever (Bello et al. 2011), so the cost estimate of dengue treatment for Cali between 2013-2015 corresponds to 5.3 million dollars. Evidently, the percentage of those treatments that were caused by minor floods is unknown and involves additional studies of spatial and temporal contagion dynamics.

Table 4.3: Estimation of mosquito control cost per neighborhood in Cali during 2013-2015 (fragment)

Neighborhood	Population	Households	Control cost (USD)
Los Comuneros I	29 043	7 643	45 858.00
Los Comuneros II	14 950	3 934	31 472.00
El Vallado	25 817	6 794	27 176.00
El Refugio	14 808	3 897	15 588.00
Mariano Ramos	28 561	7 516	15 032.00
La Base	10 886	2 865	11 460.00
Siloe	21 622	5 690	11 380.00
Jose Manuel Marroquin I	21 053	5 540	11 080.00
Union de Vivienda Popular	20 957	5 515	11 030.00
Nueva Floresta	19 498	5 131	10 262.00
El Troncal	9 617	2 531	10 124.00
Parcelaciones Pance	6 345	1 670	10 020.00
Calimio Desepaz	18 898	4 973	9 946.00

4.3.2 Traffic

Urban flooding due to intense precipitation is the main cause of weather-related disruption to the transport sector and this is expected to continue. Diversion routes, and changes to driver behavior because of floods, are often assumed without any clear rationale. Studies recognize that correlations between weather and disruption are complex, as they relate to road network capacity, drainage systems and a few other factors. Flooding is not considered in these studies (Pregnolato et al. 2017; Mark et al. 2004).

Many cities in developing countries are growing rapidly, increasing impermeable surfaces, and do not have the funds to extend and rehabilitate the existing drainage systems, thus raising the extent and frequency of urban flooding. Traffic disruptions are among indirect damages caused by water (Mark et al. 2004).

In Cali, minor flood episodes visibly affect transportation systems as vehicle speed decreases, not to mention wear and tear of pavements and vehicles under rainy conditions (Figure 4.2).

Figure 4.2: Minor floods on roads in Cali. Cañasgordas Ave. (left, source: *El País de Cali*), and Southeastern Highway (right, source: Ministry of Transportation).

This analysis focuses only on the cost of staying extra time on the road for commuters due to minor floods reported between 2000 and 2017. Economic loss estimation is based on time impedance and how much it would cost for all passengers to stay idle during that time, assuming all of them earn minimum wages.

When minor floods occur in Cali, drivers usually do not change their normal routes to avoid the flood, but rather keep driving along the flooded streets with decreased speed (Pregnolato et al. 2017). Therefore, impedance simulations with the *ArcGIS network analysis* tool give affected streets a speed penalty instead of a pass restriction, i.e., drivers still use them, but it takes longer. Vehicle speeds may decrease below 10 km/h on flooded streets (Yu et al. 2015): this analysis took that speed for the cars crossing a flooded neighborhood, except for those neighborhoods with normal average speeds already below 10 km/h (Figure 4.3). Currently there are no studies in Cali or in Colombia on average speeds or speed deceleration during minor floods to make this estimation more accurate.

Average speeds on main and secondary arterial road segments in Cali during noon rush hour were digitalized on ArcGIS from the DAPM map and used to compute travel times from and to 510 transport analysis zones (TAZ) covering the whole city, most of them coinciding with neighborhoods. Sometimes a single neighborhood is fractioned into two or more TAZ.

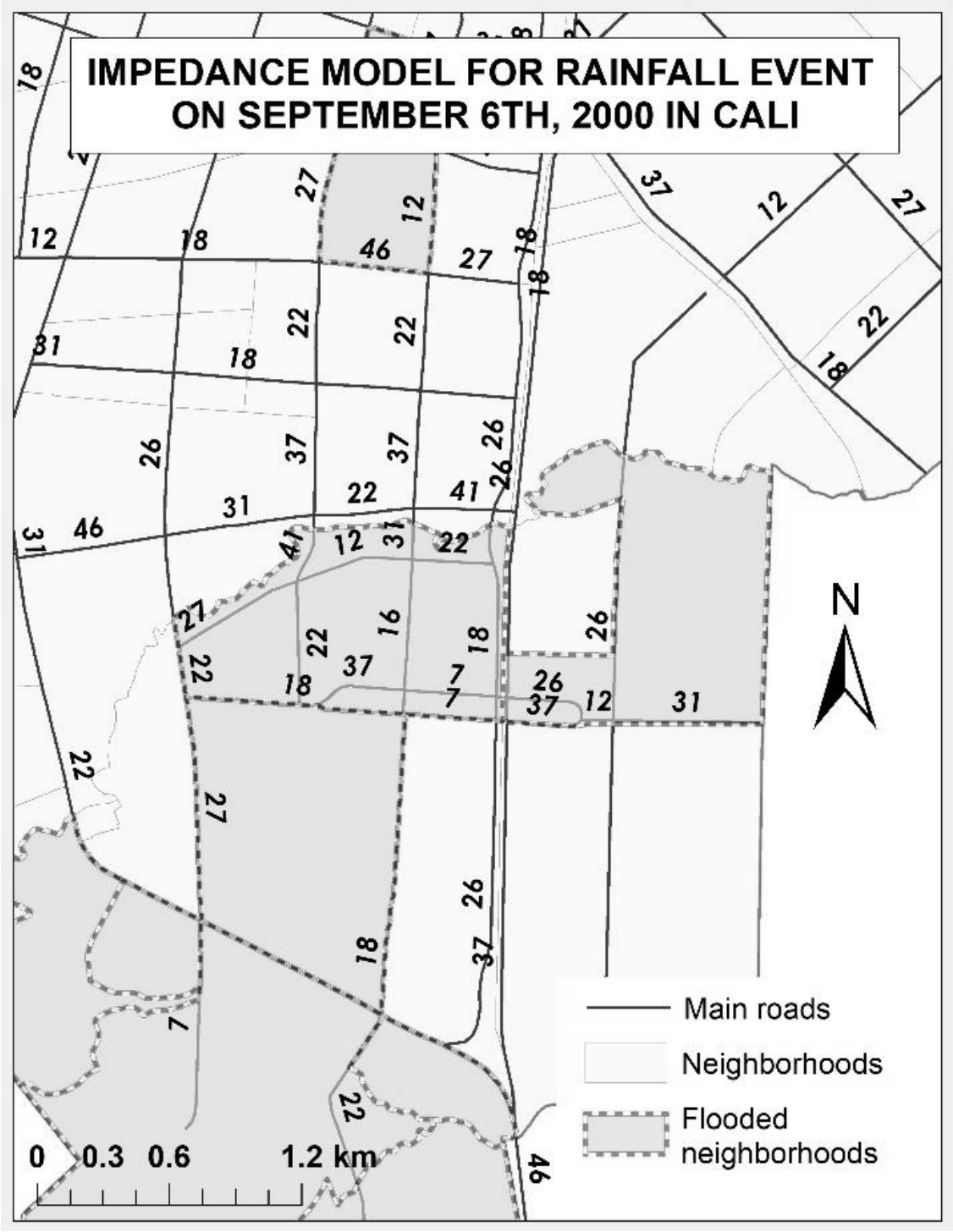

Figure 4.3: Flooded neighborhoods during a rainfall event. Commuters are assumed to cross flooded neighborhoods at 10km/h. Average speed during noon rush hour is shown along roads in km/h.

Even though there are 249,028 possible routes between the 510 TAZ, only 4,431 have reported trips in Metrocali origin/destination matrix.

For the 94 minor floods with neighborhood accuracy (Table 3.21) that took place in Cali between 2000 and 2017 during 108 days (some minor floods lasted for two or three days), a simulation was performed on ArcGIS where commuters take speed restriction as they cross the roads in flooded neighborhoods.

The average time needed to cover each one of the 4,431 routes during noon rush hour is 18.6 min. The average time to cover these same routes during the simulations of all minor floods between 2000 and 2017 increased to 33.9 min: this increment of 15.3 minutes, multiplied by all minor-flood days and all commuters during noon rush hour, equals an increase in travel time of over 200 million minutes (Table 4.4). A more didactic way to understand this figure is the following: if all citizens who ride these routes were given a stopwatch, and they were told to measure the extra time they spent on the road during the 108 minor-flood days on noon rush hour compared to a regular day, then the sum of all those stopwatches would be over 200 million minutes.

Impedance time is the most important loss for commuters during minor floods: it is time that cannot be properly used for work, for leisure or rest. This study attempts to roughly transform all losses into monetary figures with simple income/time equivalences, because it is an efficient way to summarize negative and positive impacts; however, it would take a more complex study involving several disciplines to find out the real extent of the long-term economic potential of the activities that citizens could achieve if they did not have this impedance time. Equation 4.2 shows the general estimated impedance cost in Cali between 2000 and 2017.

$$Impedance\ cost = MWM \times \sum_{i=1}^{108} \sum_{j} \sum_{k=1}^{2} PASS_{jk} \times \frac{\left(V_j - SR\right) \times L_j}{V_j \times SR} \qquad 4.2$$

where MWM = minimum wage per minute, i = minor-flood days, j = affected neighborhoods on each minor-flood day, k = public or private commuter, PASSjk = number of passengers crossing each affected neighborhood, Lj = length of roads on each

neighborhood, Vj = average speed on noon rush hour for each neighborhood, and SR = speed restriction on flooded neighborhoods (always smaller than Vj).

If every minute of impedance is worth a minimum wage minute in Colombia (COP 781,242 per month, or € 231), assuming 205.7 hours worked per month (48 hours per week), then each minute would be worth COP 63.3 or € 0.02, and the cost of minor floods for impedance affecting the citizens altogether would rise to over € 4 million.

Table 4.4: Impedance time and costs during minor-flood days in Cali (2000-2017)

Transited routes within Cali	4,431
Public trips during noon rush hour	77,882
Private trips during noon rush hour	49,643
Minor-flood days between 2000 and 2017	108
Total driving time for transited routes	82,334 min
Total driving time during minor floods	150,211 min
Total delay for all travelers	210,722,310 min
Cost of one-minute person impedance	COP 63.3 (€ 0.02)
Cost per year of impedance time	€ 157,621
2000-2017 cost of impedance time	€ 4,214,446

4.3.3 Energy

Electricity systems can collapse at country level due to something as simple as a tree falling down and disrupting electrical power lines (Byrd and Matthewman 2014), showing how fragile they can be. Furthermore, due to city growth and climate change, these power cuts will become a more frequent event in the future. Minor floods may be a cause for power cuts in a city for reasons such as:

Preventive suspension of electrical circuits due to overflow of city rivers and backwater in sewers wherever electrical circuits are underground.

Damaged primary lines due to intense winds that come along with rains, or due to falling trees and branches.

Electrical storms hitting circuits and producing overloads in the remaining circuits.

In Cali, 94 minor floods were reported between 2000 and 2017. Power cuts were reported in 35 of those 94 episodes. It is assumed that these power cuts spanned

for as many days as minor floods are reported in the neighborhoods (most minor floods last one day, but some last for two or three days).

Economic losses in the community are considered for two types of facilities, i.e., healthcare service providers, and educational institutions. These facilities are of utmost importance before, during, and after a main disaster, because they improve a society's capacity to prevent, mitigate and recover (Rodríguez M 2015).

Healthcare services

During power cuts, public healthcare institutions must reduce their services to the critical minimum and run with power plants. How many services are not provided and how much money would that represent for the city during 35 episodes of power cuts? Health care facilities do not explicitly acknowledge power cuts as one of the many causes of delays in appointments and services.

An average appointment/procedure fee of COP 200,000 (€ 59.48) is used to represent the cost that users would incur due to a power cut, whether they must go somewhere else to pay for the service, or as a symbolic cost of enduring the discomfort and health risk of having to wait for a subsequent appointment while sick. Once again, a much more complex study would be necessary to estimate the real health loss when a patient must wait longer than usual for an appointment or a procedure.

The number of missed appointments per minor-flood day is assumed equivalent to the average number of appointments given per day at the institutions located on the affected neighborhoods (Escobar G 2016, Table 4.5).

The appointment/procedure fee, multiplied by these missed daily appointments and procedures, and multiplied by the days each neighborhood had a power cut in those 35 episodes, gives an estimate of the economic loss in health care in Cali between 2000 and 2017 (Table 4.6).

Table 4.5: Daily average appointments and procedures from healthcare institutions on affected neighborhoods (fragment). GP stands for General Practitioner, PED for Paediatrician, and OS for Outpatient Surgery

Healthcare Institutions		Minor flood dates				Appointments				Procedures	
Clinic	Neighborhood	4.30.17	3.10.17	12.1.16	9.30.16	GP	Specialist	PED	OS	Deliveries	Cytology
Sebastián de Belalcázar	Juanambú				1	7	25	0	12	3	0
Nuestra Señora de Fátima	Granada				1	368	271	35	26	0	7
Valle Salud	Granada				1	546	401	61	35	14	36
Señora de los Remedios	San Vicente	1	1			0	158	10	63	7	122
Comfenalco Unilibre	San Vicente	1	1			0	815	26	59	27	0
Versalles	San Vicente	1	1			2718	575	71	86	29	79
Burgos	La Base	1				546	401	61	35	14	36
Tequendama Comfandi	Tequendama			1		0	308	6	16	0	0
Basilia psiquiatría	Tequendama			1		364	267	41	23	10	24
Los Andes	Tequendama			1		0	2	0	0	0	0
Centro Médico Imbanaco	San Fernando Nuevo	1				613	60	293	0	0	0
San Fernando	Santa Isabel			1		364	267	41	23	10	24
De Oftalmología de Cali	Nueva Tequendama			1		0	0	0	26	11	8
San José	Tequendama			1		0	0	0	17	0	4
Tequendama	Tequendama			1		807	6	0	6	0	0

Table 4.6: Estimated cost of missed appointments and procedures in neighborhoods affected by minor-flood power cuts in Cali between 2000 and 2017.

Appointments	***Missed due to minor floods***	***Cost (COP)***
General Practitioner	71,709	14,341,800,000.00
Specialist	5,920	1,184,000,000.00
Pediatrics	1,583	316,600,000.00
Gynecology	763	152,600,000.00
Dentistry	3,214	642,800,000.00
Ophthalmology	1,332	266,400,000.00
Procedures		
In-patient Surgery	1,181	236,200,000.00
Outpatient Surgery	743	148,600,000.00
Deliveries	290	58,000,000.00
Cytology	547	109,400,000.00
Immunizations	1,163	232,600,000.00
Total	**88,445**	**17,689,000,000.00**
		(€ 4,991,337)

Educational institutions

Education provides structures to build cultural capital, which can in turn be converted into economic or social capital. Interruptions in educational institutions affect the overall vulnerability of a society by reducing its knowledge, aptitudes, and status. In Cali, air conditioning is an imperative service for studying, working in offices, and maintaining food quality, which are all activities related to educational institutions (Byrd and Matthewman 2014).

The economic loss in educational institutions as a consequence of power cuts during minor floods was estimated as the fraction of tuition fees, or government budget, corresponding to those days when classes could not be offered due to lack of energy. From the 35 minor floods bringing power cuts between 2000 and 2017, eight were discarded because affected neighborhoods did not coincide with the location of high

schools and higher education institutions; from the 27 remaining minor floods (representing 30 days because some of them last more than one day), eight were discarded for being on holidays, Sundays, or vacation time, and thus not affecting academic activities: nineteen days remained on for the analysis.

According to the mayor's office in Cali, the annual average budget for 2017 that a school needs in order to provide services for a single student is COP 1,424,112 (€ 425) (Azcárate, Ocoró 2016); a typical school year is offered in 40 weeks, so the daily cost of providing services per student would be € 2.13 (€ 425 divided by 40 weeks and by 5 days).

Total losses in the educational system due to power cuts were estimated by multiplying this daily budget by the number of students enrolled at the institutions located on the affected neighborhoods and by the number of days each neighborhood was affected by minor floods (Table 4.7). Number of students enrolled at each high school institution in Cali was given by the Education Secretariat in Cali.

Regarding higher education, the daily cost (Table 4.7) of providing services for a student was obtained for each institution as the average of the semester fees for three main undergraduate programs (Table 4.8) divided by 16 weeks of class per semester and then by six days (in higher education is more common to study on Saturdays). The total loss corresponds to the representative fee of each institution multiplied by its number of students enrolled and multiplied by the days it got affected by minor floods with power cuts. Number of students enrolled at each higher education institution in Cali was given by the Ministry of Education (Ministerio de Educación Nacional 2017).

Table 4.7: Minor-flood dates affecting educational institutions (fragment). Annual budget for public high schools and semester fees from higher education institutions are transformed to daily values, then multiplied by students enrolled and then by number of minor-flood days.

Annual budget (million COP)	Educational Institutions High School	Neighborhood	Students enrolled	Minor flood dates 6.13.16	5.6.15	3.30.15	Total cost million COP
1.42	Guillermo Valencia	Popular	322			1	4.59
1.42	José Manuel Saavedra	Industrial	901	1			12.83
1.42	Manuel María Mallarino	Las Ceibas	1019		1		7.26
1.42	Juan de Ampudia	La Base	1658		1		11.81
1.42	Juana Caicedo y Cuero	El Lido	1714			1	61.02
1.42	Julio Caicedo y Téllez	Nueva Floresta	1904			1	27.12
1.42	Rafael Navia Varón	Departamental	1988	1			14.16
1.42	Las Américas	Las Américas	2036		1		14.50
1.42	La Esperanza	Alto Jordán	3237	1			69.15
1.42	Eustaquio Palacios	Lido	3944			1	140.42
Semester fee (million COP)	**Higher Education**						
9.67	Universidad Javeriana	Pance	16624	1			10 046.17
8.94	Universidad Libre	Santa Isabel	15961			1	2 973.29
9.69	Universidad ICESI	Pance	14820	1			8 972.28
2.29	Escuela Nacional del Deporte	Champagnat	6016			1	143.22
3.15	Fundación Lumen Gentium	Pance	6436	1			1 266.40
2.15	Institución Antonio Camacho	San Vicente	14097	1	1	1	1 262.86
1.91	Centro de Estudios Profesionales	Champagnat	8736			1	173.76
1.91	Academia de Dibujo Profesional	Santa Monica	4799		1	1	382.54
11.72	Escuela Militar de Aviación	Base Aerea	1518		1	1	370.60

Table 4.8: Chosen undergraduate programs to compute average semester fee for each Higher Education Institution.

Higher Education Institution	Main Undergraduate Programs
Pontificia Universidad Javeriana	Law Civil engineering Medicine
Universidad de San Buenaventura	Law Electronic engineering Psychology
Universidad Libre	Law Systems engineering Medicine
Universidad ICESI	Industrial Design Anthropology Economy
Universidad Autónoma de Occidente	Economy Electronic engineering Film and digital media
Escuela Nacional del Deporte	Business administration Sports professional Sports technologist
Fundación Universitaria Católica Lumen Gentium	Law Industrial engineering Psychology
Institución Universitaria Antonio José Camacho	Business administration Systems engineering Anthropology
Centro Colombiano de Estudios Profesionales	Technician in Foreign trade Technician in Mechatronics Technician in Environmental administration
Fundación Academia de Dibujo Profesional	Single registration fee
Corporación de Estudios Superiores Salamandra	Single registration fee
Escuela Militar de Aviación Marco Fidel Suárez	Single registration fee for men Single registration fee for women

Total estimated cost of power cuts during minor floods affecting educational institutions is over 11 million euros (Table 4.9)

Table 4.9: Estimated cost of classes missed during minor-flood power cuts in Cali.

Education level	*Institutions affected*	*Days missed*	*Students affected*	*Cost of days missed (COP)*
Secondary	51	89	102,048	1,357,513,402.00
Higher	12	50	122,291	38,262,688,186.00
			Total	**39,620,201,588.00**
				(€ 11,179,704)

4.4 Analysis of results

4.4.1 Aedes aegypti breeding

The trend in the values of Aedic Index of getting triggered on minor-flood days and fading out about a month later was more or less the same across all affected neighborhoods in different communes and on different SEL (Figure 4.1), revealing that minor floods set the minimum conditions that *Aedes aegypti* need to lay eggs, to allow them to develop into larvae and pupae and to reach the final stage all over the city. Evidence showed that commune 17, with a high SEL and a regular trash collection system, also reported a large number of dengue cases (Rojas 2016b): those authors could not explain why so many dengue cases occurred in this area, but for this analysis this was to be expected, as this commune has experienced numerous minor floods in the last 18 years.

Mosquito eggs can survive in dry conditions for a few months, and two days in contact with water can be enough for the mosquito to emerge from the pupal stage (EPA 2017). This period coincides with the expected duration of a minor flood, after which stagnated water can stay even longer in drainages given factors such as topography, sewage cleaning and evaporation after the precipitation event.

Aedic Index surveys taken exactly on the day of the minor flood in the affected neighborhoods is rather low, probably because rain itself and its impacts discourage such activities; this could be improved if the coverage and the frequency of these surveys is improved, or if data takers get equipped with appropriate protective clothing

to carry out campaigns right on minor-flood days as they are detected, since this would be an important breaking point in the trend.

On another issue, the comparison between the cost of preventing mosquitoes from entering a house (about US$ 2.00 per month) and the cost of treating a patient with dengue (between US$ 599.00 and US$ 2,361.00) shows once again that prevention is ultimately better than the cure. How much better would be to prevent stagnated water from increasing the number of mosquitos in the city and reduce household prevention measures?

4.4.2 Traffic impedance

The total delay for all travelers during minor-flood days is clearly underestimated, since it was only computed for noon rush hour, and for main and secondary roads in the absence of more detailed information, both in time and space. If tertiary roads crossing neighborhood blocks were included, distances would be longer, and so would delays. Evidently, noon rush hour is the worst-case scenario regarding number of commuters affected, but at the same time is the least problematic scenario regarding speed reduction, since speeds are already low at this hour during non-minor-flood days; the worst-case scenario regarding speed would be during non-rush hours when commuters can travel normally at higher speeds: such information is currently also missing.

It is worth noting that pavement distress, exemplified by pavement deterioration and shortening of service life due to environmental conditions (Moreno-Navarro et al. 2016; Peyman Babashamsi et al. 2015), which were beyond the scope of this study, would certainly increase the traffic impedance and the frequency of accidents (Sabir et al. 2011) anytime of the year, and not only on minor-flood days, as well as cost overruns for citizens in gasoline and auto parts (Agbelie et al. 2016).

Trips to and from Cali were also not considered due to lack of origin/destination detail, but since one of the two interstate roads to the Pacific harbor crosses Cali (Route 1901: *Cali-Loboguerrero-Buenaventura*), any delays within the city would directly affect freight costs for cargo transportation.

4.4.3 Power cuts

In countries with little to no access to reliable energy, the quickest and easiest way to measure losses due to power cuts – which also gives the lower costs – is to count how many kilowatts per hour (KWh) were not provided and then multiply them by their commercial value (Franco et al. 2017). Since the cost of electricity in a hydropower-based country like Colombia is quite low, only a few hundred euro would be incurred. The affected healthcare institutions in Cali consumed a total of 2,003.6 KWh during the 28 minor floods (33 days) with power cuts: with € 0.16/KWh (EMCALI 2019), this energy loss would only amount to € 318. However, when it comes to electricity, the real loss is not how much it costs to have it but how much it costs not to have it.

Services in health institutions are highly restricted during power cuts, even if they count on power plants since they are dedicated to emergency services and keeping medicines and substances frozen. Every time there is a power cut, general and specialist appointments are postponed, and patients must wait longer than usual, even if their appointment was not on the day of the power cut (this study only counted appointments on the power cut day).

Moreover, nosocomial infections (infections acquired in hospitals), which thrive in hospitals where hygiene management is not optimal, have more chances of emerging during power cuts because lighting and air conditioning is reduced, which hampers cleaning activities.

Deficits created by power cuts in educational institutions are also not so visible, because all students finish the academic year on a fixed calendar date regardless of whether there have been power cuts or not. However, the rush to finish the topics not dealt with during power cut days, the slow pace to catch up activities after the interruptions, and the discomfort during classes without air conditioning, computers and lights are situations that altogether disturb the learning experience, leading to problems that eventually may come to light during further professional work.

4.4.4 Economic losses in the city reinforcing illegal practices

Summing up all economic loss estimations performed in this analysis gives a rather underestimated figure of 20 million euros between 2000-2017.

Illegal microloans (*"préstamos gota a gota"*) are a phenomenon that has spread over Cali: these microloans are offered by criminal organizations that mainly seek to money launder incomes from drug trafficking. Authorities estimate that every day in all communes of the city, there are 400 to 500 debt collectors threating, beating, and even killing debtors (El País de Cali 2019). The lending activity itself is not considered a crime and thus not punished, because victims access these credits voluntarily.

Debtors borrow the money at a minimum interest rate of 20%: usual borrowed amounts are below COP 1 million (€ 283). Prosecutor's office in Cali has estimated that these organizations may handle annual cash inflows over COP 200 million (around € 57,000.00, (ADN Cali 2019)).

Multiplying this figure by the 18 years of the analysis time frame (2000 to 2017) results in over € 1 million: comparing this figure with the silent 20 million euros that people in Cali lose without knowing should give an idea that the hidden risks from minor floods push people to get involved in illegal practices.

4.5 Recommendations

Developing countries like Colombia where annual average income per capita is over US$ 10,000 may fall into what is known as the 'average income trap', because this is followed by sustained periods of little to no economic growth, and it seems difficult to attain higher development levels again (Turriago Hoyos 2018).

The big challenge this trap poses is that while it slowly drives the country to a previous and more precarious stage, it does not feel like an unwelcome situation to most citizens, who have reached certain prosperity in the conventional economy sectors.

There are ways to overcome this trap, like boosting the economy by improving working force productivity, and breaking into new markets through capacity building leading to increasing demand for new occupations.

Underestimations of the consequences of only three aspects regarding minor floods in Cali added up to € 20 million in less than 20 years, which easily equals 20% of the current annual capital resources for Cali, or the average annual budget for three small towns in the Valle del Cauca state (Cali Chamber of Commerce 2017).

These expenses have nothing to do directly with extreme events or climate change scenarios. They are the cumulated cost of poorly designed works combined with cultural malpractices over decades in the city. If more minor adverse events, like forest fires, landslides, earthquakes, water pollution, or combinations of them were considered, economic loss could easily increase five-fold. The money lost is not for covering basic needs, but for investment in innovation, and for expanding businesses to create employment, e.g., for heads of households of the more than 4,000 families still living on the Cauca River dike waiting for better opportunities.

Monitoring minor floods in a more accurate way and tracing the infrastructure weaknesses and cultural malpractices that lead to them (such as dumping waste in forbidden places and connecting illegal sewerage to the drainage network) is an initial step to reduce economic losses.

The presence of *Aedes aegypti* mosquitoes in Cali can be reduced by keeping potential nesting spots water-free. This study shows how places affected by minor floods considerably enhance AI, thus any effort to reduce stagnated water along with other solutions at household level will also help reduce the presence of mosquitoes.

Power cuts are a consequence of an electricity system based almost completely on aerial power lines, which are extremely vulnerable to wind gusts and falling trees and branches. Installing electricity lines underground must be considered.

5 HYDRODYNAMIC SIMULATION OF DRAINAGE NETWORK RESPONSE TO RAINFALL EVENTS IN A NEIGHBORHOOD IN CALI

Drainage networks in Cali convey storm water from neighborhoods through pipelines connected downstream to open channels that deliver the water to the *Cauca* River. Most neighborhoods in Cali have experienced minor floods at least once (229 neighborhoods out of a total of 336, Figure 5.1), which makes it difficult to choose only one for the analysis. However, spatial autocorrelation tests like Moran test (performed in R through function *moran.test*) can help identify regions within the city where neighborhoods have similar behaviors towards minor floods.

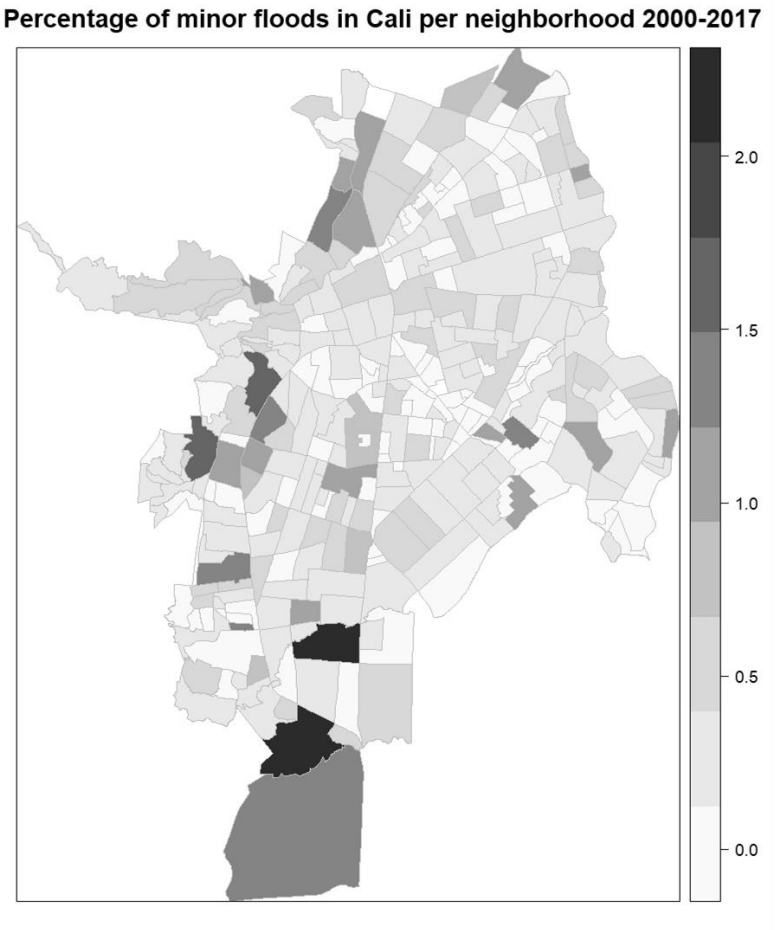

Figure 5.1: Minor floods reported per neighborhood in Cali as percentages of the total (603 times neighborhoods have been reported as flooded).

Spatial autocorrelation tests such as Moran I test (Moran 1950) compare the behavior of each neighborhood with its surroundings (at least three other neighborhoods, Figure 5.2 left), based on the neighborhoods location and their associated values (in this case Events) simultaneously. Moran tests assess whether the spatial pattern of these values is grouped, disperse, or random, based on how far the surrounding values deviate from the value of the neighborhood under consideration.

The Moran test then clusters the neighborhoods in one of four categories: high-high, for neighborhoods with high count of minor floods experienced surrounded also by other neighborhoods with high numbers of minor floods reported; high-low, for neighborhoods with high numbers of minor floods surrounded by neighborhoods with low numbers of minor floods; low-high, for neighborhoods with low numbers of minor floods surrounded by neighborhoods with high count of minor floods; and low-low, for neighborhoods with low numbers of minor floods surrounded also by other neighborhoods with low numbers of minor floods. The test classifies high and low values according to those maximum and minimum number of minor floods experienced per neighborhood in the database (13 and 0).

For this analysis, the neighborhoods with high-high combination are of greater interest because it means that the improvements and changes made to them are likely to improve conditions in their surrounding neighborhoods as well.

Seven high-high neighborhoods were statistically significant (Figure 5.2, right): *El Ingenio*, *El Lido*, *Pance*, *San Vicente*, *Santa Mónica*, *Ciudad Jardín*, and *Tequendama*. From these neighborhoods, Santa Mónica was chosen for the following relative advantages over the other six: it lies on the piedmont, thus having a wide range of slopes; it is far from the Cauca river, so direct backflow effects from it are not likely to cause minor floods; it has a medium-high socioeconomic level on average, so it is not expected that poor infrastructure and planning are relevant explanations to flooding; and it has a varied land use, including residential areas, industry and commerce.

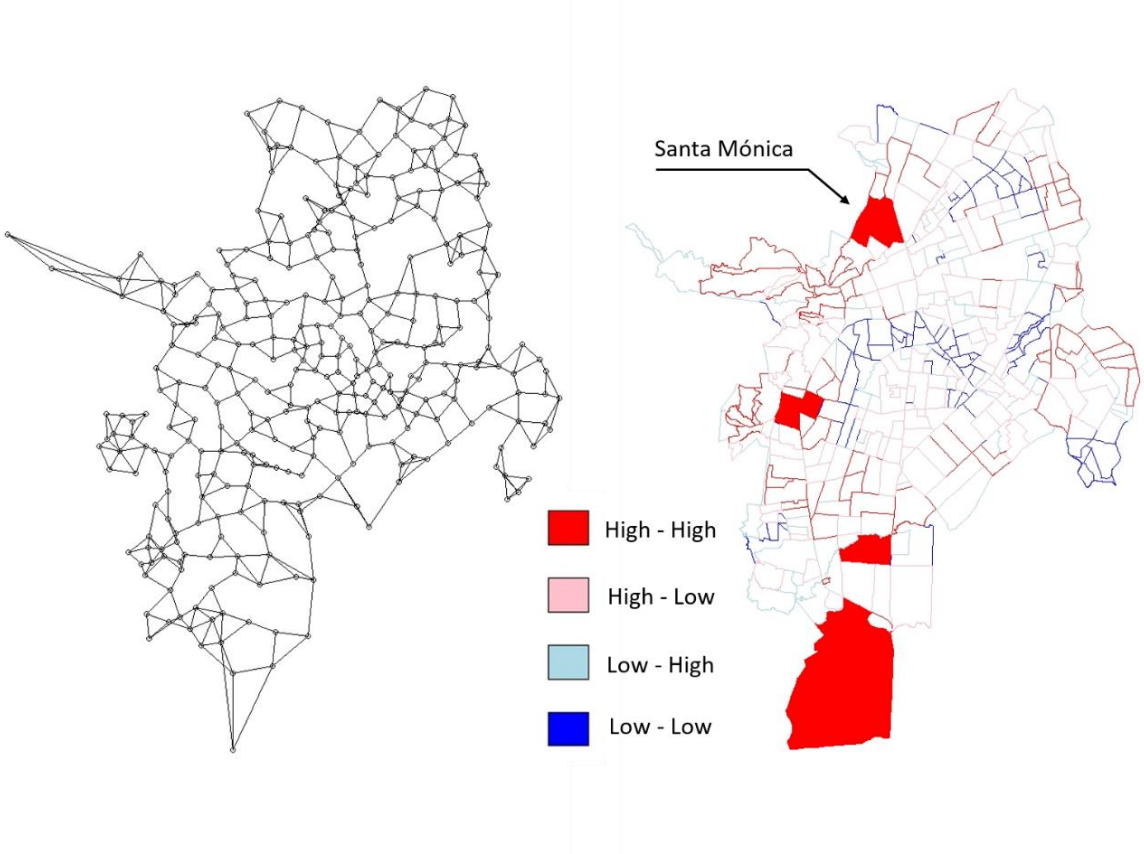

Figure 5.2: Each neighborhood is connected to at least three other neighborhoods for the network used in Moran I test (left); results from Moran I test with neighborhoods in solid color are statistically significant (right).

5.1 Input data

For this analysis, Santa Monica neighborhood was divided into micro-basins in order to have a high-resolution detail that allowed to identify streets and manholes, their flooding volume and flooding time. Since minor floods are related both to drainage response and topographic features, a software that includes these effects (EPA Storm Water Management Model-SWMM, EPA and CDM 2012) was used to simulate storms and the neighborhood's drainage response.

SWMM is a well-known free open-source software, easy to couple with GIS tools and to perform sensitivity analysis of its parameters (Huang and Jin 2019). Its dynamic rainfall-runoff simulation of runoff quantity and quality can be made for single events or long-term consecutive rainfall events in urban areas (EPA and CDM 2012).

Besides simulating stormwater flow under normal conditions, SWMM was also used to simulate the effects of installing LIDS and of clogging conditions in the drainage network.

5.1.1 Neighborhood input data

- A slope map is derived from the previous terrain data, keeping its 5-meter horizontal resolution and 1-meter vertical resolution (ArcMap Surface to Slope tool).
- Flow direction is obtained for each pixel after removing sinks and peaks (Figure 5.3), which are errors in the elevation of single pixels due to rounding of elevations to integer numbers, which make them look illogically higher or lower than expected from the rest of the terrain. Objects on and below the ground level, such as buildings or empty water bodies, sometimes are not removed from the terrain data and can also produce these peaks and sinks, as long as they are smaller than the size of a pixel (5m X 5m), which is not expected for this high resolution. ArcMap fill tool removes these sinks and peaks.

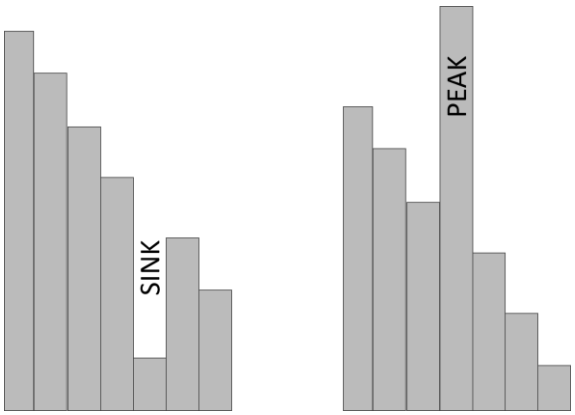

Figure 5.3: Single pixels considered as sinks or peaks, because of their out-of-sequence standing with respect to pixels nearby that may indicate errors in elevation.

- Flow direction has eight possible routes (North, Northeast, East, Southeast, South, Southwest, West and Northwest), based on elevation differences among

pixels (Figure 5.4, below). Pipelines and channels may have opposite slopes compared to the terrain.

- Land use is classified in three categories for Santa Monica: residential areas, service facilities, and mixed use, the latter including residential areas, commercial buildings, specialized services, and low-impact industry (Figure 5.5, upper left). Mixed use category is composed by residential areas in 50% (Alcaldía de Santiago de Cali 2018).

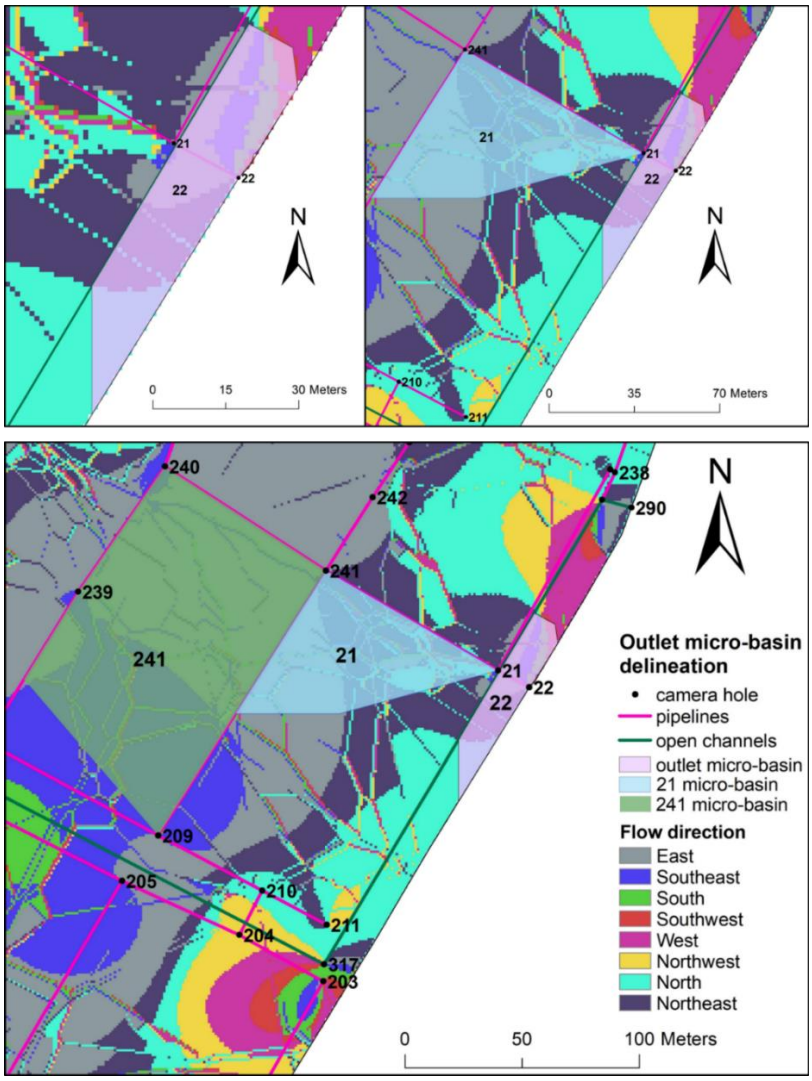

Figure 5.4: Micro-basin delineation. Micro-basin #22 drains to manhole #22 (upper left); micro-basin #21 drains into manhole #21, draining in turn to #22 (upper right); micro-basin #241 drains into manhole #241, and then into #21 (below).

- Built areas are shown as polygons (Figure 5.5, upper right) (IDESC Geoportal 2018).
- Urban partitions, also shown as polygons, are units within the neighborhood that include all built and green areas, leaving out only streets and roads, seen in white (Figure 5.5, upper left).
- The drainage network is presented in shape files detailing pipelines, channels and manholes (Figure 5.5, below). Some attributes are also available (Table 5.1). Information was supplied by the Utility services company (EMCALI 2017b), except for the width and depth of open channels, checked on site.

Table 5.1: Attributes available for drainage network components

Component	Fields
Pipe	ID, name, diameter, length, material, start and end invert elevation
Channel	Depth,width, side slopes, and length
Network	Type of sewer system (storm drain, sewer, or combined)
Manhole	ID, location, and rim elevation

5.2 Methodology

Time series from rainfall events, land-use and soil information, topography, and demographics for every micro-basin in Santa Monica, along with drainage network details for the neighborhood must be entered to SWMM model.

5.2.1 Micro-basin delineation for Santa Monica

Flow direction was used to delineate micro-basins, as water seeks the lowest point to drain; drainage pipelines are also an aid to delineate micro-basins despite being underground, because they are laid alongside streets with sidewalks and façades that convey water downward; since one of the main differences between a normal flood and a minor flood is that in the latter water does not flow into homes, maximum water depth allowed in the simulations cannot go past door thresholds (about 30 cm above ground level). Open channels were also used as limits for micro-basins.

The delineation process starts by the perimeter outlets (only those manholes draining water out of the neighborhood): the micro-basin for each perimeter outlet is

defined as all the surface area draining to it (Figure 5.4, upper left). The process repeats itself afterwards by visually defining micro-basins draining to perimeter outlet micro-basins (Figure 5.4, upper right and below), until the whole neighborhood area is converted to micro-basins. At the end of the process, 170 micro-basins were delineated for Santa Monica, with an average size of 3,556.74 m^2 each (about one street block), with one as small as 2.5 m^2 and one as large as 51,850 m^2 (about five street blocks). The neighborhood area is 620,616 m^2, slightly larger than the sum of the microbasins (604,645.3 m^2) due to the presence of endorheic areas (Figure 5.6).

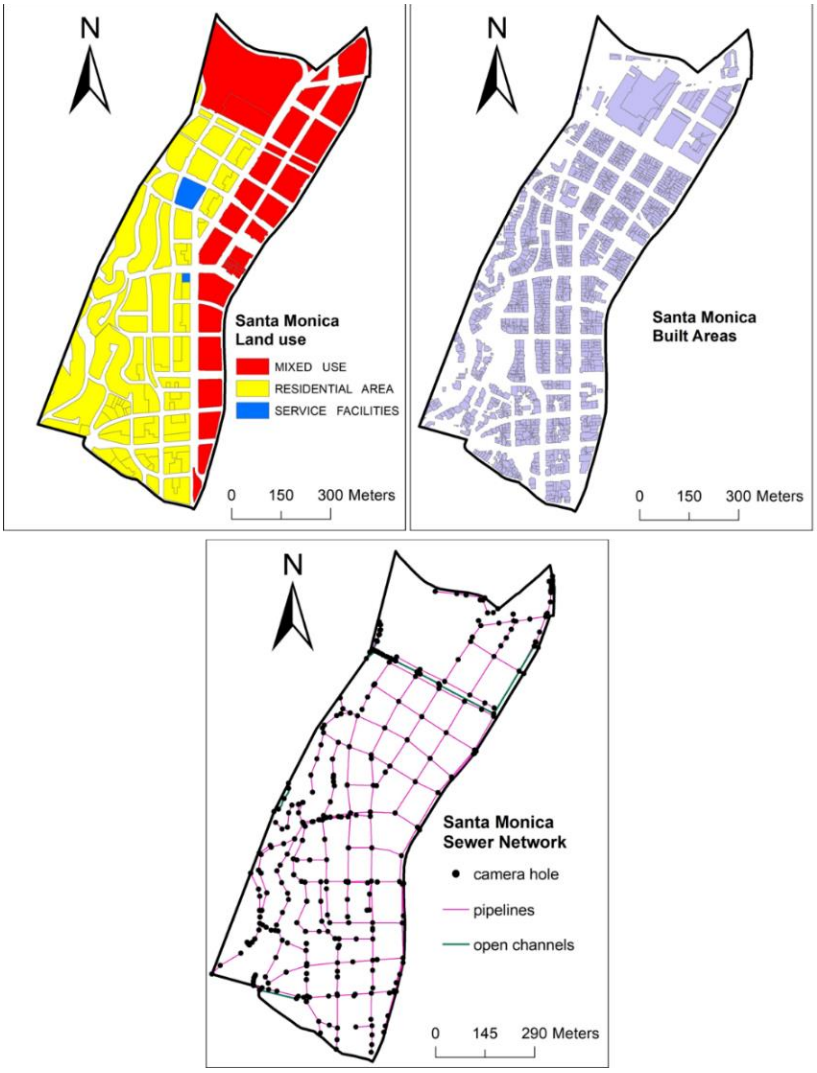

Figure 5.5: Land use in Santa Monica (upper left); built areas (upper right); drainage network components (below).

There are few areas not draining anywhere, as pixel flow direction keeps bringing flow inwards. These areas are considered endorheic micro-basins (Figure 5.6); validation of such behavior was made on site, where local people confirmed that two of these areas get frequently flooded during rains. No floods were noticed for the third one (Figure 5.6, bottom), but some people did observe floods just a block away.

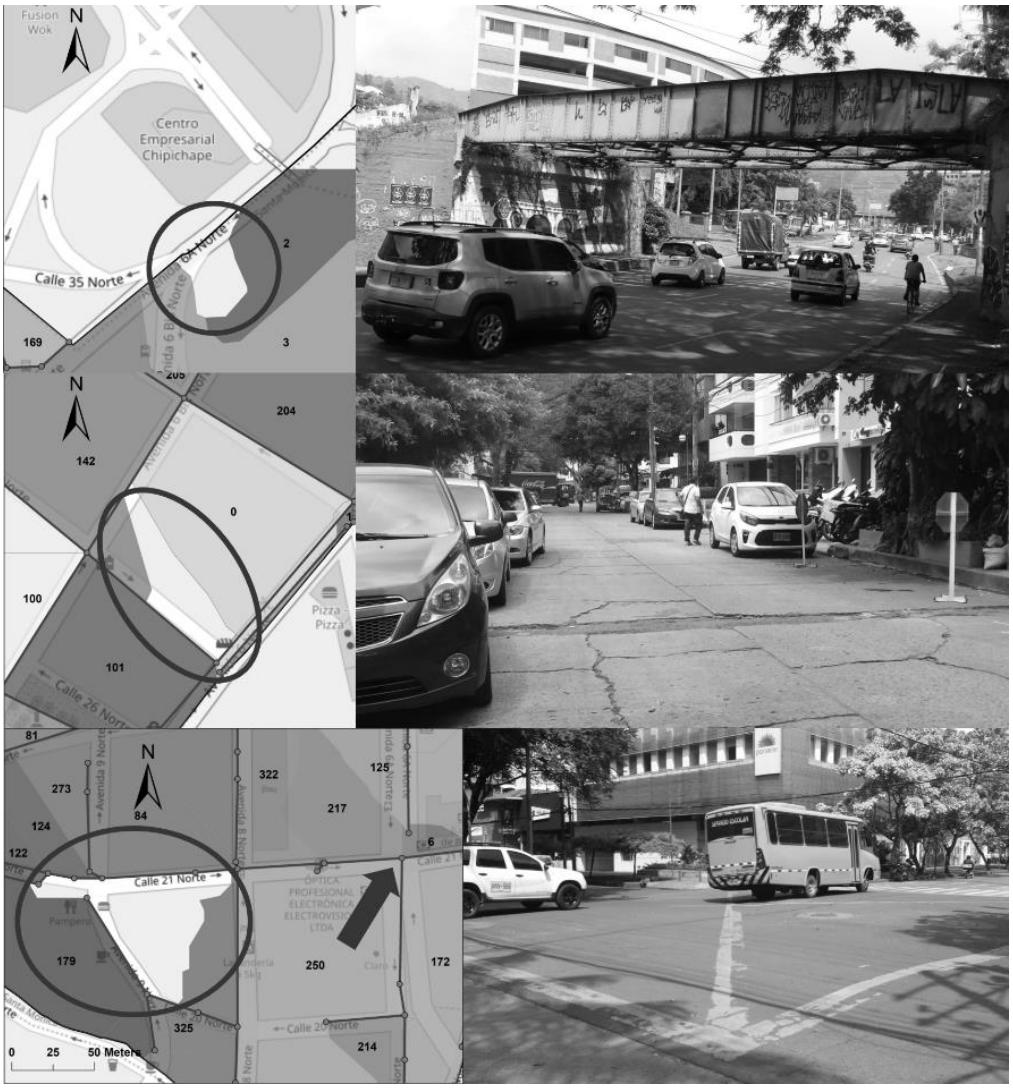

Figure 5.6: Endorheic micro-basins in Santa Monica: 6th Ave. underpass (top), business street (center), and junction pointed on map by red arrow (bottom).

5.2.2 Micro-basin attributes

Demographics, land use/land coverage, soil properties, and micro-basin characterization were estimated as input data for SWMM model:

- *Land cover*: Each micro-basin contains built area, green area, and/or paved roads (Figure 5.7). Through map algebra (equation 5.1) and ArcMap intersection tools, all land cover areas are computed

$$PRA = MA - UP$$
$$GA = UP - BA \quad 5.1$$

*w*here PRA = paved-road area, MA = micro-basin area, UP = urban partition area, GA = green area and BA = built area.

- *Population*: Santa Monica has a projected population for 2017 of 3,796 inhabitants (DANE 2010); dividing it by the neighborhood area (620,616 m^2) gives a population density of 61.17 Person/Ha. People living on each micro-basin are estimated with this density, considering that mixed-use areas are 50% residential (equation 5.2)

$$POP = DENS \times \left(RA + \frac{MU}{2}\right) \quad 5.2$$

where POP = micro-basin population, DENS = population density for Santa Monica, RA = residential area in the micro-basin, and MU = mixed-use area in the micro-basin.

- *Width (m)*: it is computed as the micro-basin area divided by its maximum draining length, which is the longest distance that the water must travel to reach the micro-basin outlet.

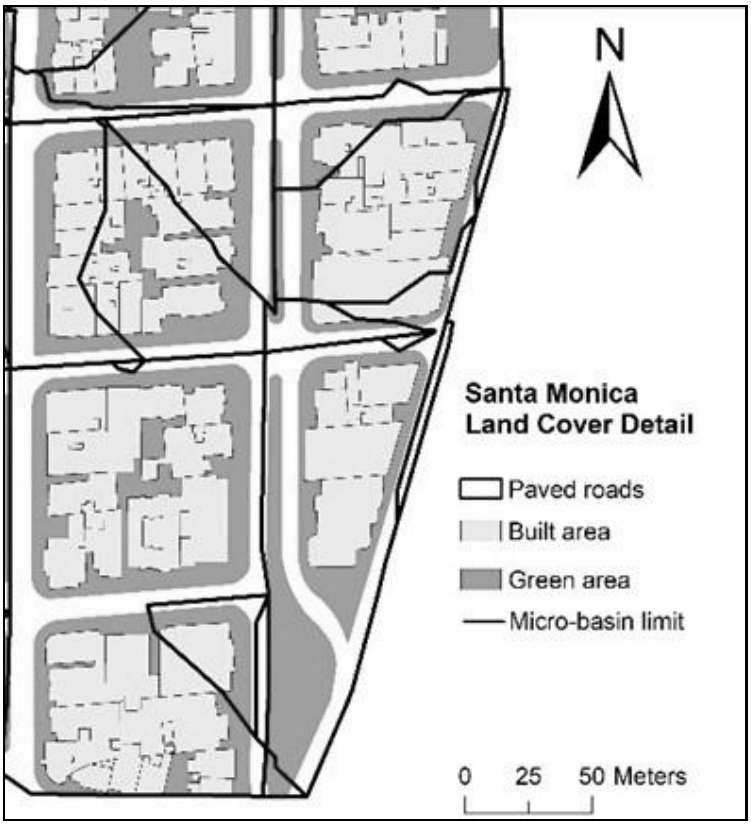

Figure 5.7: Detail of land-cover in Santa Monica.

- Infiltration parameters: soil properties determine infiltration parameters for SWMM. Hydraulic conductivity, suction head, and initial moisture deficit are the parameters requested by SWMM for infiltration calculations and they depend on the type of soil (clay, silt, sand, among others). Micro-basin areas were intersected with geotechnical zones from previous seismic studies in the city (Alvarado A et al 2005) that also describe and delineate the type of soils present (Table 5.2).
- Surface roughness: roughness was expressed for both impervious and pervious areas as Manning's n coefficients. For impervious areas, roughness is the area-weighted average between streets and roads (n=0.013) and buildings (n=0.014). Pervious areas had a constant value (n=0,024 for dense green areas).

Table 5.2: Soil and hydraulic properties of geo-technical zones in Santa Monica.

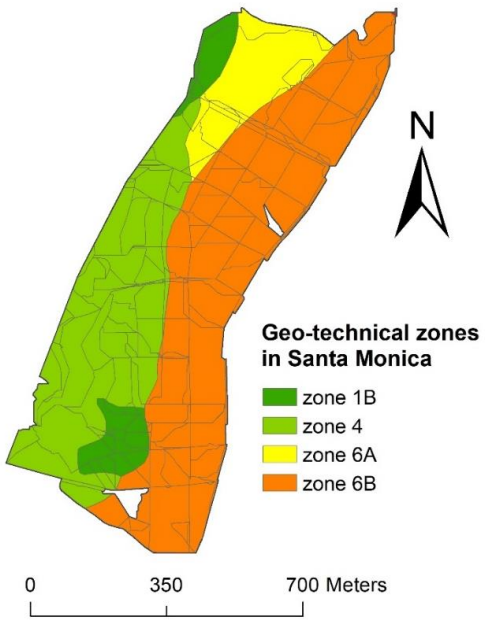

Zone	Soil description
1B	Sedimentary rock and material (CL, MH, SC)
4	Colluvial soil (CL, MH, CH)
6A	*Menga* and *El Bosque* alluvial fan (CH, MH)
6B	Cali middle alluvial fan (MH, CH, ML)

CL **Lean clay;** ***MH*** **Heavy silt;** ***SC*** **Clayey sand;**
CH **Heavy clay;** ***ML*** **Lean silt**

Zone	Ksat	ψ	IMD
1B	1.44	206.3	0.46
4	0.51	233.0	0.47
6A	1.78	204.5	0.47
6B	3.39	193.0	0.48

Ksat **Hydraulic conductivity [mm/h];**
ψ suction head [mm]
IMD initial moisture deficit [fraction]

5.2.3 Settings for Storm Water Management Model

SWMM model conceptualizes a drainage system as a series of environmental compartments: atmosphere, land surface, groundwater, and transport (Figure 5.8). Interactions between these compartments are mostly pre-established, but a few selections must be made according to user needs.

- *Infiltration model*: SWMM uses five different models to describe rainfall infiltration from the pervious area of a sub-catchment into the unsaturated upper soil zone (classic and modified Horton, classic and modified Green-Ampt, and SCS Curve Number). For this study, Horton models were discarded because there were no empirical data from infiltration rates; nonetheless, there were enough secondary data on soil properties, and sensitivity analysis from model defaults to perform the Green-Ampt model, which depletes moisture deficit in the top soil layer during initial periods of low rainfall, giving a more realistic infiltration behavior for urban basins during storms with initial rainfall intensities

under soil's saturated hydraulic conductivity (EPA and CDM 2012). This model considers compaction of urban soil and antecedent conditions (Rosa et al. 2015).

- *Routing model*: flow routing within a conduit is governed by the conservation of mass and momentum equations for gradually varied, unsteady flow. SWMM user chooses the level of sophistication to solve Saint-Venant equations (steady, kinematic, and dynamic). Steady and kinematic flow routing cannot account for channel storage, backwater effects, flow reversal or pressurized flow, and are insensitive to time steps used; dynamic wave routing was then selected because it represents fully pressurized flow in closed conduits: it is the only routing model that can simulate flooding, and take flooded water out of the system or pond it atop nodes to re-enter the drainage system. It is the chosen method to simulate backwater effects due to downstream flow restrictions, and its numerical stability for thirty-second or shorter time steps (EPA and CDM 2012).
- *Depression storage (m)*: it is the height of water that a micro-basin can store above its surface. As it was assumed before, this height cannot go past door sills, otherwise it would be a normal flood. The depression storage is set to 30 cm.

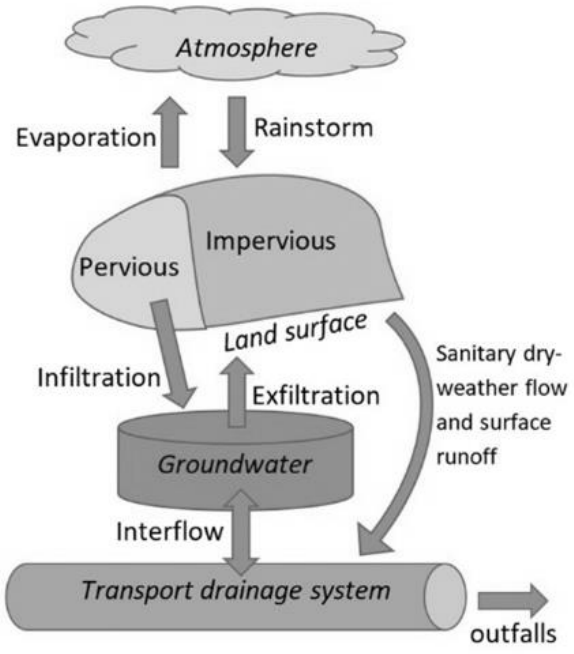

Figure 5.8: SWMM interactions between compartments of a drainage system.

5.2.4 Rainfall event simulations on Santa Monica with SWMM

Four original FNFA rainfall events that caused minor floods in Santa Monica were used as input for the model (Figure 5.9). Due to the closeness between Santa Monica and *Colegio San Luis* rainfall station, rainfall data is taken only from this station.

Rainfall events chosen are considered only until the end of the reported minor-flood day (midnight), since further rainfall would not be the cause of the beginning of the minor flood. Rainfall events cover different durations (from hours to a few days), different average intensity values (1.24 mm/h – 5.44 mm/h) and different time distributions (skewed towards the beginning, skewed towards the end, intermittent, and homogeneous). Evaporation daily rates recorded at a sugar cane research center in Cali (Cenicaña 2019) were entered to SWMM for the corresponding rainfall event dates.

Total rainfall values from all 744 events were fitted into a Pearson 6 probability distribution function (PDF) using EasyFit software (Mathwave Technologies 2013), which gave it a significant goodness of fit ranked third (Kolmogorov Smirnov and Chi-Squared) and second (Anderson Darling) among 61 different PDFs. Parameters from Pearson 6 are $\alpha1=0.97545$, $\alpha2=4.7215$, and $\beta=274.55$. The probability of occurrence for each of the four historic events according to this chosen PDF is shown in Figure 5.9.

5.2.5 Simulation considering flood in surrounding neighborhoods

The drainage network is composed by junctions, links and subcatchments in SWMM: junctions correspond to manholes, links can be pipelines or open channels, and subcatchments are the micro-basins previously defined for Santa Monica, feeding rainfall water to manholes. A drainage network can function properly inside a neighborhood if water is drained out of it. Nevertheless, whenever a rainfall event occurs on a neighborhood, it is likely that surrounding neighborhoods experience that same rainfall event too and get congested (especially in the Santa Monica case with its high-high Moran test category, Figure 5.2).

Rainfall event 1 (skewed towards the end)

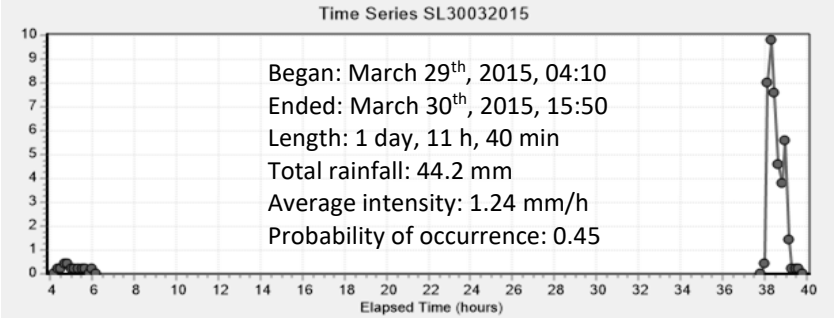

Rainfall event 2 (skewed towards the beginning)

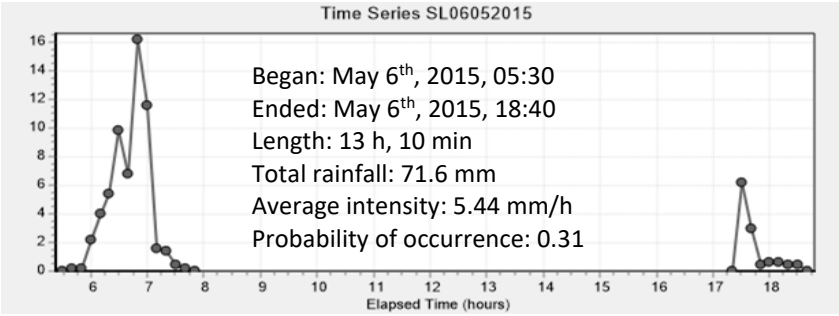

Rainfall event 3 (intermittent)

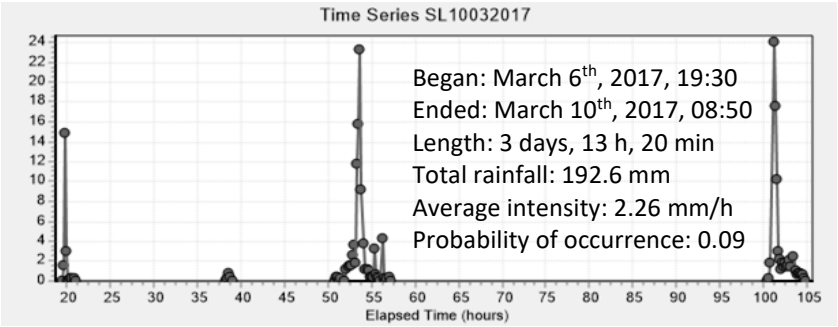

Rainfall event 4 (homogeneous)

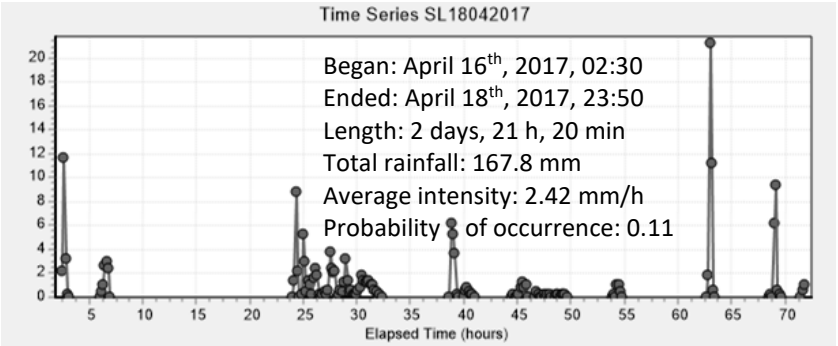

Figure 5.9: Historic rainfall events over Santa Monica that have caused minor floods and have been chosen for simulation in SWMM.

Perimeter outlets – pipelines that drain water out of the neighborhood – do not end in junctions, but in outfalls, which are terminal nodes that determine final downstream boundaries. In order to simulate floods in the neighborhoods downstream Santa Monica, these boundaries were gradually changed from a condition of empty pipelines in the downstream neighborhoods (0% outlet diameter), through flowing full (100% outlet diameter), and finally to flow under 2-meter hydrostatic pressure.

Flooding volume refers to the volume of water coming out from the manholes that cannot go back into the drainage network and cannot stay in the neighborhood, thus causing minor floods in neighborhoods downstream.

Depth storage is the flooding level of the minor flood: it is the height of water level that micro-basins can hold on top and send back to the drainage network in impermeable areas, or infiltrate to the soil in permeable areas: it cannot be higher than 30 cm (height limit between a minor flood and a regular flood).

Infiltration is the volume of water that went into the soil in permeable areas.

Simulation under blocked pipelines in the neighborhood

This simulation reduced the cross-section area of every pipeline and open channel in the neighborhood to find out the effects of partially blocked pipelines on flooding loss volumes compared to normal conditions (0% cross section blocked). The default condition was rainfall event 4 with 0% water level in surrounding neighborhoods and 5-mm depth storage (Table 5.4).

Simulation with LIDS

LIDS are systems that mimic natural processes of infiltration, evapotranspiration and use of stormwater to reduce peak flows in urban areas and protect water quality and aquatic habitat (EPA 2018). Examples of LIDS are: permeable pavement, rain gardens, bio-retention cells, and green roofs (EPA and CDM 2012).

LIDS in SWMM are a combination of vertical layers with properties defined on a per-unit-area basis, which allows them to be easily projected on different micro-basins. SWMM performs a moisture balance within each layer and keeps track of how much water moves in between layers and is stored within (EPA and CDM 2012).

Table 5.3: Flooding and infiltration volumes in Santa Monica under simulation of flood in surrounding neighborhoods.

		Water level filling perimeter outlets						
		0%	40%	80%	100%	200%		
	Rain 1	Precipitation inflow: 267.3 x 100 m³						
Depth storage		Volume (x 100 m³)						
5 mm	Flooding volume	165.7	166.0	166.3	166.4	167.0	Infiltration	78.6
10 mm	Flooding volume	140.6	141.0	141.2	141.3	141.9	Infiltration	84.7
20 mm	Flooding volume	92.2	92.6	92.8	92.9	93.5	Infiltration	95.4
	Rain 2	Precipitation inflow: 432.9 x 100 m³						
Depth storage		Volume (x 100 m³)						
5 mm	Flooding volume	289.6	290.0	290.3	290.5	291.2	Infiltration	120.0
10 mm	Flooding volume	262.8	263.1	263.4	263.6	264.3	Infiltration	128.1
20 mm	Flooding volume	212.3	212.6	212.9	213.1	213.8	Infiltration	140.9
50 mm	Flooding volume	76.6	76.9	77.2	77.3	78.1	Infiltration	163.1
	Rain 3	Precipitation inflow: 1,164.6 x 100 m³						
Depth storage		Volume (x 100 m³)						
5 mm	Flooding volume	882.2	883.1	883.8	884.2	886.0	Infiltration	258.0
10 mm	Flooding volume	847.6	848.5	849.2	849.5	851.3	Infiltration	273.5
20 mm	Flooding volume	782.6	783.3	783.9	784.2	785.7	Infiltration	301.3
50 mm	Flooding volume	588.1	588.7	589.3	589.6	590.9	Infiltration	383.1
100 mm	Flooding volume	342.7	343.3	343.8	344.1	345.4	Infiltration	403.4
150 mm	Flooding volume	155.9	156.2	156.6	156.7	157.4	Infiltration	403.4
	Rain 4	Precipitation inflow: 1,014.6 x 100 m³						
Depth storage		Volume (x 100 m³)						
5 mm	Flooding volume	708.6	709.3	710.0	710.4	711.9	Infiltration	280.3
10 mm	Flooding volume	673.6	674.3	674.9	675.3	676.9	Infiltration	296.1
20 mm	Flooding volume	613.9	614.6	615.2	615.6	617.1	Infiltration	318.0
50 mm	Flooding volume	457.2	457.8	458.3	458.6	459.8	Infiltration	353.2
100 mm	Flooding volume	249.6	250.1	250.4	250.6	251.7	Infiltration	354.8
150 mm	Flooding volume	62.5	62.8	63.0	63.1	63.7	Infiltration	354.8

Table 5.4: Flood volume increase when simulating reduction in pipeline cross-sections

Rain 4 (0% water level)	**Blocked cross-section area**					
	0%	10%	30%	50%	70%	90%
Flooding volume (m^3)	70,860	73,694	79,718	86,095	92,968	100,409
Flooding increase (%)	0	4	12.5	21.5	31.2	41.7

EPA SWMM may send LIDS outflow directly to the drainage network or to the pervious area from each micro-basin. Both options are executed during the simulations.

LIDS settings are classified into six process layers: surface layer, pavement layer, soil layer, storage layer, drain system, and drainage mat. Not all the latter layers are present in every LIDS: it depends on the specific parameters of each one.

Simulations for porous pavement, rain gardens and green roofs were performed, and all parameters from each LIDS were entered covering their entire range of values to see which ones optimize LIDS overall performance; each parameter is modified at a time, leaving default values in the others. Flooding loss (in hundreds of m^3) was used to compare normal drainage performance and performance with LIDS.

Rainfall event 3 with no flooding in surrounding neighborhoods and 5-mm depth storage is the default event shown (Table 5.5, Table 5.6 Table 5.7), but all 4 rainfall events with similar conditions were used for all simulations.

Porous pavement

Permeable pavement systems are excavated areas filled with gravel and paved over with a porous concrete or asphalt mix (EPA and CDM 2012). SWMM controls parameters in five process layers: surface, pavement, soil, storage, and drain system (Figure 5.10). The area given to porous pavement is the paved-road area (PRA, equation 5.1).

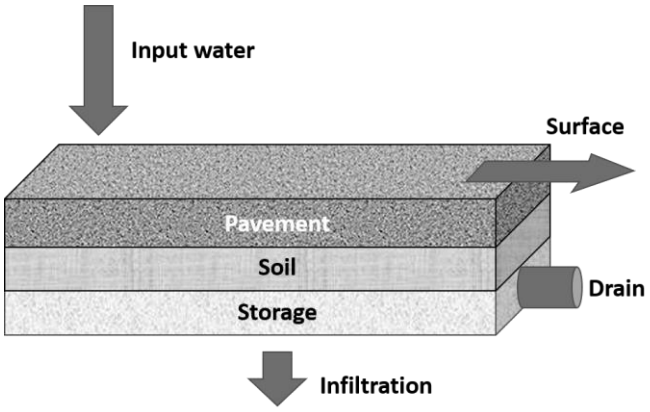

Figure 5.10: Porous pavement conveys rainfall water on the surface as flooding volume, drains it to network or permeable areas, or infiltrates it below where possible.

Table 5.5: Porous pavement performance on flooding volume under parameter adjustment.

Porous pavement for Rainfall event 3 (0% water level, 5-mm depth storage)				
Flooding loss volume (x100 m^3)	with no porous pavement (pp)		882.2	
Variable	**Default value**	**Range tested**	**Flooding (x100 m^3)**	
			To pervious	**To drainage**
Surface berm height (mm)	0	0 - 100	471.6 - 471.1	789.2 - 781.4
Surface roughness (Manning 's n)	0.1	0.009 - 0.2	471.6 - 470.4	789.7 - 782.3
Surface slope (%)	1	0 - 20	472.5 - 472.4	790.3 - 790.0
Pavement thickness (mm)	10	1.0 - 200	471.6 - 471.6	789.8 - 782.2
Void ratio	0.15	0.12 - 0.21	471.6 - 471.6	789.3 - 789.3
Permeability (mm/h)	100	1.0 - 200	471.6 - 471.6	789.1 - 789.2
Soil thickness (mm)	10	1.0 - 300	471.6 - 470.2	789.2 - 781.4
Soil porosity	0.5	0.4 - 0.5	471.6 - 471.6	789.5 -789.2
Soil field capacity	0.2	0.11 - 0.38	471.6 - 471.6	789.2 - 789.2
Soil wilting point	0.1	0.024 - 0.18	471.6 - 471.6	782.4 - 789.2
Soil conductivity (mm/h)	0.5	0.01 - 4.74	471.6 - 470.4	789.7 - 786.0
Soil suction head (mm)	50	49.02 - 320.04	471.6 - 471.6	789.2 - 789.2
Storage thickness (mm)	10	1.0 - 300	471.6 - 471.6	789.2 - 789.2
Storage void ratio	0.75	0.5 - 0.75	471.6 - 471.6	789.2 - 789.2
Storage seepage rate (mm/h)	0.5	0.1 - 5	471.6 - 471.6	789.2 - 789.2
Drain flow coefficient (mm/h)	100	1.0 - 500	471.6 - 471.6	789.2 - 789.2
Offset height (mm)	10	0 - 300	471.6 - 471.6	789.2 - 789.2
Best flood-reduction combination	pp draining to network		780.9 (x100 m^3)	
	pp draining to pervious area		470.6 (x100 m^3)	

The same flood reduction combination is run for rainfall events chosen (Table 5.6):

Table 5.6: Best flood reduction combination on flooding volume using porous pavement.

		Rain 1	**Rain 2**	**Rain 3**	**Rain 4**	
	flooding volume without pp	165.7	289.6	882.2	708.6	x100 m^3
Best flood reduction combination	pp draining to network	90.6	210.7	780.9	612.0	x100 m^3
	pp draining to pervious area	27.2	107.2	470.6	339.2	x100 m^3

Rain gardens

Rain gardens are a type of bio-retention cell consisting of just the engineered soil layer with no gravel bed below it (EPA and CDM 2012). Rain gardens have parameters in three process layers: surface, soil, and storage (Figure 5.11). For the simulation, 30% of the built area from every micro-basin (BA, 5.1) is replaced by rain gardens (Table 5.7).

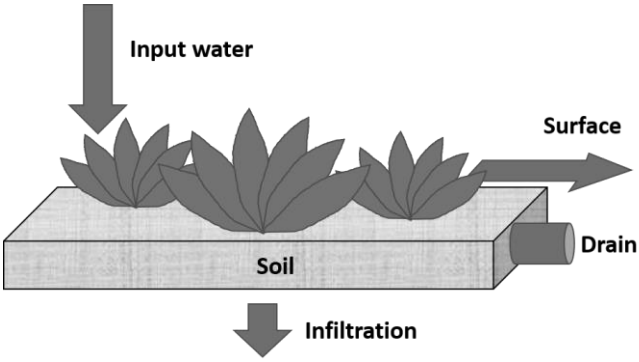

Figure 5.11: Rain gardens convey rainfall water on the surface as flooding volume, drain it to network or permeable areas, or infiltrate it below where possible.

Table 5.7: Rain gardens performance on flooding volume under parameter adjustment.

Rain gardens for Rainfall event 3 (0% water level, 5-mm depth storage)				
Flooding loss volume (x100 m^3)	with no rain gardens (rg)		882.2	
Variable	**Default value**	**Range tested**	**Flooding (x100 m^3)**	
			To pervious	**To drainage**
Surface berm height (mm)	0	0 - 100	536.8 - 537.5	881.3 - 880.3
Vegetation volume fraction	0	0 - 0.2	536.8 - 536.8	881.3 - 881.3
Surface roughness (Manning's n)	0.1	0.009 - 0.2	538.0 - 537.5	882.4 - 881.1
Surface slope (%)	1	0 - 20	538.3 - 536.9	881.7 - 882.4
Soil thickness (mm)	450	450 - 900	536.8 - 536.8	881.3 - 881.3
Soil porosity	0.5	0.4 - 0.5	537.8 - 536.8	881.3 -881.3
Soil field capacity	0.2	0.11 - 0.38	536.8 - 536.8	881.3 - 881.3
Soil wilting point	0.1	0.024 - 0.18	536.8 - 536.8	881.2 - 881.3
Soil conductivity (mm/h)	0.5	0.01 - 4.74	538.0 - 536.8	883.0 - 880.5
Soil suction head (mm)	50	49.02 - 320.04	536.8 - 537.7	881.3 - 880.9
Storage seepage rate (mm/h)	0.5	0.1 - 5	536.8 - 536.8	881.3 - 881.3
Best flood reduction combination	rg draining to network		881.3 (x100 m^3)	
	rg draining to pervious area		536.8 (x100 m^3)	

The same flood reduction combination is run for Rainfall events 1, 2 and 4 (Table 5.8):

Table 5.8: Best flood reduction combination on flooding volume using rain gardens.

	Rain 1	Rain 2	Rain 3	Rain 4	
flooding volume without rg	165.7	289.6	882.2	708.6	x100 m^3
rg draining to network	163.6	287.7	881.3	707.6	x100 m^3
rg draining to pervious area	92.6	161.1	536.8	395.8	x100 m^3

Green roofs

Green roofs are another variation of a bio-retention cell that have a soil layer laying atop a special drainage mat material that conveys excess percolated rainfall off of the roof (EPA and CDM 2012). Green roofs have parameters in three process layers: surface, soil, and drainage mat. For the simulation, 70% of the built area from every micro-basin (BA, 5.1) is replaced by green roofs, as 30% was considered for rain gardens before.

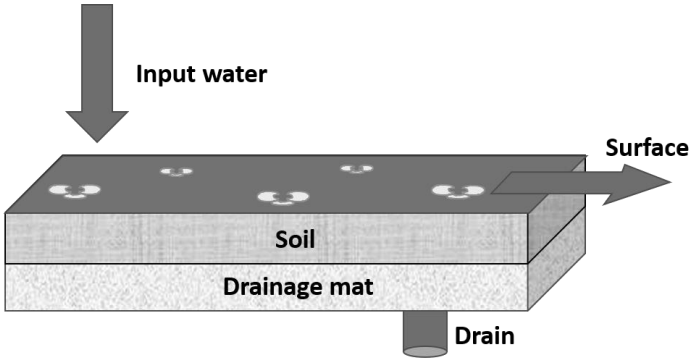

Figure 5.12: Green roofs convey rainfall water on the surface as input water for the rest of the micro-basin, or drain it to network or permeable areas.

Table 5.9: Green roofs performance on flooding volume under parameter adjustment.

Green roofs for Rainfall event 3 (0% water level, 5-mm depth storage)				
Flooding loss volume (x100 m^3)	with no green roofs (gr)		882.2	
Variable	**Default value**	**Range tested**	**Flooding (x100 m^3)**	
			To pervious	**To drainage**
Surface berm height (mm)	0	0 - 100	541.1 - 540.4	881.7 - 879.1
Vegetation volume fraction	0	0 - 0.2	541.1 - 541.1	881.7 - 881.7
Surface roughness (Manning's n)	0.1	0.009 - 0.2	542.6 - 541.1	882.1 - 880.8
Surface slope (%)	1	0 - 20	542.3 - 542.8	882.1 - 881.9
Soil thickness (mm)	75	75 - 150	541.1 - 541.0	881.7 - 881.1
Soil porosity	0.5	0.4 - 0.5	541.3 - 541.1	881.9 - 881.7
Soil field capacity	0.2	0.11 - 0.38	541.4 - 541.7	881.7 - 881.7
Soil wilting point	0.1	0.024 - 0.18	541.5 - 540.7	881.5 - 881.8
Soil conductivity (mm/h)	0.5	0.01 - 4.74	541.5 - 540.1	881.5 - 881.1
Soil suction head (mm)	50	49.02 - 320.04	541.5 - 541.3	881.7 - 881.0
Drainage mat thickness (mm)	25	25 - 50	541.1 - 541.1	881.7 - 881.7
Drainage mat void fraction	0.5	0.5 - 0.6	541.1 - 541.1	881.7 - 881.7
Drainage mat roughness (Manning's n)	0.1	0.1 - 0.4	541.1 - 540.7	881.7 - 881.7
Best flood reduction combination	gr draining to network		881.7 (x100 m^3)	
	gr draining to pervious area		541.1 (x100 m^3)	

The same flood reduction combination is run for the other rainfall events (Table 5.10):

Table 5.10: Best flood reduction combination on flooding volume using green roofs.

	Rain 1	**Rain 2**	**Rain 3**	**Rain 4**	
flooding volume without gr	165.7	289.6	882.2	708.6	x100 m^3
gr draining to network	163.3	287.5	881.7	707.7	x100 m^3
gr draining to pervious area	88.3	158.2	541.1	393.3	x100 m^3

5.3 Analysis of results

5.3.1 Simulation considering flood in surrounding neighborhoods

Flooding volume does not change considerably as water level in surrounding neighborhoods increase (Table 5.11); however, the percentage of rainfall water that becomes flooding volume with 0% water level (no flooding in surrounding neighborhoods) is very high – between 62% and 75.8% -, suggesting that network design could be a more important factor to determine floods than backwater effects, at least for this neighborhood, as it was somehow expected, for being far from Cauca River and

having piedmont slopes. Flooding volume from Santa Monica cannot convey through its drainage network and cannot stay on top of the street (5 mm depth storage), so it is conveyed to surrounding neighborhoods.

Table 5.11: Flooding volume increase as water level increases in surrounding neighborhoods. Depth storage of 5 mm is taken for all cases.

				Water level filling perimeter outlets			
		Flooding volume		40%	80%	100%	200%
	Inflow (m^3)	(m^3)	% of inflow	Flooding increase (%) compared to 0%			
Rain 1	26 730	16 570	62.0	0.18	0.36	0.42	0.78
Rain 2	43 290	28 960	66.9	0.14	0.24	0.31	0.55
Rain 3	116 460	88 220	75.8	0.10	0.18	0.23	0.43
Rain 4	101 460	70 860	69.8	0.10	0.20	0.25	0.47

Rainfall event 1 has the lowest total volume and the smallest percentage of rainfall becoming flooding volume (62%), but this flooding volume has the highest increase as surrounding neighborhoods get flooded. On the other side, Rainfall event 3 has the highest total volume and the highest percentage of rainfall becoming flooding volume (75.8%), but also the smallest percentage of change in flooding volume (0.43%) as surrounding neighborhoods get flooded.

Depth storage is the water depth that can stay atop of the streets without flowing out. The higher depth storage is in a neighborhood, the smaller is the flooding volume that it conveys to other neighborhoods (Table 5.12): a neighborhood that remains flooded is preventing surrounding neighborhoods to get flooded.

Table 5.12. Flooding volume with different depth storages, compared to 5-mm depth storage. 0% water level in surrounding neighborhoods is taken for all cases.

				Depth storage (mm)				
		Flooding volume (0% water level)		10	20	50	100	150
	Inflow (m^3)	(m^3)	% of inflow	Flooding volume change (%)				
Rain 1	26 730	16 570	62.0	-15.1	-44.4	---	---	---
Rain 2	43 290	28 960	66.9	-9.3	-26.7	-73.5	---	---
Rain 3	116 460	88 220	75.8	-3.9	-11.3	-33.3	-61.2	-82.3
Rain 4	101 460	70 860	69.8	-4.9	-13.4	-35.5	-64.8	-91.2

Model calibration through manholes with highest flood volumes

A proper calibration of the model was not possible since flooding volumes have never been measured or estimated in Santa Monica or in any other neighborhood in Cali: it means that flooding volume percentages (Table 5.11) may have been actually different. Nevertheless, regardless of this inexistent flooding volume calibration, those manholes that get the highest flood volumes in the simulation should also be the most flooded in reality.

Manholes with highest flood volumes under the 100% water level filling scenario were visited on site and local people were asked to confirm whether minor floods had occurred exactly there (Table 5.13 and Figure 5.13). Floods were observed in five out of the seven manholes (confirmed status). Manhole J16 is in one of the endorheic micro-basins previously detected (Figure 5.6). All confirmed areas were characterized by their flat topography. In general, the time that manholes stay flooded in the simulation is longer than what it usually takes for a minor flood to disappear (between 6 and 48 hours).

Table 5.13: Most frequently flooded manholes during simulation of 100% water level filling perimeter outlets and confirmation status on site.

Rainfall event	Manhole ID	Location	Status	Flood (x10 m^3)	Hours flooded
3	J284	6th Ave. commerce	Confirmed	163.14	129.0
3	J223	6A Ave. hardware store	Confirmed	102.03	128.0
3	J98	26 N and 6A junction	Not confirmed	46.2	128.0
3	J16	6th Ave underpass	Confirmed	34.78	112.0
3	J285	6th Ave. commerce	Confirmed	26.93	111.0
4	J96	26 N St. garden	Confirmed	11.28	111.0
4	J198	7th Ave. hostel	Not confirmed	9.47	109.0

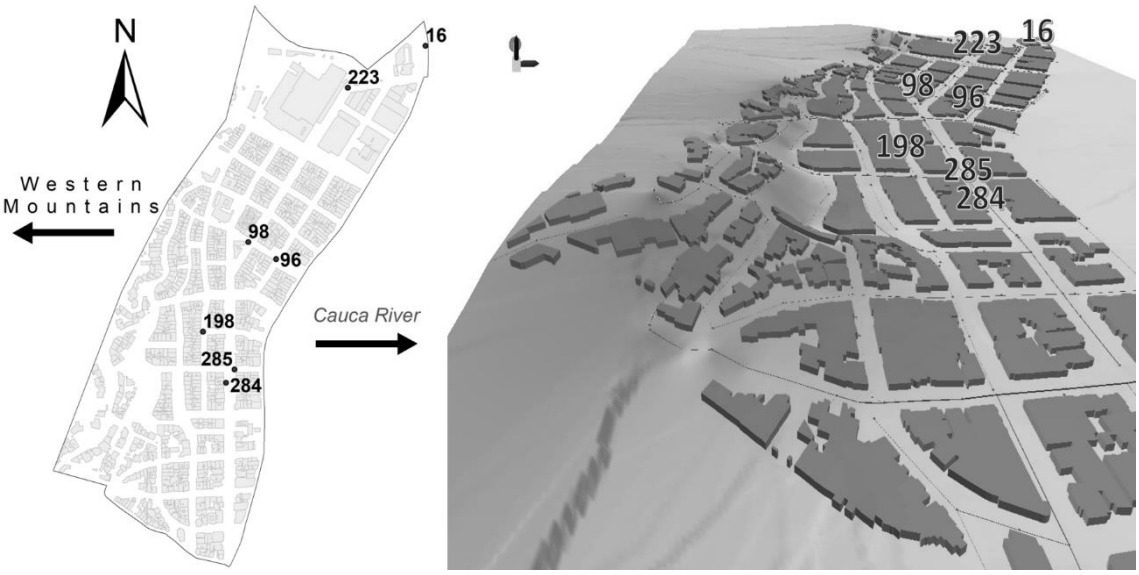

Figure 5.13: Location of manholes with highest flood volumes during simulation with 100% water level filling perimeter outlets.

5.3.2 Simulation under blocked pipelines in the neighborhood

Flooding volume increases significantly more with reduction of pipeline cross-section areas than with flooded surrounding neighborhoods. Flooding volume increases 41.7% with a reduction of 90% in cross-section for all pipelines (Table 5.4).

Most manholes with highest flood volumes during pipeline cross-section reduction include several of the most flooded manholes already detected during simulation with 100% water level filling perimeter outlets (Table 5.13). None of the additional manholes accounted for cross-section reduction simulation had been seen flooded according to local people when validating the results on site (Table 5.14 in bold).

The areas around these additional manholes are in the upper part of the neighborhood, they have steep slopes and do not seem to get easily flooded based on topography, so probably backflow from pipelines explains the model results. However, the time that manholes stay flooded in this simulation are more realistic when compared to minor-flood observations.

Table 5.14: Most flooded manholes during simulations of reductions in pipeline cross-sections. Manholes detected exclusively in this simulation are shown in bold.

Reduction	Manhole ID	Location	Status	Flood (x10 m^3)	Hours flooded
30%	J223	6A Ave. hardware store	Confirmed	21.97	7.36
70%	J198	7th Ave. hostel	Not confirmed	9.91	6.81
50%	J284	6th Ave. commerce	Confirmed	8.25	7.05
90%	J285	6th Ave. commerce	Confirmed	7.45	7.49
30%	J98	26 N and 6A junction	Not confirmed	7.13	7.29
90%	**J200**	**High-sloped junction**	**Not confirmed**	**7.12**	**7.51**
90%	**J271**	**9th Ave. restaurant zone**	**Not confirmed**	**4.65**	**7.53**
90%	**J262**	**High-sloped junction**	**Not confirmed**	**3.24**	**7.48**
90%	**J61**	**High-sloped residential area**	**Not confirmed**	**1.15**	**7.49**
30%	**J114**	**High-sloped residential area**	**Not confirmed**	**0.07**	**7.04**

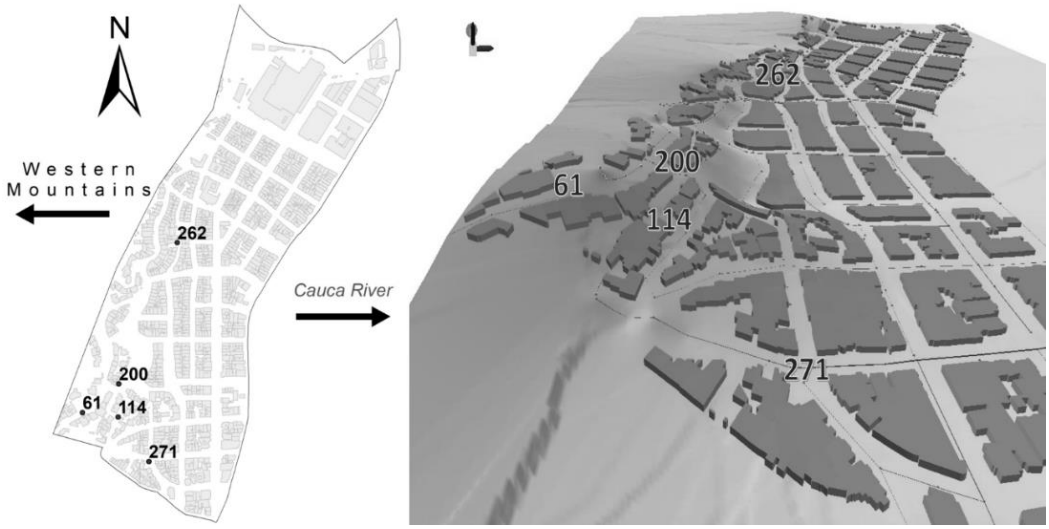

Figure 5.14: Location of manholes exclusively affected during simulation of reduction in pipeline cross-sections.

5.3.3 Simulation of LIDS to reduce flooding volume

Porous pavement

Porous pavement reduced flooding volume in different amounts depending on how it conveys its infiltrated water: if pavement drains water directly into the drainage network, flooding volume is reduced a maximum of 45.3% for rainfall event 1 (Table 5.6) and as little as 11.5% for rainfall event 3; however, when porous pavement drains first to a permeable area within the micro-basins (green area), the reduction increases considerably, ranging between 46.7% (rainfall event 3) and 83.6% (rainfall event 1).

Higher values in *surface berm height*, *surface roughness*, *soil thickness*, and *soil conductivity*, allow porous pavement to retain more flooding volume (Table 5.5).

Rainfall event 1 had the best results in both cases, probably because it has the smallest average intensity (1.24 mm/h). Flooding reduction is proportional to rainfall volume of each rainfall event (Figure 5.15).

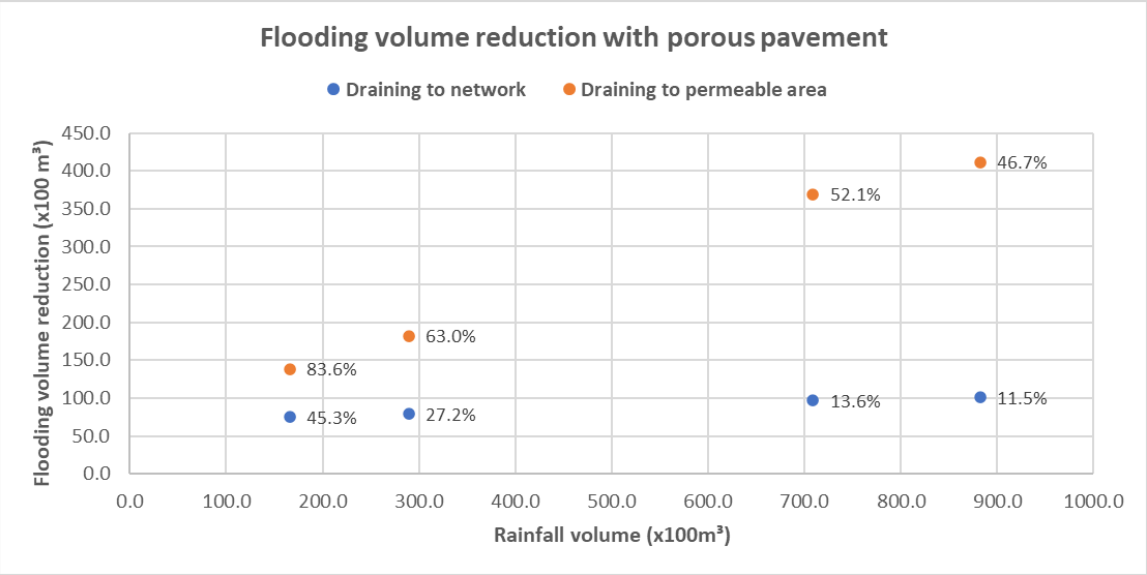

Figure 5.15: Flooding reduction with porous pavement for the 4 rainfall events chosen. Reduction percentages label both drainage options of each rainfall event.

Rain Gardens and Green roofs

For rain gardens and green roofs, the difference in results between draining to network and draining to a permeable area is more dramatic (Figure 5.16). Simulations with rain gardens and green roofs conveying water directly into the draining network practically did not reduce flooding volume in Santa Monica: maximum reduction for rain gardens was 1.3% and for green roofs was 1.4%, both in rainfall event 1. However, when water is drained to a permeable area, reduction improves to a maximum of 44.4% for rain gardens in rainfall event 2 and 46.7% for green roofs in rainfall event 1 (Figure 5.16).

For green roofs, more *ponding capacity*, higher *soil conductivity,* and rougher *materials in the drainage mat* lead to more flooding volume reduction (Table 5.9). As for rain gardens, results vary little as parameter values change (Table 5.7).

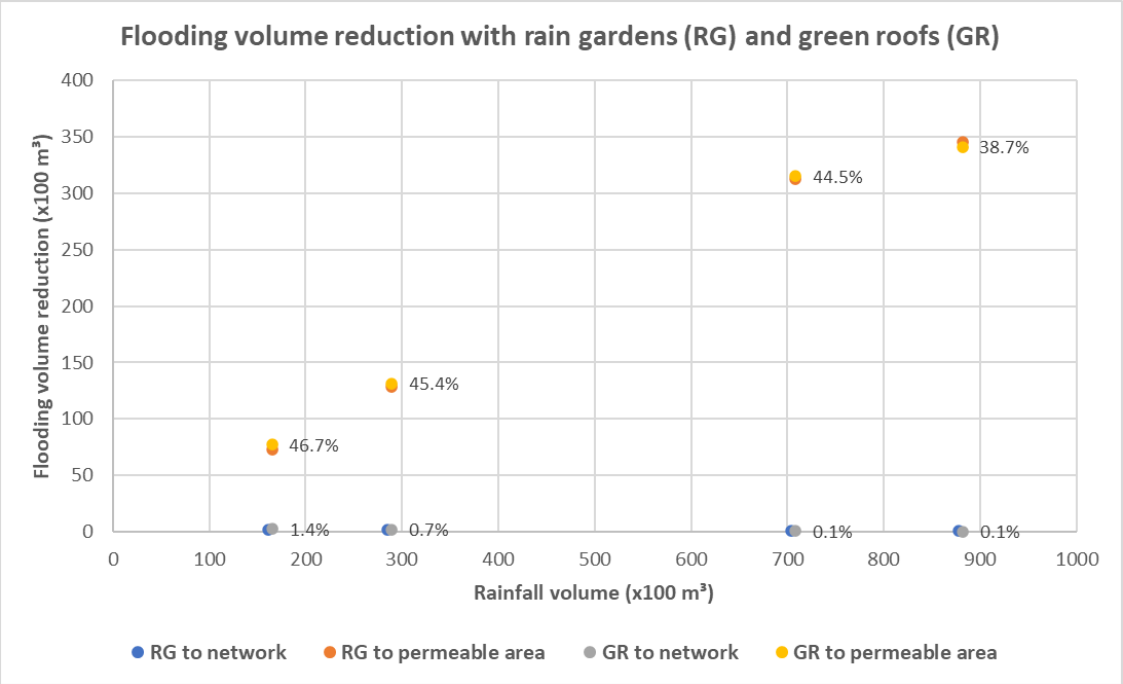

Figure 5.16: Flooding reduction with rain gardens and green roofs for the 4 rainfall events chosen. Reduction percentages label RG to network and GR to permeable area (very similar than those for GR to network and RG to permeable area respectively) of each rainfall event.

5.4 Recommendations

Flat topography influences the occurrence of minor floods more than outlet blockages and even pipeline obstructions up to certain level. Many of the top-flooded manholes in simulations were in or near an endorheic micro-basin. A high-resolution topographic map of the city would enable the preliminary detection of minor-flood prone areas, after which pipeline slope and diameter modifications can be simulated and implemented. Another way to detect minor-flood areas is by detecting stagnated water in aerial pictures taken in drone overflights during and after storms.

Porous pavement reduces significantly and efficiently (it only covers 0.021% of Santa Monica area) the flooding volume when it conveys water to a pervious area and not directly to the drainage network, in which case flood decreases in a very small percentage that would not justify the cost making all streets and roads permeable. For

this technique to work, an appropriate combination of these measures and technical facilities needs to be developed in the city and in its upstream areas outside.

Simulation with rain gardens and green roofs proves that the way water is conveyed after being retained by LIDS is as important as the solution itself: connections to pervious areas can improve flooding reduction hundreds of times (e.g. for rainfall event 3, green roofs reduced flooding volume 50 m^3 when draining to network and 34,100 m^3 when draining to permeable areas).

Flood duration estimated by the simulation is much longer than observed in minor floods, whenever they occur in flat areas. When they occur in steep slopes, they were closer to real observations. This happens because EPA SWMM forces accumulated water in a micro-basin to exit at an outlet only, and not along the pipelines, as it occurs with sinks along the streets. Better results should then be expected with higher resolution inputs that allow micro-basin delineation down to each sink on the street, at least for flat areas.

Two errors related to units were detected in EPA SWMM: it expresses runoff in cubic meters per second when it really is tenths of liter per second, and volume in 10^6 liters when it really is 10^4 liters; a review on units and dimensions is suggested for this software.

6 CONCLUSIONS AND RECOMMENDATIONS FOR FURTHER RESEARCH

Statistical analyses were performed with ArcGIS and R software to find correlations between rainfall parameters and minor floods and between neighborhood attributes and minor floods; these minor floods were reported in the city of Cali during 2000-2017. The potential losses from such minor floods were estimated over three aspects or minor disasters: *Aedes Aegyptus breeding*, *traffic impedance*, and *reduction in healthcare and educational services due to power cuts*. Finally, three common types of LIDS were tested in EPA SWMM software to determine which were more effective to reduce flooding volume; some maintenance problems were also simulated to see how they could affect flooding volumes in Santa Monica, one of the many neighborhoods in Cali that has experienced minor floods.

6.1 Summary of results

6.1.1 Correlation between rainfall parameters, neighborhood attributes and minor floods

Rainfall parameter differences between minor-flood and non-minor-flood events

All rainfall parameters (except *begin year day, peak hour,* and *asymmetry*) were statistically different in minor-flood and non-minor-flood related samples. *Total rainfall* is higher during minor-flood-related rainfall events, as well as *maximum intensity*, *peak position*, *duration*, *rain periods* and *spots*, while *triangular shape* is lower, meaning more abrupt changes in rainfall intensity. Rainfall could tend to have some of those conditions with climate change (Sofia and Tarolli 2017), such as heavy rainfall lasting longer (*total rainfall* and *duration*), and having fewer interruptions within a storm (*rain periods*).

Rainfall data from this study showed 16 rainfall events with *total rainfall* below 40 mm causing minor floods in the city (including a 1.4-mm event). Such low rainfall values causing minor floods could be explained by reading errors at the rainfall stations, by spatially concentrated rain showers, by highly vulnerable areas in the city collapsing with just a few millimeters of rain, or by a combination of them all.

Rainfall parameters as predictors of minor floods

T-tests showed that most individual rainfall parameters were significantly different for minor-flood and non-minor-flood events (Table 3.6). However, these are just statistical analyses of lumped historic records: individual or grouped rainfall parameters were not enough to predict whether a particular rainfall event would cause minor floods or not. When rainfall parameters were used in a joint logistic regression to predict which rainfall events would cause minor floods, the result gave a pseudo-R^2 of **0.262** (Table 3.10). Even though high R^2 values are not expected in urban hydrology analyses, this R^2 value is rather low and implies that there must be another set of meteorological variables (other than rainfall parameters) that help determine whether minor floods occur or not.

Rainfall parameters as predictors of number of neighborhoods affected by minor floods

The variable 'Occurrences' gives information about the severity of minor floods over the city by including the number of neighborhoods affected. All rainfall parameters except *begin year day* and *peak hour* significantly explained the variable 'Occurrences' (individual Poisson regressions). Nevertheless, in the joint Poisson regression, the pseudo-R^2 value for prediction of number of neighborhoods affected for a particular rainfall event was only **0.196** (Table 3.14), so once again, rainfall parameters alone could not accurately predict the impact of a given rainfall event over the city. It is likely that some unrecorded variables on the ground (related to waste management) or underground (related to drainage network maintenance) have also influence on the impact of minor floods.

Neighborhood attributes predicting number of minor floods per neighborhood

Distance to river, *slope range*, and *population density* are attributes that significantly explained the number of minor floods registered per neighborhood in Cali (Table 3.15).

Odds ratios from Poisson regression illustrated how much a one-unit change in neighborhood attributes modified the probability of having an extra minor-flood report on average per neighborhood.

Predictive margins for attributes and interactions between categories

Through predictive margins, it can be seen how higher SEL expected more minor floods than lower SEL, but they also showed a higher variability, which reflects the lack of criteria regarding network drainage conditions to define SEL (see section 3.1.2): a neighborhood can be classified in a high SEL, but at the same time it can have a poorly designed drainage network or very little green area, which would not affect its classification. Well-designed/maintained drainage infrastructure and minimum urban soil sealing practices are not present in all high SEL levels.

Higher *slope range* values predict more minor floods in neighborhoods with SEL 1: high slope ranges allow drainage networks to convey water effortlessly by gravity under certain design and maintenance conditions; if these conditions are not met, which is more likely in lower SEL, then the natural topographic advantages turn into drawbacks, leading to water ponding and flash floods.

Minor floods per neighborhood increase along with *population density* for lower SEL neighborhoods; densification in low-SEL neighborhoods usually occur with no infrastructure planning, increasing their vulnerability, while higher SEL increases in population are usually a consequence of new urban plans where basic infrastructure has been previously implemented. However, neighborhoods with SEL 6 were more susceptible to minor floods as *population density* decreased: a reason could be that some communities with financial power decided to live away from city centers and settled in countryside villas far between, giving more concern to the architecture of the houses than to having a proper drainage infrastructure.

Rainfall parameters predicting types of minor floods

Only one rainfall parameter predicted significantly one type of minor flood: *peak hour* predicting *trees falling* with an estimate of **0.113** (Table 3.19): Pacific jet-winds tend to be stronger in the afternoon and in the night time in the Cauca valley and mountains (Yepes et al. 2019), thus battering vegetation harder as they accompany rainfall.

Triangular shape (p=0.08) was close to significantly predict *traffic congestion and accidents*: *triangular shape* indicates that very abrupt rainfall events would alter traffic more and cause more automobile accidents than uniform rainfall events.

Asymmetry (p=0.09) and *spots* (p=0.08) also were close to significantly predict *river overflow*. Estimates indicated that rainfall events with higher volumes after the peak and fewer spots detecting rainfall are more likely to cause rivers to spill over. Rivers in the Cauca Valley drag a large amount of sediments: loose material in banks and mountains has more chances of being dragged if long rainfall volumes follow the peak. A rainfall event detected by few rainfall stations may indicate that it is taking place outside the district area of Cali, either on top of the Andes mountains or upstream Cauca River before getting to Cali.

Impact variables explaining each other

From the five pairings highlighted in the analysis, three showed significant correlations: *trees falling* explaining *power cuts*, *trees falling* explaining *traffic congestion and accidents*, and *power cuts* explaining *educational and health centers affected* (Table 3.20). On the other hand, *river overflow* did not significantly explain either *sewer blockage* nor *death, missing and wounded*. Rainfall events with falling trees increased their chances of causing power cuts over nine times and traffic congestion and accidents over six times.

6.1.2 Estimation of economic losses due to minor floods

Aedes aegypti breeding

The trend of Aedic Index values getting triggered on minor-flood days and fading out about a month later was uniform across all affected neighborhoods, showing that minor floods provided conditions for mosquitoes to reach their final stage.

The estimated cost of controlling *Aedes aegypti* breeding caused by minor floods is € 536,823.00 with over 880,000 people affected.

Traffic impedance

Impedance time lost by commuters during the 108 days of minor floods was over 200 million minutes, equivalent to € 4,214,446.00 by simply multiplying the minutes by the cost of the minimum wage minute in Colombia.

Power cuts

During power cuts, public healthcare institutions must reduce their services to the critical minimum and run on emergency power plants. With an average appointment/procedure fee of COP 200,000 (€ 59.48), the estimated cost of missed appointments and procedures during minor-flood days was € 4,991,337.00**.**

Educational institutions also must interrupt their activities during power cuts in minor-flood days. The total estimated cost of power cuts during minor floods affecting educational institutions is € 11,179,704.00.

Economic losses in the city reinforcing illegal practices

All economic loss estimations in this analysis due to minor floods summed over 20 million euros between 2000 and 2017. Meanwhile, Prosecutor's office in Cali has estimated that illegal microloan organizations handle annual cash inflows over COP 200 million (around € 57,000.00).

Multiplying this latter figure by 18 (the years of the analysis time frame, 2000-2017) results in over € 1 million: it is very likely that people in Cali would resort less in such illegal alternatives, had they not lost these 20 million euros related to minor floods in the first place, especially considering that most loans are small (around 25 € per person, El País de Cali 2019).

6.1.3 Hydrodynamic simulations of draining network response in a neighborhood in Cali

Simulation considering flood in surrounding neighborhoods

Flooding volume remained considerably steady in Santa Monica as surrounding neighborhoods go from experiencing no flood to having their outlet manholes filled with water up to twice their diameter. The percentage of rainfall water that becomes flooding

volume varies between 62% and 75.8%, suggesting that the network design could already present some problems other than backwater effects from surrounding neighborhoods.

Model calibration through manholes with highest flooding volumes

A proper calibration of the model was not possible since flooding volumes have never been measured or estimated in Santa Monica or in any other neighborhood in Cali. Nevertheless, manholes with the highest flooding volumes in the simulation should also be the most flooded in reality. These manholes were visited on site and local people were asked to confirm whether minor floods had occurred exactly there: floods were observed in five out of the seven manholes. In general, the time that manholes stay flooded in the simulation is longer than what it usually takes for a minor flood to disappear (between 6 and 48 hours)

Simulation under blocked pipelines in the neighborhood

Flooding volume increased significantly more with reduction of pipeline cross-section areas than with flooded surrounding neighborhoods. Flooding volume increased 41.7% with a reduction of 90% in cross-section for all pipelines.

Most flooded manholes during pipeline cross-section reduction include several of the most flooded manholes already detected during simulation of flooded surrounding neighborhoods. None of the additional manholes accounted for cross-section reduction simulation were confirmed when calibrating the results on site by asking local people. Flood duration in this simulation is more realistic when compared to minor-flood observations.

Simulation of LIDS to reduce flooding volume

Porous pavement

When pavement drains water directly into the drainage network, flooding volume is reduced a maximum of 45.3% for rainfall event 1 and as little as 11.5% for rainfall event 3; however, when porous pavement drains first to a permeable area within the micro-

basins (green area), the reduction increases considerably, ranging between 46.7% (rainfall event 3) and 83.6% (rainfall event 1).

Rain Gardens and Green roofs

The difference in results between draining to network and draining to a permeable area was more dramatic: when conveying into the draining network, maximum reduction for rain gardens was 1.3% and for green roofs 1.4%, both in rainfall event 1. However, when water was drained to a permeable area, reduction improves to a maximum of 44.4% for rain gardens in rainfall event 2 and 46.7% for green roofs in rainfall event 1.

6.2 Contribution of the study

The significant correlations between rainfall parameters and minor floods showed which types of rainfall events were more prone to cause minor floods in the city.

The significant correlations between neighborhood attributes and minor floods help to prioritize which neighborhoods should be intervened first, especially with a restricted city budget. In 2019, CVC became interested in knowing which places in Cali should harbor Sustainable Drainage Systems (SUDS) to reduce urban flood risks.

Economic estimations of losses due to minor floods in the city serve as a basis for the government, institutions, and the community to weigh the consequences of not including minor floods as an integral part of flood risk management.

Simulations with LIDS highlight clearly that having green areas to drain water to is as important as building the solutions themselves (rain gardens, green roofs, and porous pavements). In some cases, connecting LIDS directly to draining networks had practically no effect on dampening peak flow on the streets. Currently this is critical as government expects to reduce minor floods by forcing new construction projects, both public and private, to include LIDS or SUDS within their sites.

6.3 Recommendations for future research

Even though groundwater dynamics take place on longer time scales than rainfall-runoff processes and do not seem to be strongly related to minor floods, aquifer zones can be useful to define those permeable areas where SUDS and LIDS could drain rainfall water

to, in order to reduce minor floods. Therefore, an aquifer map with a better resolution than the current official one for Cali is required.

Due to some very small rainfall events causing minor floods in Cali, CVC should periodically calibrate the rainfall stations, EMCALI should check critical infrastructure points in neighborhoods to reduce vulnerability, and research on spatial distribution of rainfall events must be made, since some events may fall in very small areas in between stations and thus cannot be detected by them.

In order to make data collection on minor floods more systematic and accurate, aid organizations and institutions should train part-time workers to collect information immediately after a rainfall event takes place; another option is to rely upon high space-time resolution satellite radar imagery (Sentinel-1, ALOS) taken as early as possible after rainfall events occur, as a tool to make ex-post analysis to spot minor floods overall: this gives data collectors more time to elaborate the reports.

Since minor floods do not directly take human lives or physically damage equipment, there is no need for evacuation plans, but rather for taking long-term actions to reduce minor floods in most vulnerable spots, such as infrastructure improvements, and maintenance and protection, which requires continuous data monitoring and analyses; unlike flood hazard maps, the location of minor floods and critical neighborhoods changes in a more dynamic way and it is very sensitive to cultural practices and modifications in infrastructure.

Neighborhood attributes that significantly correlate to minor floods (*population density*, *distance to rivers*, and *slope range*) are associated with urban pressure on river buffering areas. National and local authorities must propose land-use plans that include protective measures for existing and new buildings on the floodplains.

Underestimations of the consequences of only three aspects regarding minor floods in Cali added up to € 20 million in less than 20 years, which easily equals 20% of the current annual capital resources for Cali. These expenses have nothing to do directly with extreme events or climate change scenarios: they are the cumulated cost of poorly designed works combined with cultural malpractices over decades in the city. Reducing these adverse effects would improve expansion of businesses and employment.

The presence of *Aedes aegypti* mosquitoes in Cali is practically impossible to avoid due to its weather and topography; however, their amount and impact on the city's inhabitants can be reduced by keeping nesting spots free of water. Any effort to reduce the presence of stagnated water along with other household solutions will help reduce the presence of mosquitoes.

Power cuts are a consequence of an electricity system based almost completely on aerial power lines, which are extremely vulnerable to wind gusts and falling trees and branches. Putting the electricity lines underground must be considered.

A high-resolution topographic map of the city would enable the preliminary detection of minor-flood prone areas, after which pipeline slope and diameter modifications can be simulated and implemented. Another way to detect minor flood areas is from aerial pictures taken in drone overflights during storms.

LIDS such as porous pavement, rain gardens and green roofs reduce significantly and efficiently flooding volume as long as they convey water to a pervious area and not directly to the drainage network, in which case flood decreases in a very small percentage that would not justify the cost of converting all streets and roads to permeable, and of installing such structures in buildings. In fact, it would be just as effective to drain regular roofs and gardens directly into permeable areas to reduce flooding volume. For this strategy to work, an appropriate combination of these measures and technical facilities needs to be developed in the city.

EPA SWMM estimates longer flooding durations than those observed. This probably happens because EPA SWMM forces accumulated water in a micro-basin to exit at an outlet only, and not along the pipelines, as it occurs with sinks along the streets. Better results should then be expected with higher resolution inputs that allow micro-basin delineation down to each sink on the street, at least for flat areas.

7 BIBLIOGRAPHIC REFERENCES

- ADN Cali editorial office (2016). Preparación para lluvias, preocupa. *ADN Cali*, jun-22, p:3.
- ADN Cali editorial office (2019). Con los ojos en los 'gota a gota'. *ADN Cali*, apr-3, p:3.
- Agbelie B, Volovski M, Zhang Z et al (2016). Updating State and Local Highway Cost Allocation and Revenue Attribution. Transp Res Rec 2597:1-10. DOI: 10.3141/2597-01.
- Alcaldía de Santiago de Cali (2014). Revisión ordinaria del Plan de Ordenamiento Territorial de Santiago de Cali. DAPM, Cali.
- Alcaldía de Santiago de Cali (2018). Circular con carácter de doctrina del acuerdo 0373 de 2014. DAPM, Cali.
- Alcaldía de Santiago de Cali (2019). Director del Banco Mundial conoció la importancia del proyecto Plan Jarillón de Cali. Available online at http://www.cali.gov.co/gestiondelriesgo/publicaciones/147296/director-del-banco-mundial-conocio-la--importancia-del-proyecto-plan-jarillon-de-cali/.
- Alvarado A, Sandoval J, Daza R (2005). Estudio de microzonificación sísmica de Santiago de Cali. Ingeominas, Cali.
- Argüeso D, Di Luca A, Evans, J (2016). Precipitation over urban areas in the western Maritime Continent using a convection-permitting model. Clim Dyn 47 (3-4):1143–1159. DOI: 10.1007/s00382-015-2893-6.
- Avila H, Avila L, Sisa A (2016). Dispersed Storage as Stormwater Runoff Control in Consolidated Urban Watersheds with Flash Flood Risk. J Water Resour Plann Manage 142(12). DOI: 10.1061/(ASCE)WR.1943-5452.0000702.
- Azcárate L, Ocoró C (2016). Plan anual de contratación del servicio educativo 2017. Alcaldía de Santiago de Cali.
- Bahamón A (2014). Colombia geografía y destino: visión geopolítica de sus regiones naturales. Universidad Militar Nueva Granada, Bogotá.
- Bangert M, Molyneux D, Lindsay S et al (2017). The cross-cutting contribution of the end of neglected tropical diseases to the sustainable development goals. Infect Dis Poverty 6(1), i15. DOI: 10.1186/s40249-017-0288-0.
- Bello S, Díaz E, Malagón-Rojas J et al (2011). Medición del impacto económico del dengue en Colombia: una aproximación a los costos médicos directos en el período 2000-2010. Biomédica 31:110–145.
- Blanco-Vogt A, Schanze J (2014). Assessment of the physical flood susceptibility of buildings on a large scale: conceptual and methodological frameworks. Nat Hazards Earth Syst Sci 14 (8):2105–2117. DOI: 10.5194/nhess-14-2105-2014.
- Buitrago O, Paredes S, Motta N (2011). De los farallones al Cauca: situaciones ambientales, actores e imaginarios. Editorial Universidad del Valle, Cali.

- Byrd H, Matthewman S (2014). Exergy and the City: The Technology and Sociology of Power (Failure). J Urban Technol 21(3):85–102. DOI: 10.1080/10630732.2014.940706.
- Cali Chamber of Commerce (2017): Balance económico de Cali y el Valle del Cauca en 2016. Executive report.
- Campos A, Holm-Nielsen N, Díaz C et al (2012). Análisis de la gestión del riesgo de desastres en Colombia: un aporte para la construcción de políticas públicas. World Bank Colombia, Bogotá.
- Cardona O, Carreño M (2011). Updating the Indicators of Disaster Risk and Risk Management for the Americas. IDRiM Journal 1(1):27–47. DOI: 10.5595/idrim.2011.0014.
- Cea L, Fraga I (2018). Incorporating Antecedent Moisture Conditions and Intraevent Variability of Rainfall on Flood Frequency Analysis in Poorly Gauged Basins. Water Resour Res 54(11):8774–8791. DOI: 10.1029/2018WR023194.
- Cenicaña (2019). Boletines diarios de la Red Meteorológica Automatizada. Available online at https://www.cenicana.org/apps/meteoportal/public/diarios.
- Chen Y, Yeh C, Yu B (2016). Flood damage assessment of an urban area in Taiwan. Nat Hazards 83(2):1045–1055. DOI: 10.1007/s11069-016-2362-5.
- Cooley A, Chang H (2017). Precipitation Intensity Trend Detection using Hourly and Daily Observations in Portland, Oregon. Climate 5(1). DOI: 10.3390/cli5010010.
- Corfee-Morlot J, Cochran I, Hallegatte S et al (2011). Multilevel risk governance and urban adaptation policy. Climatic Change 104(1):169–197. DOI: 10.1007/s10584-010-9980-9.
- Corporación OSSO (2012). Informe de Avance No 2: Contrato de Consultoría No 101 de 2012 celebrado entre el Fondo Adaptación y Corporación OSSO. Fondo Adaptación, Bogotá.
- Cutter S, Gall M (2015). Sendai targets at risk. In Nat Clim change 5, 707 EP -. DOI: 10.1038/nclimate2718.
- CVC, Universidad del Valle (2007). El Río Cauca en su valle alto: un aporte al conocimiento de uno de los ríos más importantes de Colombia. Lemoine Editores, Cali.
- DANE (2010). Proyecciones nacionales y departamentales de población 2005-2020. Estudios Postcensales (7).
- Dash P, Punia M (2019). Governance and disaster: Analysis of land use policy with reference to Uttarakhand flood 2013, India. Int J Disast Risk Re 36, p. 101090. DOI: 10.1016/j.ijdrr.2019.101090.
- Decree 4819 (2010). Diario Oficial 47937 dec-29 p. 218. Bogotá.
- Dommar C, Lowe R, Robinson M et al (2014). An agent-based model driven by tropical rainfall to understand the spatio-temporal heterogeneity of a

chikungunya outbreak. Acta Tropica 129:61–73. DOI: 10.1016/j.actatropica.2013.08.004.

- Dottori F, Kalas M, Salamon P et al (2017). An operational procedure for rapid flood risk assessment in Europe. Nat Hazards Earth Syst Sci 17(7):1111–1126. DOI: 10.5194/nhess-17-1111-2017.
- El País de Cali editorial office (2019). El 'gota a gota': franquicias de la criminalidad. *El País de Cali*, apr-28, A14-A15.
- EMCALI (2017a). Norma técnica de recolección de aguas residuales y lluvias. Criterios de diseño en sistemas de alcantarillado. EMCALI, Cali.
- EMCALI (2017b). Sewer system spatial information. Grupo de Información Geográfica y Análisis. Confidential information.
- EMCALI (2019). Tarifas de Energía: Mercado Regulado. Resolución UPME-0355. Available online at https://www.emcali.com.co/web/energia/mercado-regulado.
- EPA (2017). Mosquito life cycle. Environmental Protection Agency. Available online at https://www.epa.gov/mosquitocontrol/mosquito-life-cycle.
- EPA (2018). Urban Runoff: Low Impact Development. United States Environmental Protection Agency. Available online at https://www.epa.gov/nps/urban-runoff-low-impact-development.
- EPA, CDM (2012). SWMM. Version 5.1. Cincinnati, Ohio: EPA. Available online at www.epa.gov/swmm.
- Escobar G (2016). Cali en cifras 2015. Departamento Administrativo de Planeación, Cali.
- ESRI (2015). ArcGIS Desktop. Version 10.3.1. Environmental Systems Research Institute. Redlands, CA
- European Parliament (2007). Directive 2007/60/EC of the European Parliament and of the Council of 23 October 2007 on the assessment and management of flood risks. Official Journal of the European Union (L 288):27–34.
- Franco A, Shaker M, Kalubi D et al (2017). A review of sustainable energy access and technologies for healthcare facilities in the Global South. Sustain Energy Technol Assess 22:92–105. DOI: 10.1016/j.seta.2017.02.022.
- Friedman J, Hastie T, Tibshirani R (2010). Regularization Paths for Generalized Linear Models via Coordinate Descent. J Stat Softw V33-01:1–22.
- Garcia-Urquia E, Axelsson K (2015). Rainfall thresholds for the occurrence of urban landslides in Tegucigalpa, Honduras: an application of the critical rainfall intensity. Geogr Ann A 97(1):61–83. DOI: 10.1111/geoa.12092.
- Gariano S, Sarkar R, Dikshit A et al (2019). Automatic calculation of rainfall thresholds for landslide occurrence in Chukha Dzongkhag, Bhutan. Bull Eng Geol Environ 78(6):4325–4332. DOI: 10.1007/s10064-018-1415-2.

- Genovese E, Green C (2014). Assessment of storm surge damage to coastal settlements in Southeast Florida. J Risk Res 18(4):407–427. DOI: 10.1080/13669877.2014.896400.
- González C, Alfaro A (2001). El desplazamiento interno detonante de la vulnerabilidad ante amenazas naturales en Barrancabermeja, Colombia. Segundo Congreso Iberoamericano de Ingeniería Sísmica, Madrid.
- Gonzalez O (2012). Características climatológicas de ciudades principales y municipios turísticos. IDEAM, Bogotá.
- Guzmán D, Cadena M, Ruiz F (2015). Regionalización de Colombia según el régimen pluvial anual. IDEAM, Bogotá.
- Heydari N, Larsen D, Neira M et al (2017). Household Dengue Prevention Interventions, Expenditures, and Barriers to Aedes aegypti Control in Machala, Ecuador. IJERPH 14(2). DOI: 10.3390/ijerph14020196.
- Hoyos N, Escobar J, Restrepo J et al (2013). Impact of the 2010-2011 La Niña phenomenon in Colombia, South America: the human toll of an extreme weather event. Appl Geogr 39:16–25.
- Huang M, Jin S (2019). A methodology for simple 2-D inundation analysis in urban area using SWMM and GIS. Nat Hazards 97(1):15–43. DOI: 10.1007/s11069-019-03623-2.
- IDESC Geoportal (2018). DAPM, Version 3.3. Available online at http://idesc.cali.gov.co/.
- Jann B (2013). Predictive margins and marginal effects in Stata. German Stata Users' Group Meetings 2013 11, Stata Users Group. Available online at https://ideas.repec.org/p/boc/dsug13/11.html.
- Jiménez N, Velásquez A (2011). Distribución del suelo y construcción de riesgos en Cali durante la segunda mitad del siglo XX. Historia de Cali Siglo XX, Tomo I:336-352. Universidad del Valle, Cali.
- Kobayashi K, Takara K, Sano H et al (2016). A high-resolution large-scale flood hazard and economic risk model for the property loss insurance in Japan. In J Flood Risk Manag 9(2):136–153. DOI: 10.1111/jfr3.12117.
- Liang P, Ding Y (2017). The long-term variation of extreme heavy precipitation and its link to urbanization effects in Shanghai during 1916–2014. Adv Atmos Sci 34(3):321–334. DOI: 10.1007/s00376-016-6120-0.
- Lisonbee J, Ribbe J, Wheeler M (2019). Defining the north Australian monsoon onset: A systematic review. Prog Phys Geog. DOI: 10.1177/0309133319881107.
- Lumley T (2017). Pseudo-R2 statistics under complex sampling. Aust N Z J Stat 59(2):187–194. DOI: 10.1111/anzs.12187.
- Manz B, Rodríguez J, Maksimović Č et al (2013). Impact of rainfall temporal resolution on urban water quality modelling performance and uncertainties. Water Sci Technol 68(1). DOI: 10.2166/wst.2013.224.

- Mark O, Weesakul S, Apirumanekul C et al (2004). Potential and limitations of 1D modelling of urban flooding. J Hydrol 299(3-4):284–299. DOI: 10.1016/j.jhydrol.2004.08.014.
- Mathwave Technologies (2013). EasyFit, version 5.6. Mathwave Technologies. Available online at www.mathwave.com.
- McGrath H, Stefanakis E, Nastev M (2015). Sensitivity analysis of flood damage estimates: a case study in Fredericton, New Brunswick. Int J Disaster Risk Reduct 14:379–387. DOI: 10.1016/j.ijdrr.2015.09.003.
- Ministerio de Educación Nacional (2017). Matriculados en Educación Superior Colombia 2016. SNIES, Bogotá.
- Mokhtarian P (2016). Discrete choice models' ρ 2: a reintroduction to an old friend. J Choice Model 21:60–65. DOI: 10.1016/j.jocm.2016.02.001.
- Moran P (1950). Notes on Continuous Stochastic Phenomena. Biometrika 37(1/2). DOI: 10.2307/2332142.
- Moreno-Navarro F, Sol-Sánchez M, Tomás-Fortún E et al (2016). High-Modulus Asphalt Mixtures Modified with Acrylic Fibers for Their Use in Pavements under Severe Climate Conditions. J Cold Reg Eng 30(4). DOI: 10.1061/(ASCE)CR.1943-5495.0000108.
- Palanisamy B, Chui T (2015). Rehabilitation of concrete canals in urban catchments using low impact development techniques. J Hydrol 523:309–319. DOI: 10.1016/j.jhydrol.2015.01.034.
- Peyman B, Nur I, Mohd R (2015). The effect of preservation maintenance activities in asphalt concrete pavement sustainability. Jurnal Teknologi 78(4):117-124. DOI: 10.11113/jt.v78.8008.
- Plank S (2014). Rapid Damage Assessment by Means of Multi-Temporal SAR — A Comprehensive Review and Outlook to Sentinel-1. Remote Sensing 6(12):4870–4906. DOI: 10.3390/rs6064870.
- Pregnolato M, Ford A, Wilkinson S et al (2017). The impact of flooding on road transport: a depth-disruption function. Transport Res D-Tr E 55:67–81. DOI: 10.1016/j.trd.2017.06.020.
- Ramos-Cañón A, Prada-Sarmiento L, Trujillo-Vela M et al (2016). Linear discriminant analysis to describe the relationship between rainfall and landslides in Bogotá, Colombia. Landslides 13(4):671–681. DOI: 10.1007/s10346-015-0593-2.
- Rodríguez M (2015). Vulnerabilidad poblacional al riesgo de desastres en Bolivia. UNFPA, La Paz.
- Rojas J (2016a). Boletín Epidemiológico 2016. Alcaldía de Santiago de Cali, Cali.
- Rojas J (2016b). Boletín epidemiológico: semana epidemiológica No. 39. Secretaría de Salud de Cali, Cali.
- Rosa D, Clausen J, Dietz M (2015). Calibration and Verification of SWMM for Low Impact Development. J Am Water Resour As 1–12.

- RStudio Team (2015). RStudio: Integrated Development for R. Boston, MA. Available online at http://www.rstudio.com/.
- Sabir M, Van Ommeren J, Koetse M et al (2011). Adverse Weather and Commuting Speed. Netw Spat Econ 11(4):701–712. DOI: 10.1007/s11067-010-9130-y.
- Sánchez M, Silva M, Zúñiga J et al (2007). Es mejor prevenir: módulo Inundaciones. Vol 13. Red Cross International, Managua.
- Scorzini A, Leopardi M (2017). River basin planning, from qualitative to quantitative flood risk assessment: the case of Abruzzo Region (central Italy). Nat Hazards 88(1)71–93. DOI: 10.1007/s11069-017-2857-8.
- Secretaría de Educación de Cali (2018). Información de cupos en colegios de Cali. Letter to Cesar Canon-Barriga, Cali.
- Sedano K, Carvajal Y, Ávila A (2013). Análisis de aspectos que incrementan el riesgo de inundaciones en Colombia. luaz (37). DOI: 10.17151/luaz.2013.37.13.
- Sheela A, Sarun S, Justus J et al (2015). Assessment of changes of vector borne diseases with wetland characteristics using multivariate analysis. Environ Geochem Health 37(2):391–410. DOI: 10.1007/s10653-014-9655-y.
- Sofia G, Tarolli P (2017). Hydrological Response to ~30 years of Agricultural Surface Water Management. Land 6(1). DOI: 10.3390/land6010003.
- StataCorp LP (2015). Stata Statistical Software. Version Release 14. College Station, Tx.
- Turriago A (2018). La 'Trampa' del ingreso medio: análisis. *Dinero*, feb-23. Available online at https://www.dinero.com/economia/articulo/la-trampa-del-ingreso-medio-por-alvaro-turriago-hoyos/255666.
- UNISDR (2015). Making development sustainable: the future of disaster risk management. Global assessment report on disaster risk reduction, 4.2015. United Nations, Geneva.
- University of Maryland, Texas A&M University (2018). The Growing Threat of Urban Flooding: A National Challenge. University of Maryland and Texas A&M University.
- Uribe H, Holguín C (2012). A propósito de la oleada invernal, el papel del estado frente al manejo del dique del Río Cauca en Cali, Colombia. Eleuthera 6:228–245.
- World Health Organization (2012). Health Indicators of Sustainable Cities in the Context of the Rio+20 UN Conference on Sustainable Development. National Institute of Environmental Health Sciences, USA.
- Wijayanti P, Zhu X, Hellegers P et al (2017). Estimation of river flood damages in Jakarta, Indonesia. Nat Hazards 86(3):1059–1079. DOI: 10.1007/s11069-016-2730-1.
- Williams R (2012). Using the Margins Command to Estimate and Interpret Adjusted Predictions and Marginal Effects. Stata J (12):308–331.

- World Meteorological Organization (2009). Integrated flood management concept paper. WMO, Geneva.
- Wu X, Zhou L, Gao G et al (2016). Urban flood depth-economic loss curves and their amendment based on resilience: evidence from Lizhong Town in Lixia River and Houbai Town in Jurong River of China. Nat Hazards 82(3):1981–2000. DOI: 10.1007/s11069-016-2281-5.
- Yamin L, Ghesquiere F, Cardona O et al (2013). Modelación probabilista para la gestión del riesgo de desastre: el caso de Bogotá, Colombia. The World Bank, Washington, DC. ISBN: 978-958-695-840-0.
- Yepes J, Poveda G, Mejía J et al (2019). CHOCO-JEX: A Research Experiment Focused on the Chocó Low-Level Jet over the Far Eastern Pacific and Western Colombia. Bull Amer Meteor Soc 100(5):779–796. DOI: 10.1175/BAMS-D-18-0045.1.
- Yu L, Gao Y, Yu L et al (2015). Floating car data-based method for detecting flooding incident under grade separation bridges in Beijing. IET Intell Transp Sy 9(8):817–823. DOI: 10.1049/iet-its.2014.0228.

ACKNOWLEDGEMENT

Special thanks to DAAD BMZ and Fiat Panis Foundation for sponsoring this research, and to EMCALI, CVC, OSSO Corporation, and the Mayor's Office in Cali for sharing data for the analysis.